NASA CR-121137

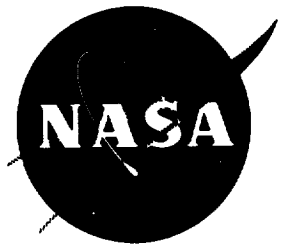

Volume I Final Report

Composite Propulsion Feedlines For Cryogenic Space Vehicles

by

C. A. Hall, D. J. Laintz, and J. M. Phillips

MARTIN MARIETTA CORPORATION

Prepared for

NATIONAL AERONAUTICS AND SPACE ADMINISTRATION

NASA Lewis Research Center
Contract NAS3-14370

Joseph Notardonato, Project Manager

1. Report No.	2. Government Accession No.	3. Recipient's Catalog No.
NASA CR-121137		

4. Title and Subtitle	5. Report Date
Composite Propulsion Feedline for Cryogenic Space Vehicles	August 1973
	6. Performing Organization Code: 04236

7. Author(s)	8. Performing Organization Report No.
C. A. Hall, D. J. Laintz, J. M. Phillips	
	10. Work Unit No.

9. Performing Organization Name and Address	11. Contract or Grant No.
Martin Marietta Corporation P. O. Box 179 Denver, Colorado 80201	NAS3-14370
	13. Type of Report and Period Covered: Final Report, June 1970 to December 1972

12. Sponsoring Agency Name and Address	14. Sponsoring Agency Code
National Aeronautics and Space Administration Lewis Research Center Cleveland, Ohio 44135	

15. Supplementary Notes

16. Abstract

Thin metallic liners that provide leak-free service in cryogenic propulsion systems are overwrapped with a glass-fiber composite that provides strength and protection from handling damage. The resultant tube is lightweight, strong and has a very low thermal flux. Several styles of tubing ranging from 5 to 38 cm (2 to 15 in.) in diameter and up to 305 cm (10 ft) long were fabricated and tested at operating temperatures from 294 to 21 K (+70 to -423°F) and operating pressures up to 259 N/sq cm (375 psi). The primary objective for the smaller sizes was thermal performance optimization of the propulsion system while the primary objective of the larger sizes was weight optimization and to prove fabricability. All major program objectives were met resulting in a design concept that is adaptable to a wide range of aerospace vehicle requirements. Major items of development included bonding large diameter aluminum end fittings to the thin Inconel liner; fabrication of a 38 cm (15 in.) diameter tube from 0.008 cm (0.003 in.) thick Inconel; and evaluation of tubing which provides essentially zero quality propellant in a very short period of time resulting in a lower mass of propellant expended in chilldown.

17. Key Words (Suggested by Author(s))	18. Distribution Statement
Composite Cryogenic Feedline Chilldown Overwrap	Distribution of This Document is Unlimited

19. Security Classif. (of this report)	20. Security Classif. (of this page)	21. No. of Pages	22. Price*
Unclassified	Unclassified		

* For sale by the National Technical Information Service, Springfield, Virginia 22151

FOREWORD

The work described herein was conducted by the Martin Marietta Corporation, Denver Division, under NASA Contract NAS3-14370. Work was done under the management of the NASA Project Manager, Mr. Joseph Notardonato, Liquid Rocket Technology Branch, NASA-Lewis Research Center, Cleveland, Ohio. Messrs. James Faddoul, James Barber and Al Pavli also served as Project Managers during some phases of the contract.

In addition to the stated authors, several persons provided major assistance in the performance of this activity including Messrs. Clifford S. Foster, Earl F. Wollam, Rex P. Moore, Walter L. McKenna, Lyle L. Bartels, Timothy P. Quinn and Donald A. Stang.

TABLE OF CONTENTS

VOLUME I

VOLUME II

FIGURES

FIGURES (Continued)

TABLES

TABLES

ABSTRACT

Thin metallic liners that provide leak-free service in cryogenic propulsion systems are overwrapped with a glass-fiber composite that provides strength and protection from handling damage. The resultant tube is lightweight, strong and has a very low thermal flux. Several styles of tubing ranging from 5 to 38 cm (2 to 15 in.) in diameter and up to 305 cm (10 ft) long were fabricated and tested at operating temperatures from 294 to 21 K (+70 to -423°F) and operating pressures up to 259 N/sq cm (375 psi). The primary objective for the smaller sizes was thermal performance optimization of the propulsion system while the primary objective of the larger sizes was weight optimization and to prove fabricability. All major program objectives were met resulting in a design concept that is adaptable to a wide range of aerospace vehicle requirements. Major items of development included bonding large diameter aluminum end fittings to the thin Inconel liner; fabrication of a 38 cm (15 in.) diameter tube from 0.008 cm (0.003 in.) thick Inconel; and evaluation of tubing which provides essentially zero quality propellant in a very short period of time resulting in a lower mass of propellant expended in chilldown.

COMPOSITE PROPULSION FEEDLINES FOR CRYOGENIC SPACE VEHICLES

By Charles A. Hall, Daniel J. Laintz
and John M. Phillips
MARTIN MARIETTA CORPORATION

SUMMARY

This is the final report of a 16-month program that was conducted under Contract NAS3-14370. The objective of the program was to develop lightweight composite tubing and attendant fittings for use as cryogenic plumbing on space vehicles. Tubing representative of four different requirements was fabricated in sizes ranging from 5 to 38 cm (2 to 15 in.) diameter and up to 305 cm (10 ft) in length.

The smaller tubes were joined together into two separate systems representative of the Orbital Maneuvering System (OMS) liquid oxygen (LOX) and liquid hydrogen (LH_2) feed systems for the Phase B Space Shuttle configuration.

The larger 38 cm (15 in.) diameter tubes were fabricated in 305 cm (10 ft) lengths. One tube represented a section of the LOX main engine feedline and one represented a section of the LH_2 main engine feedline for the Phase B Shuttle configuration.

An analysis program assessed thermal, structural, weight and fabrication parameters and formed the basis for the tubing design. Ultimately, thin metallic liners 0.008 to 0.28 cm (0.003 to 0.011 in.) thick were selected as the primary load-carrying member. These liners were overwrapped with glass-fibers impregnated with a resin matrix suitable for cryogenic service to strengthen the liners and protect them from handling or flight dynamics damage. Concurrent with the analysis effort, preliminary tests were performed to aid in selecting materials of construction. Tensile tests were performed on composite cloth segments. Metallographic analyses evaluated the end fitting configurations to assist in the development of an explosively bonded joint between the liner and its end fitting. A preliminary 38 cm (15 in.) diameter specimen, approximately 90 cm (36 in.) long was fabricated and used as a test bed for resolution of problems with the liner fabrication and the explosive bonding of the end fitting.

Next, the 11 tubes required for test were fabricated and verified ready for test. Tube fabrication included liner welding, joining of the liners to end fittings, instrumentation installation, overwrapping and curing, and a series of in-process leak checks and other quality determinations.

The main engine tubes were subjected to a series of tests including pressure cycling, temperature cycling, torsion, bending and burst. The LOX main engine tube was destroyed during post-overwrap proof testing and the test was, therefore, limited to temperature cycling of the Inconel to aluminum joint. The failure during proof testing occurred at one of the explosive bonded aluminum end fittings to Inconel liner joints and was understandable since the joint was known to contain an unbonded area covering about 10% of the tube circumference. The tube contained two aluminum fittings, each bonded to the Inconel liner by explosives. Damage which occurred at one end while welding the completed tube into a system was repaired but residual work-hardening of the Inconel prevented a completely successful rebonding. The LH_2 tube performed very satisfactorily throughout the entire program.

The OMS tubes were subjected to a series of tests including chilldown, steady-state flow, steady-state heat input in both the insulated and uninsulated configuration, thermal and pressure cycling, radial thermal conductivity, vibration and application of pressure to failure. The OMS tubes performed satisfactorily during all tests, although small leaks created some difficulty in the high-vacuum testing.

The results of this and the earlier program[1] clearly verify the advantages of using glass-fiber composite tubing in cryogenic propellant service. Some of the advantages include low thermal flux, lightweight construction, low-heat-soakback from engines, rapid chilldown, high strength and handling ease. This can be accomplished with only a moderate increase in cost -- in many cases for less than $60 per kg ($25 per pound) of weight reduced.

Additional work is needed to more fully develop the explosive bonding concept, more adequately demonstrate the diameters used in large propulsion systems, and eliminate the leakage problems in some designs.

---

(1) C. A. Hall, T. J. Pharo, J. M. Phillips, and J. P. Gille: Low Thermal Flux Glass-Fiber Tubing for Cryogenic Service. Martin Marietta Corporation, Denver, Colorado, NASA CR-72797, March, 1971.

INTRODUCTION

In the continuing development of optimum performance cryogenic propulsion systems, there is considerable interest in the reduction of system heat gains and in minimizing total system weight. Considering the high heat leak rates through conventional tubing systems, it is desirable that techniques be developed to produce feedlines using a low heat leak material such as composites, particularly if these feedlines also contribute to weight minimization.

In a recently completed program, Contract NAS3-12047, Glass-Fiber Tubing for Cryogenic Service,[1] Martin Marietta Corporation analyzed, designed, fabricated and tested a series of composite propulsion feedlines designed to limit the heat transfer through this portion of the propulsion system. These feedlines incorporated a thin metal liner to eliminate leakage and provide compatibility with cryogenic propellants. These thin metal liners were overwrapped with a glass-fiber material using a suitable matrix. Because the glass-fiber overwrap is a very good thermal insulator and the thin metal liner has a very small cross-sectional area, the thermal conductivity was reduced considerably in both radial and longitudinal directions. Program results confirm the desirability of this concept. Some of the advantages, in addition to low radial and axial thermal flux, are lightweight construction, low axial heat-soakback from engines or vaporizers, rapid chilldown, strength, and resistance to handling damage.

The 0.10 cm (0.040 in.) minimum wall thickness used for all-metal feedlines in a great majority of propulsion systems is dictated by handling and maintainability, not stresses. For example, an Inconel 718 or stainless steel tube with a 0.003 cm (0.001 in.) wall thickness could carry all internal pressure loads for many propulsion feedlines and tank vents but could not be handled without incurring damage. Since composite tubing can be fabricated with the metal liner wall thickness near 0.003 cm (0.001 in.) and the handling and maintenance requirements can be met with a material having a low density and a low thermal conductivity, lighter feedlines with reduced thermal flux characteristics result.

Several problems must be solved before lightweight low thermal flux tubing can be used on a space vehicle such as the Space Shuttle. The solution of these problems for the main engines, Orbiter Maneuvering System (OMS) engines, and the Attitude Control Propulsion System (ACPS) cryogen plumbing was the intent of this program. The objective of the work was to design, fabricate, and evaluate glass-fiber composites for both the OMS and the main engine feedline systems for application on the MDAC/MMC Phase B Space Shuttle vehicle configuration as developed under Contract NAS8-26016. Tubing specimens were designed, fabricated and subjected to various portions of the specified test program. The Phase B Shuttle

configuration, as of 1 July 1971, was considered as the baseline, and although this baseline includes a cryogenic OMS system which has since been deleted, the technology developed will be applicable to any cryogenic system of similar size.

The program consisted of two technical tasks, Task I - OMS Feedlines, and Task II - Main Engine Feedlines. Each of these tasks consisted of system design, analysis, test item and fixture fabrication, testing and analysis of results. Specific items that were performed to accomplish the program objectives included:

1) Selecting a set of boundaries for analysis and for use as design parameters;

2) Modifying existing analytical models to incorporate the analysis of glass-fiber overwrapped, metal-lined tubing;

3) Using the analytical models to assist in the design of the metal-lined tubing including the selection of an optimum location for the tubing, selection of thermal barriers, effects of various temperatures at each end of the tubing, system weight and overall system performance;

4) Designing the test items using several designs to simulate the main engine and the OMS feedline;

5) Fabricating the 38 cm (15 in.) diameter main engine feedlines and the 5 to 9.4 cm (2 to 3.7 in.) diameter OMS feedlines;

6) Testing the tubing to determine its capability to withstand the necessary flight loads and requirements;

7) Correlating the experimental and analytical data to show the capability of the analytical model to predict the tubing performance; and

8) Reporting future modifications or changes that would be incorporated into flight-qualified feedlines.

The first effort consisted of selecting the candidate feedlines; performing thermal, structural, weight and fabrication analyses; and designing the test items and test fixtures.

Tube fabrication followed the design phase and included liner welding, joining of the liners to end fittings, instrumentation installation, overwrapping and curing, and a series of in-process leak checks. Much of the metal fabrication was subcontracted to highly experienced thin metal bellows manufacturers. The test fixtures were fabricated concurrent with this effort. The fabrication effort included the following:

5 sections of LH_2 OMS tubing;

4 sections of LOX OMS tubing;

1 section of LH_2 main engine tubing; and

1 section of LOX main engine tubing.

For the OMS tubing, a series of thermal performance tests including chill-down, steady-state heat input, radial thermal conductivity, and heat capacity were performed. Thermal and pressure cycling, vibration and burst tests were also performed. The LH_2 main engine test item was subjected to structural testing including thermal cycles, pressure cycles, bending cycles, torsion cycles, and burst. The LOX main engine test item was only subjected to a proof test and thermal cycles.

A complete analysis of the fabrication and test data was performed to document the effectiveness, cost, reliability, and desirability of glass-fiber composite tubing for cryogenic space vehicle applications. Structural integrity and thermal quality were evaluated and compared to the predicted performance. Recommendations for design improvements based on the above comparison were established. The design criteria established in the initial design phase were updated as indicated by the data analysis.

All major program objectives were accomplished resulting in a usable concept for effectively reducing thermal inputs and weight of propulsion systems.

DATA REVIEW AND BASELINE DEFINITION

The specific objectives of this program were to analyze, design, fabricate and test cryogenic feedlines for space vehicles. The Phase B Space Shuttle configuration as of 1 July 1971 was defined as the baseline for these activities.

The configuration and performance requirements of the shuttle propellant feed systems were determined by a detailed review of the Phase B reports from the McDonnell Douglas/Martin Marietta contract studies on the Space Shuttle Vehicle. The primary sources of information were the Part II-2(A) Technical Summary[2] and Part II(A) Detail Mass Properties[3] reports for the orbiter and the Part II-3 Technical Summary[4] and Part III(B) Detail Mass Properties[5] reports for the booster. The information listed below was obtained from this review and was used as criteria for the feedline designs:

1) Engine starts per mission:
   Booster and orbiter main engines - 1 each,
   OMS engines - 10,
   ACPS pressurization - multiple;

2) Cooldown techniques:
   Booster and orbiter main engines - wet, fill through feedline, active recirculation system,
   OMS engines - LH_2, thermodynamic vent cooling,
   LOX, recirculation plus 0.75% of full flow to cooldown pump and line,
   ACPS - LH_2 and LOX, thermodynamic vent cooling;

3) Time allowed to obtain start quality:
   Since the OMS burns are long, usually 100 to 200 seconds, a fairly long cooldown time of 2 to 3 minutes will be permissible although not desirable;

4) Flowrates:

   OMS - LH_2, 5.1 kg/sec (11.2 lb/sec) or 2.5 kg/sec (5.6 lb/sec)
   LOX, 25.6 kg/sec (56.4 lb/sec) or 12.8 kg/sec (28.2 lb/sec)

   ACPS - LH_2, 6.6 kg/sec (14.6 lbs/sec)
   LOX, 20.6 kg/sec (45.4 lbs/sec)

   Booster main engine -
   LH_2, 97 kg/sec (214 lb/sec) in each engine duct
   LOX, 3498 kg/sec (7716 lb/sec) in each of two lines

Orbiter main engine -

LH_2, 194 kg/sec (428 lb/sec)

LOX 1178 kg/sec (2572 lb/sec);

5) Line environment - temperature profile for a mission:

Orbiter - on-orbit nominal external temperature = 283 K ($50^{o}F$)

Booster - wet, maximum for checkout, etc. 339 K ($150^{o}F$)

6) System pressures (tank top):

OMS and ACPS -

LH_2, 22 N/sq cm (32 psi)

LOX, 28 N/sq cm (41 psi)

Booster main engine -

LH_2, 19 N/sq cm (28 psi)

LOX, 13.5 N/sq cm (19.5 psi)

Orbiter main engine -

LH_2 and LOX, 19 N/sq cm (28 psi).

Other data required for analytical models were also obtained by this review and are listed in Appendix A of this report. Data not available in the Phase B reports were developed as required during the program.

SELECTION OF CANDIDATE SYSTEMS AND COMPARISON WITH SHUTTLE REQUIREMENTS

The following orbiter and booster propellant feed systems from the MDAC/MMC Phase B Space Shuttle vehicle configuration as developed under Contract NAS8-26016, were chosen as candidate systems.

Orbiter:

- Main Engine LOX Feedline
- Main Engine LH_2 Feedline
- OMS LOX Feedline
- OMS LH_2 Feedline
- ACPS LOX Feedline
- ACPS LH_2 Feedline

Booster:

- Main Engine LOX Feedline
- Main Engine LOX Feed Ducts
- Main Engine LOX Fill and Drain
- Main Engine LH_2 Feed Ducts
- Main Engine LH_2 Fill and Drain
- APU Exhaust Ducts

Candidate systems were chosen as those systems which afforded the largest total system weight savings, including consumables, and met the temperature and pressure constraints for composite tubing as developed under NAS3-12047.

The work performed does not include finalized detailed designs of the feedline systems but rather conceptual designs sufficient to determine the configuration; including bends, size, length, etc., and the location of pumps, engines, tanks, bellows, and etc. Configuration layouts and detail specifications on lengths and diameters are included in Appendix B of this report.

The Phase B study configuration as baselined for the activity in this contract includes a cryogenic OMS and ACPS. The current baseline includes an earth storable propulsion system for these requirements. A vehicle which will probably utilize LOX and LH_2 as propellants is the Space Tug. The Baseline Tug Definition Document[6], Rev. A, shows a cryogenic propulsion

system with feedlines configured approximately as shown in Figure 1. A comparison of working pressures and diameters between this program and the Tug is shown in Table 1. The similarities are evident and the need for lightweight, thermally efficient feedlines is well established.

The main engine feedlines and auxilliary lines for the Phase B study are similar to the currently proposed configuration. The major system change to expendable cryogenic tanks has not altered the generalized concept for the fill and drain lines, the LOX feedline which is currently abour 43 cm (17 in.) diameter, or the 10 cm (4 in.) LOX recirculation line. The LH_2 pressurization and vent line is currently about 25 cm (10 in.) diameter and exceeds 33 meters (100 ft) in length. A major portion of the LH_2 feedline is currently located inside of the LH_2 tank but it may still be a candidate for composites.

Figures 2, 3 and 4 depict a typical external tank plumbing configuration. This configuration is subject to considerable change as a result of trade studies and the selection of a contractor for the external tanks. Table 2 shows the details of the various lines and potential weight reduction based upon this one configuration.

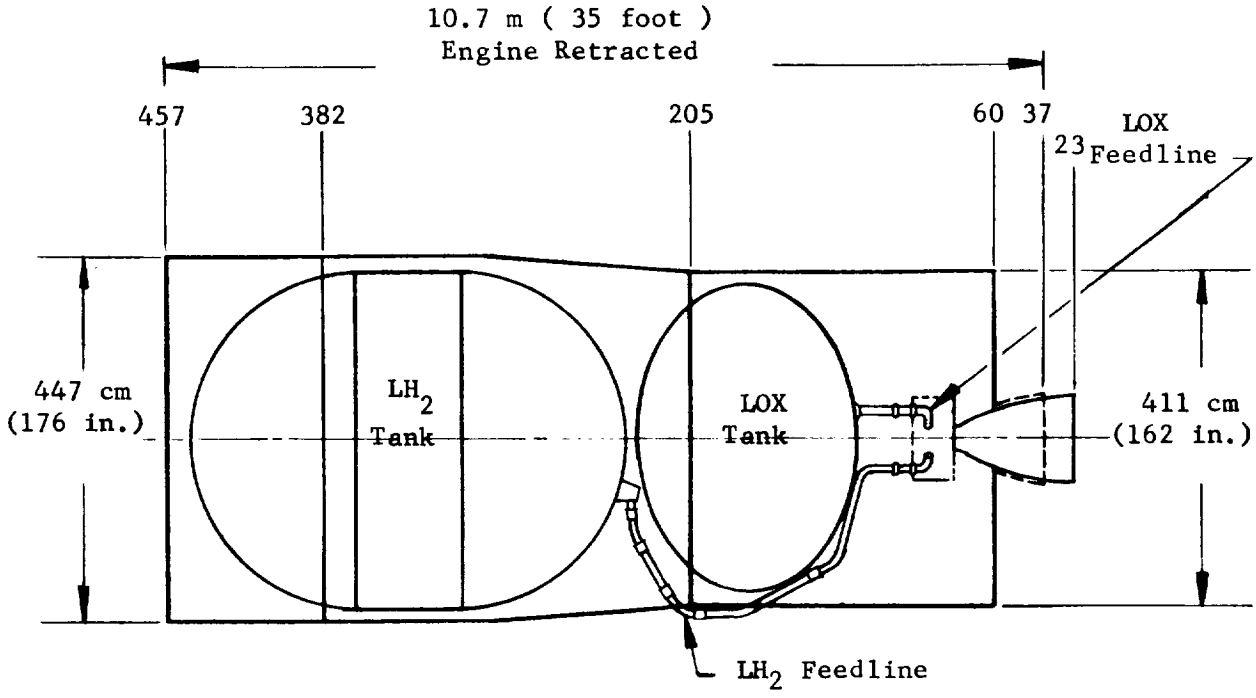

Figure 1. - Baseline Tug Overall Configuration

TABLE 1. - FEEDLINE REQUIREMENTS COMPARISON-BASELINE SPACE TUG vs NAS3-14370

Description	Baseline Space Tug	Baseline NAS3-14370
Line Diameter - LOX (cm)	7.4	7.9 - 9.4
Line Diameter - LH_2 (cm)	6.1	5.1 - 6.4
Working Pressure* - LOX (N/sq cm)	21	45
Working Pressure* - LH_2 (N/sq cm)	21	31
Required Thermal Efficiency	Good	Good
Chilldown - Conditioning - LH_2	Recirculating System to Maintain Cold Line	Need Rapid Chilldown and Low Thermal Characteristics
Chilldown - Conditioning - LOX	None	Recirculating System to Maintain Cold Line

* Includes head and 3g Acceleration for the Space Tug. The numbers are approximate.

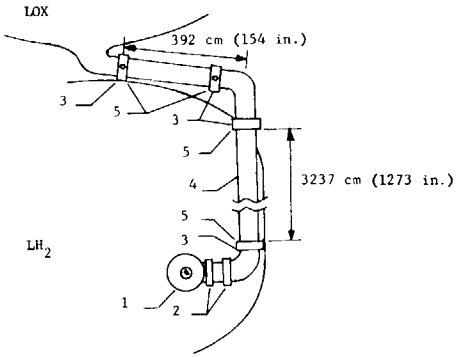

LOX Feedline

LEGEND - ALL-METAL LINES

1 - Disconnect Valve

2 - Gimbal Joint

3 - Pin Joint

4 - Line-Aluminum (2219) 43 cm (17 in.) Diameter x 0.355 cm (0.140 in.)

5 - Flange Joint (Aluminum to Stainless Steel)

COMPOSITE LINE LEGENDS

1 - Line, 392 cm (154 in.) long = 392 cm (154 in.)

6 - Lines, 539 cm (212 in.) long = 3234 cm (1272 in.)

TOTAL: 3626 cm (1426 in.)

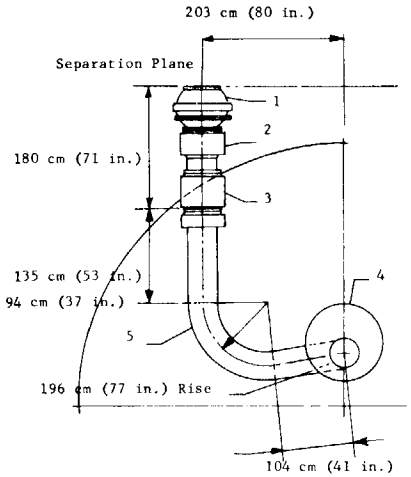

LH_2 Feedline

LEGEND - ALL-METAL LINES

1 - Disconnect Valve

2 - Bellows

3 - Tank Fitting

4 - Siphon Inlet

5 - Line - Stainless Steel (304) 43 cm (17 in.) Diameter x 0.254 cm (0.100 in.) Wall

COMPOSITE LINE LENGTHS

1 - Line, 128 cm (48 in.) long = 122 cm (48 in.)

1 - Line, 109 cm (43 in.) long = 109 cm (43 in.)

1 - Line, 76 cm (30 in.) long = 76 cm (30 in.)

TOTAL: 307 cm (121 in.)

Figure 2. - Proposed External Tank Plumbing Configurations - Feedline

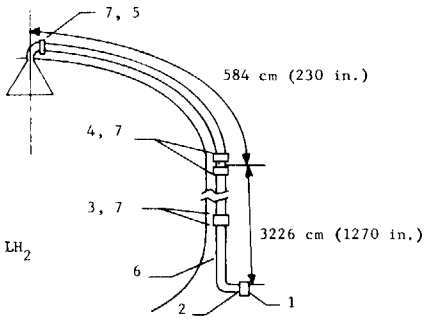

LH_2 Pressure Line

LEGEND - ALL-METAL LINES

1 - Disconnect Valve

2 - Gimbal Joint

3 - Pin Joint

4 - Sliding Bellows

5 - Bellows

6 - Line-Aluminum (2219) 25 cm (10 in.) Diameter x 0.160 cm (0.063 in.) Wall

7 - Flange Joing (Aluminum to Stainless Steel)

COMPOSITE LINE LENGTHS

2 - Lines, 292 cm (115 in.) long = 584 cm (230 in.)

11- Lines, 293 cm (115.5 in.) long = 3226 cm (1270 in.)

1 - Line, 117 cm (46 in.) long = 117 cm (46 in.)

1 - Line, 84 cm (33 in.) long = 84 cm (33 in.)

TOTAL: 4011 cm (1579 in.)

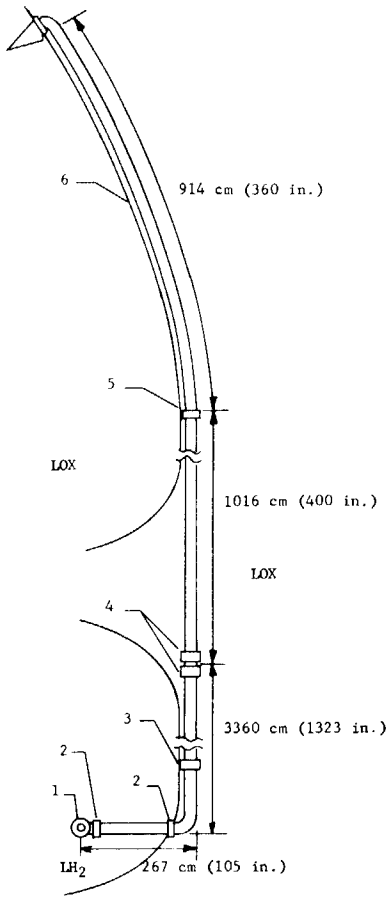

LOX Pressure Line

LEGEND - ALL-METAL LINES

1 - Disconnect Valve

2 - Gimbal Joint

3 - Pin Joint

4 - Sliding Bellows

5 - Bellows

6 - Line-Steel (304) 15 cm (6 in.) Diameter x 0.117 cm (0.046 in.) Wall

COMPOSITE LINE LENGTHS

3 - Lines, 305 cm (120 in.) long = 914 cm (360 in.)

3 - Lines, 338 cm (133 in.) long = 1014 cm (399 in.)

11- Lines, 305 cm (120 in.) long = 3353 cm (1320 in.)

1 - Line, 244 cm (96 in.) long = 244 cm (96 in.)

TOTAL: 5525 cm (2175 in.)

Figure 3. - Proposed External Tank Plumbing Configurations - Pressure/Vent Lines

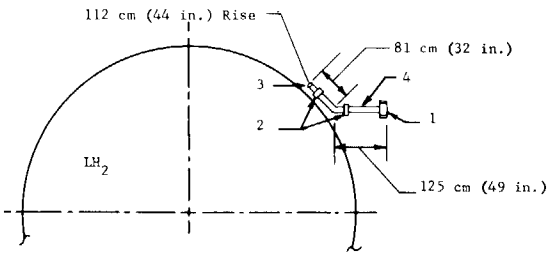

LH_2 Recirculation Line

LEGEND - ALL-METAL LINES

1 - Disconnect Valve

2 - Gimbal Joint

3 - Pin Joint

4 - Line-Steel (304
10 cm (4 in.) Diameter x
0.165 cm (0.065 in.) Wall

COMPOSITE LINE LENGTHS

1 - Line, 112 cm (44 in.) long =
112 cm (44 in.)

1 - Line, 81 cm (32 in.) long =
81 cm (32 in.)

1 - Line, 125 cm (49 in.) long =
125 cm (49 in.)

TOTAL: 318 cm (125 in.)

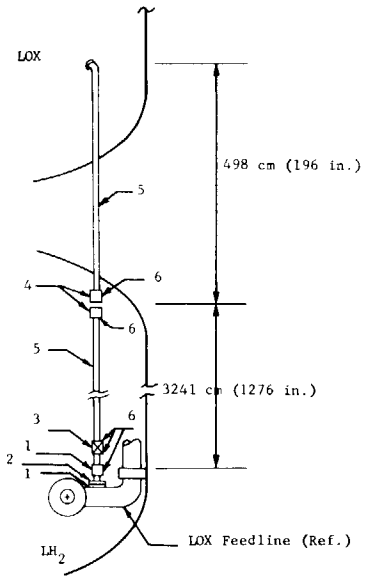

LOX Recirculation Line (Anti-Geysering)

LEGEND - ALL-METAL LINES

1 - Gimbal Joint

2 - Sliding Bellows (Welded)

3 - Shutoff Valve

4 - Sliding Bellows

5 - Line-Aluminum (2219)
10 cm (4 in.) Diameter x
0.318 cm (0.125 in.) Wall

6 - Flange Joint (Aluminum to
Stainless Steel)

COMPOSITE LINE LENGTHS

2 - Lines, 249 cm (98 in.) long =
498 cm (196 in.)

11 - Lines, 295 cm (116 in.) long =
324 cm (1276 in.)

TOTAL: 3739 cm (1472 in.)

Figure 4. - Proposed External Tank Plumbing Configuration - Recirculation Links

Table 2.- DROP TANK LINE CONFIGURATIONS [Proposed & Preliminary]

Description	Diameter		Length		Working pressure		Working Temperature		Current Weight		Composite Weight	
	cm	in	m	ft	N/sq cm	psi	K	F	kg	lb	kg	lb
LOX Feedline	43	17	36	118	172	250	91 to 347	-297 to 165	522	1150	243	535
LOX Pressurization	15	6	55	181	21	30	91 to 667	-297 to 740	248	546	113	249
LOX Recirulation	10	4	38	123	172	250	91 to 347	-297 to 165	119	261	52	114
LH_2 Feedline	43	17	3	10	32	46	21 to 347	-423 to 165	127	280	44	96
LH_2 Press. & Vent	25	10	40	131	31	45	21 to 445	-423 to 340	201	443	139	307
LH_2 Pressurization	13	5	40	131	31	45	21 to 445	-423 to 340	183	403	101	223
LH_2 Tank Recirculation	10	4	3	10	41	60	21 to 347	-423 to 165	32	70	12	27

NOTE: The weight reduction indicated by this table is based on the following assumptions:

- o Only the straight or slightly curved sections of the lines will be replaced by composite lines.
- o The weights shown include no components such as bellows, sliding joints, etc.
- o E glass is used for the composite line overwrap material.
- o The minimum wall thickness for the current lines is 0.117 cm (0.046 in.).
- o A high temperature overwrap can be developed for the LOX pressurization lines.
- o The LH_2 pressurization and vent line may be combined as a single line or the vehicle vents may proceed immediately to the ground based equipment. In the latter case, only pressurization sizing will be required.

ANALYSIS

The purpose of the analytical effort was to develop the techniques required to predict the performance of the metal-lined glass-fiber composite feedlines and to establish criteria for the feedline design. All analyses were based on information and criteria developed by the Phase B Space Shuttle studies.

The ultimate objective of this program is to increase the payload capability of the Space Shuttle vehicle. This objective can be accomplished by reducing the weight of the propulsion system components and by limiting the propellant lost due to boiloff and overboard bleed during feedline cooldowns. The analysis activity during the program was, therefore, directed at the following items:

1) Propellant expended in cooling feedlines prior to engine restarts;

2) Boiloff of propellants due to radial heat input and conduction down the feedline;

3) Flange and/or connector design and weights;

4) Basic feedline structural weight;

5) Weight of insulation necessary on or in the feedline;

6) Weight of a vacuum jacket;

7) Effect of the number of feedline fills required for system restarts;

8) Weight of the pressurization system as a function of pressure drop;

9) Various planned flowrates.

The analysis performed in this program predicted the thermal characteristics and the structural requirements of the OMS, ACPS and main engine feedlines. The analyses performed and the results obtained are summarized in the following paragraphs.

Steady-State Heat Input Analysis. - The purpose of this analysis was to determine the propellant loss due to boiloff from the feedline filled with liquid oxygen or liquid hydrogen. This analysis was performed on the flight configuration of the OMS LOX and LH_2 feedlines and on the test configuration of the OMS LOX feedline. The mass of the engine at the feedline outlet and the mass of a flow initiating valve in the feedline were included in the analysis for each condition.

OMS LOX flight configuration: This analysis was performed on the flight configuration of the OMS LOX feedline for each of the following conditions:

1) Bare line - all-metal -- emissivity (e) reflective;

2) Bare line - composite -- (e) not reflective;

3) Insulated line - all-metal;

4) Insulated line - composite;

5) Vacuum jacketed line - all-metal;

6) Vacuum jacketed line - composite;

7) Insulated and vacuum jacketed line - all-metal;

8) Insulated and vacuum jacketed line - composite.

This feedline has a length of 1130 cm (446 in.) with a diameter of 6.7 cm (2.6 in.) and a length of 280 cm (110 in.) with a diameter of 5.5 cm (2.1 in.). The smaller diameter line is connected to the engines. The configuration of this feedline is shown in Figure B-2 of Appendix B.

The following operating conditions and requirements were considered for this analysis:

1) The section of feedline next to the engine was assumed to be dry to incorporate thermal resistance in the system;

2) A mission duration of 200 hours;

3) Nominal environmental temperature of 294 K ($70^{o}F$) which intercepts the temperatures used in the Space Shuttle studies where the hot case was 317 K ($110^{o}F$) and the cold case was 278 K ($40^{o}F$);

4) The temperature of liquid oxygen was set at 91 K ($-296^{o}F$) and the heat of vaporization as 213 joules/g (91.7 Btu/lb);

5) Feedline wall thickness of 0.041 cm (0.016 in.).

Values of the heat transfer rate to the propellant were determined for the hot, cold and nominal cases for each feedline condition. These values are plotted in Figure 5 for the uninsulated all-metal and composite feedline dry end sections.

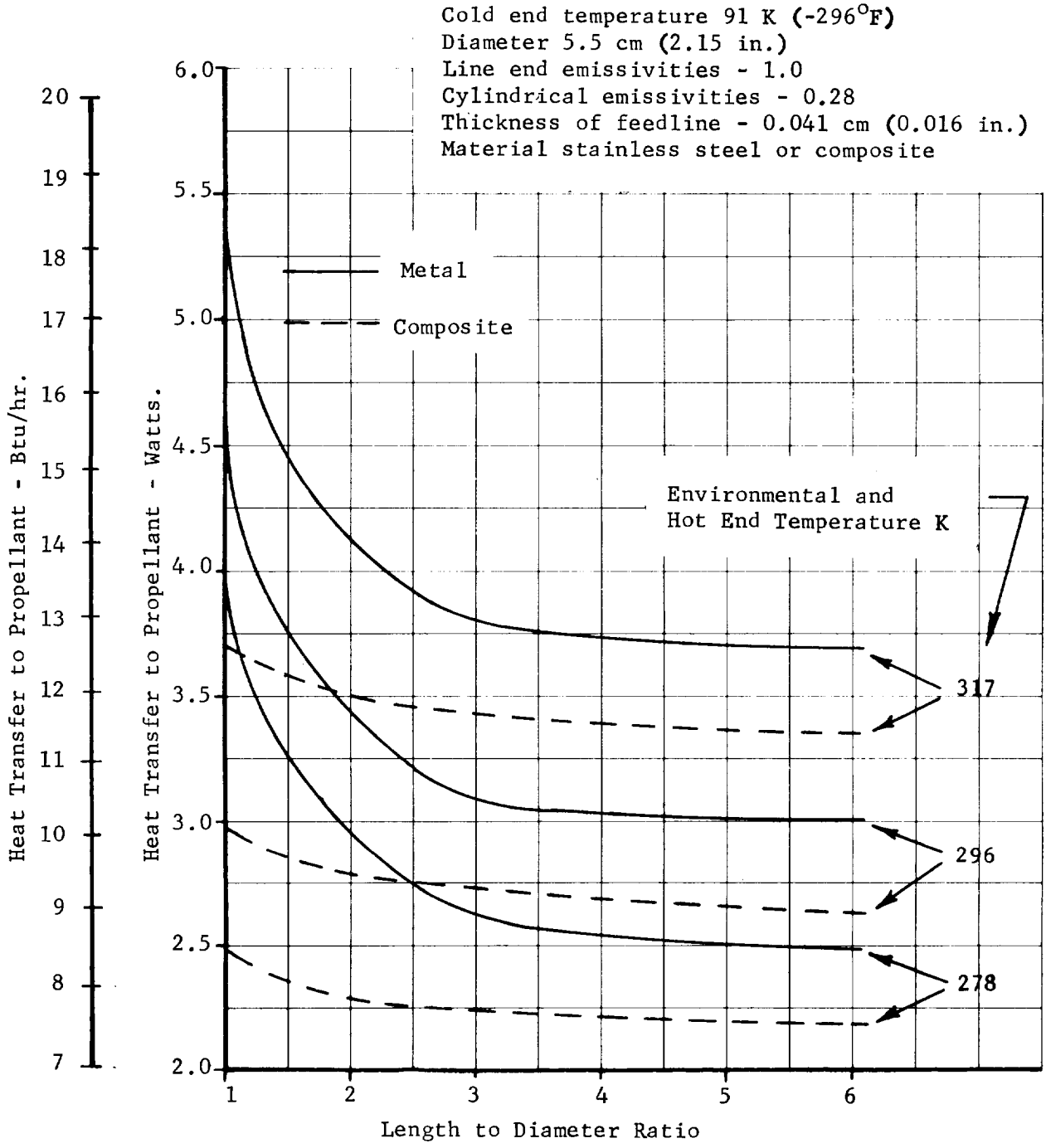

Figure 5. - Heat Transfer to Liquid Oxygen for Bare All-Metal and Composite Feedline End Sections

After the heat transferred to the propellant by the system heat leaks was determined, the propellant boiloff due to these heat leaks was calculated. A summary of the propellant boiloff for the OMS LOX feedline is shown in Table 3. The analysis shows that the radial losses of the bare composite feedline are higher than the losses of the all-metal feedline which is due to the high emissivity of the overwrap surface. The emissivity can be reduced by adding one layer of double aluminized mylar to the composite feedline. This will make the radial loss comparable to the all-metal loss with no significant weight penalty. The end losses were determined using an all-metal feedline wall thickness of 0.041 cm (0.016 in.) which is the minimum gage used in the Phase B shuttle studies. This wall thickness is probably not practical when viewed from a fabrication and installation standpoint. A more practical wall thickness would be 0.008 - 0.10 cm (0.030 - 0.040 in.) for the all-metal line and a 0.013 cm (0.005 in.) liner with a 0.05 cm (0.020 in.) overwrap for the composite line. This increased wall thickness would double the end losses for the all-metal feedline and result in some additional loss for the composite feedline. The values in Table 3 have been corrected for this change.

OMS LOX test configuration: The analysis was also performed on the test configuration of the OMS LOX feedline for the following conditions:

1) Uninsulated -- emissivity non-reflective; and

2) Insulated -- emissivity reflective thru insulation but unpolished glass on feedline.

The feedline configuration used for the analysis is shown in Figure 6. The boiloff rate for the feedline in an uninsulated condition was 0.007 m^3/hr (1.89 gal/hr) if complete contact of the liner with the overwrap was assumed. If partial contact (50%), as discussed in Appendix C, was assumed, the boiloff rate was 0.006 m^3/hr (1.6 gal/hr). With one layer of double aluminized mylar wrapped around the tube the boiloff rate was reduced to 0.0024 m^3/hr (0.63 gal/hr) and with 20 layers of double aluminized mylar the boiloff was 0.0014 m^3/hr (0.37 gal/hr).

OMS LH_2 flight configuration: This analysis was performed on the flight configuration of the OMS LH_2 feedline for each of the following conditions:

1) Vacuum jacketed line - all-metal;

2) Vacuum jacketed line - composite;

3) Insulated and vacuum jacketed line - all-metal;

4) Insulated and vacuum jacketed line - composite.

TABLE 3. - SUMMARY OF PROPELLANT LOSSES DUE TO BOILOFF FOR OMS LOX FEEDLINE

Config-uration	Feed-line Type	Thermal System	Insulation Loss		†Feedline End Loss		Vacuum Jacket Support Loss		Insulation Joint Loss		Total	
			kg	lb	kg	lb	kg	lb	kg	lb	kg	lb
LOX OMS Flight System	All-metal	Bare Line	e_s = .28		L/D = 3						1179	2593
			1135	2500	42	93						
		Insulated Line	52	115	L/D = 6				2	5	68	150
					14	30						
		Vacuum Jacket No Insulation	e_s = .026		*L/D = 6		106	234			283	623
			99	218	29	65						
		Vacuum Jacket Insulation	63	139	L/D = 6		106	234	2	5	234	514
					14	30						
	Composite	Bare Line	e_s = .85		L/D = 3						2061	4535
			2028	4468	30	69						
		One Layer MLI	e_s = .026		L/D = 6						108	238
			93	205	15	33						
		Insulated Line	52	115	L/D = 6				2	5	60	132
					5	12						
		Vacuum Jacket No Insulation	e_s = .026		*L/D = 6		106	234			263	578
			93	205	15	33						
		Vacuum Jacket Insulation	63	139	L/D = 6		106	234	2	5	225	496
					5	12						

NOTE: e_s = Surface Emissivity of Feedline

L/D = Length to Diameter Ratio of Feedline End, Dry Section

* = Boiloff Includes Wet Section Equal to Dry Section

† = Feedline End Loss Includes Two Engines

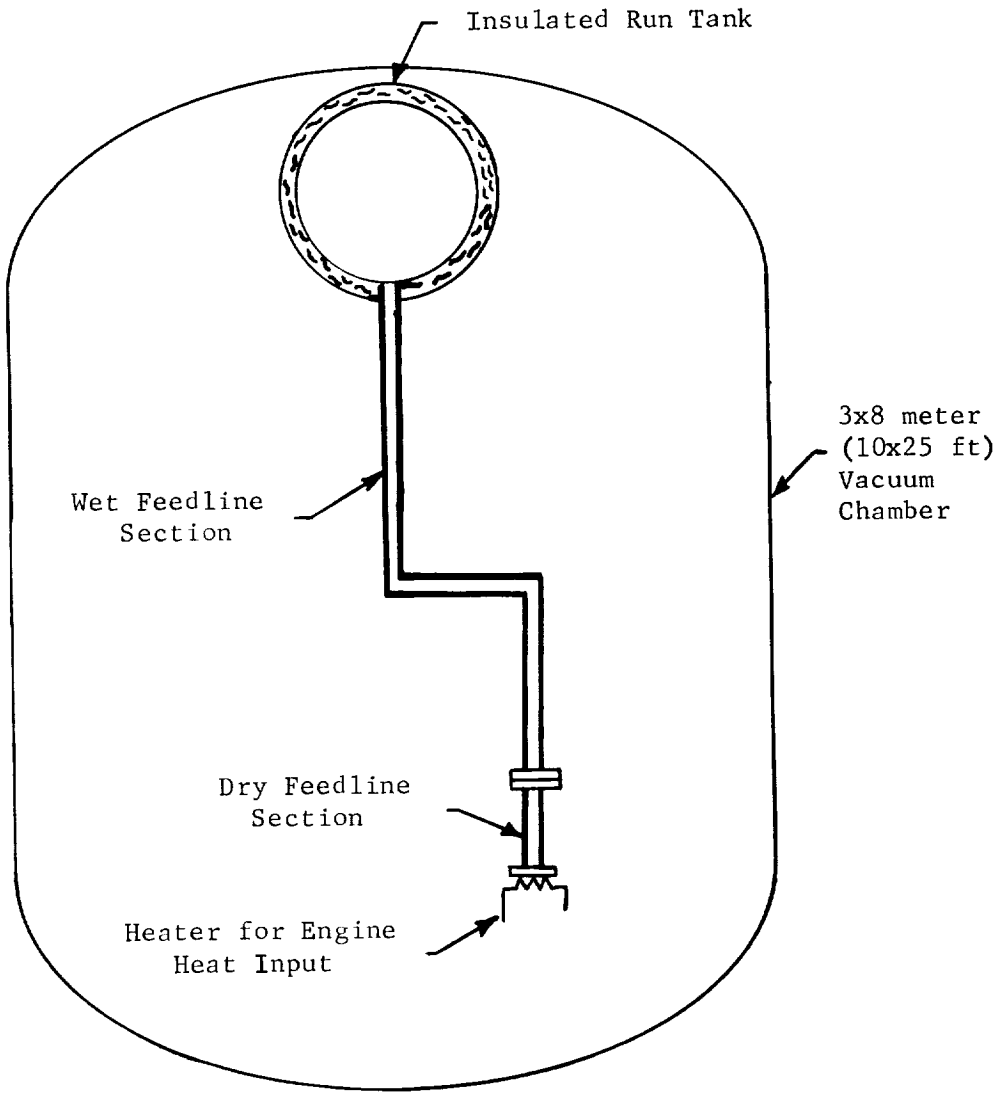

Figure 6. - LOX Test Item Installed
in Vacuum Chamber

Since no steady-state heat input tests were planned for the LH_2 line, the test configuration was not analyzed. The mass of the engine at the feedline outlet and the mass of a flow initiating valve in the feedline were included in the analysis for each condition.

The analysis for the LH_2 feedline was performed using the same methods, equations and assumptions that were used in the LOX feedline analysis. The system analyzed was the OMS LH_2 flight configuration. This feedline has a length of 2425 cm (955 in.) with a diameter of 9.9 cm (3.9 in.) and a length of 1885 cm (742 in.) with a diameter of 7.9 cm (3.1 in.). The smaller diameter line is connected to the engines. This feedline configuration is shown in Figure B-1 of Appendix B.

The operating conditions and requirements considered for the analysis of this feedline were similar to those considered for the LOX feedline. The end heat leaks for this line are plotted in Figure 7 for the all-metal and composite feedlines in the insulated and jacketed condition. A summary of the propellant boiloff for the OMS LH_2 feedline is shown in Table 4.

A detailed presentation of the steady-state heat input analysis is presented in Appendix D of this report.

OMS Feedline Valve Placement. - An analysis was performed to determine the optimum valve placement for the OMS propellant feed systems. One option included a valve at the tank outlet, defined as a dry feedline concept, and the other option included a valve at the engine inlet defined as a wet feedline concept. The purpose of this analysis was to define the wet and dry proportions of the feedlines considering feedline configurations, various insulation conductivities, mission duration, and number of engine burns.

Generally, efficient tank storage requires long, low heat leak penetrations such as a dry, evacuated and low wall conductance feedline. Conversely, a large number of orbital engine burns dictates a wet feedline for minimum propellant losses. These two opposing requirements establish the need for a trade study to define their relative importance. The approach taken was to trade the boiloff weights of a wet feedline against the cooldown requirements of a dry feedline for several different concepts and insulation conductivities. For this activity three styles were evaluated. The first was a conventional stainless steel tube with a wall 0.08 cm (0.030 in.) thick. The second was a composite concept conforming to the designs specified in this contract with an 0.008 cm (0.003 in.) thick liner, and the third was an advanced internal insulation concept having a 0.0025 cm (0.001 in.) mylar inner wall (a detailed description of this concept is included on page 36).

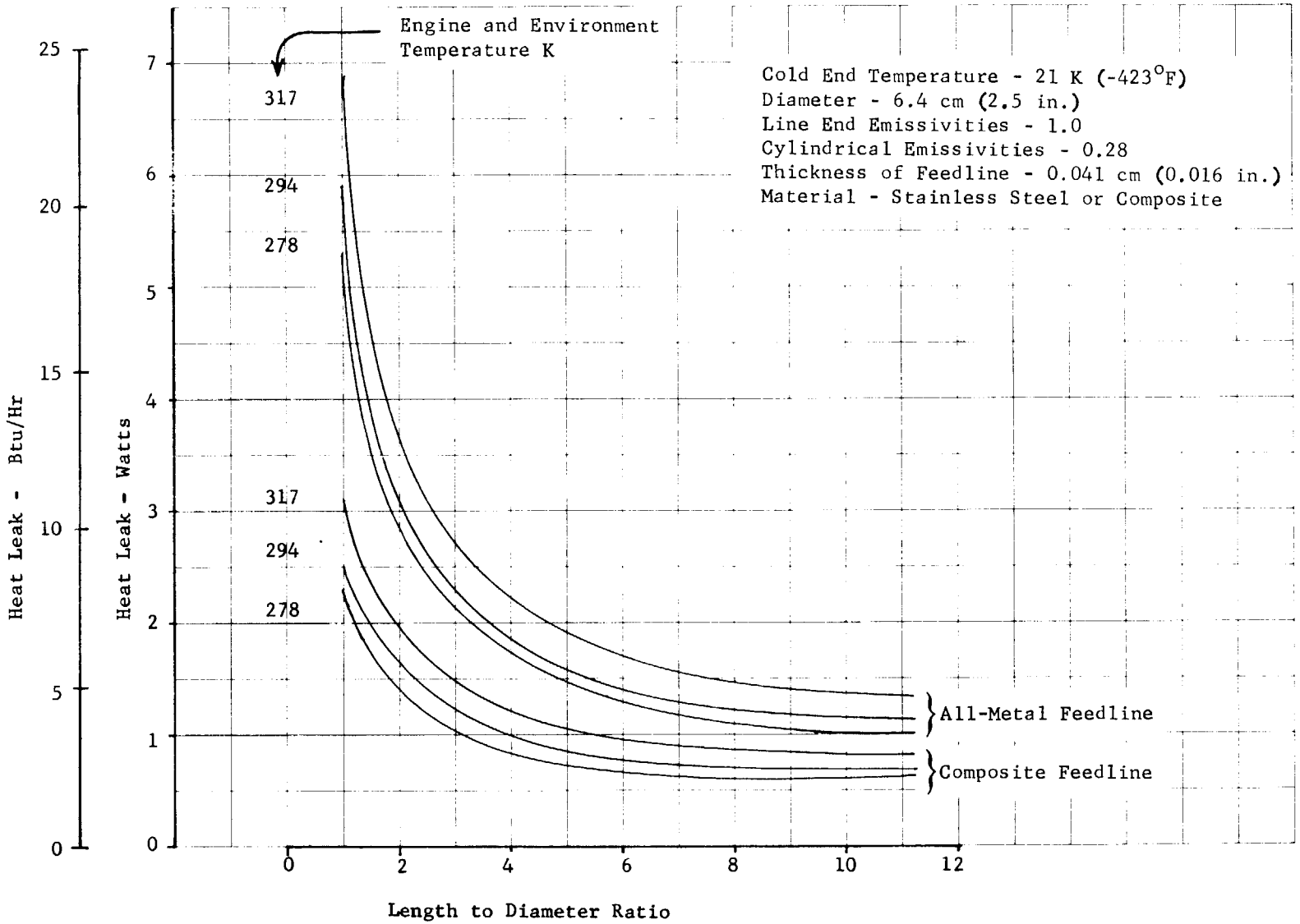

Figure 7. - End Heat Leaks for the LH_2 Insulated and Vacuum Jacketed Feedlines

TABLE 4. - SUMMARY OF PROPELLANT LOSSES DUE TO BOILOFF FOR OMS LH_2 FEEDLINE

Configuration	Feedline Type	Thermal System	Radial Loss		Feedline End Loss †		Vacuum Jacket Support Loss		Insulation Joint Loss		Total	
			kg	lb	kg	lb	kg	lb	kg	lb	kg	lb
LH_2 OMS Flight System	All-metal	Vacuum Jacket (No Insulation)	337	743	*10	*21	147	325	--	--	494	1089
		Vacuum Jacket (With Insulation)	150	331	5	10	147	325	8	17	310	683
	Composite	Vacuum Jacket (No Insulation)	329	726	*8	*17	147	325	--	--	484	1068
		Vacuum Jacket (With Insulation)	150	331	3	6	147	325	8	17	308	679

e = Surface Emissivity of Feedline = 0.28
L/D = Length to Diameter Ratio of Feedline Dry Section = 6
* = Boiloff Includes Wet Section Equal to Dry Section
† = Feedline End Loss Includes Two Engines

A typical cryogenic feed system of the type used for this analysis is shown in Figure 8.

The analysis first determined the relationship between the cooldown flowrate and the cooldown time per unit length of dry line. The cooldown time and quantity of propellant expended for a given feedline length was then determined as a function of the flowrate. This data is presented in Tables 5 and 6 for a 5 cm (2 in.) inside diameter vacuum jacketed feedline for both LOX and LH_2.

Cooldown flowrate in the OMS system will be a transient value and depends upon engine flow restriction and/or overboard bleed line sizes. Since this transient flow analysis was beyond the scope of this study, a flowrate of 0.23 kg/sec (0.5 lb/sec) was chosen for the LH_2 and LOX feedlines. This flowrate gave the quantity of cooldown propellants shown in Figure 9 for varying feedline lengths and configurations.

The days of mission time required for the boiloff losses of a wet system to exceed the cooldown requirements of a dry system are summarized in Table 7 for a mission consisting of 10 cooldowns.

The weight sensitivity to the number of cooldowns is directly proportional. Five cooldowns would require half the weight and time listed in Table 7 and 20 cooldowns twice the weight and time.

It is important to note that no recirculation system weights have been added to the total weight evaluation. Since these weights can be substantial for wet systems, their addition should be analyzed before selecting the wet concept. Also, a feedline using the internal insulation concept would have to be of a larger diameter to provide the same flow area. This would add additional weight to the propellant feed system and would require more space in the vehicle.

The results of this analysis show that the composite feedlines could be dry for a variety of missions. For example, Table 7 shows that, if a mission requiring 10 cooldowns were to extend over 4 days, the LH_2 feedline should be dry and if the mission would extend over 24 days, both systems should be dry. For a mission of this type, the LH_2 thermodynamic vent cooling system and the LOX recirculating systems would not be required resulting in a considerable increase in payload capability.

A detailed presentation of the techniques used in this analysis and the assumptions made is included in Appendix D of this report.

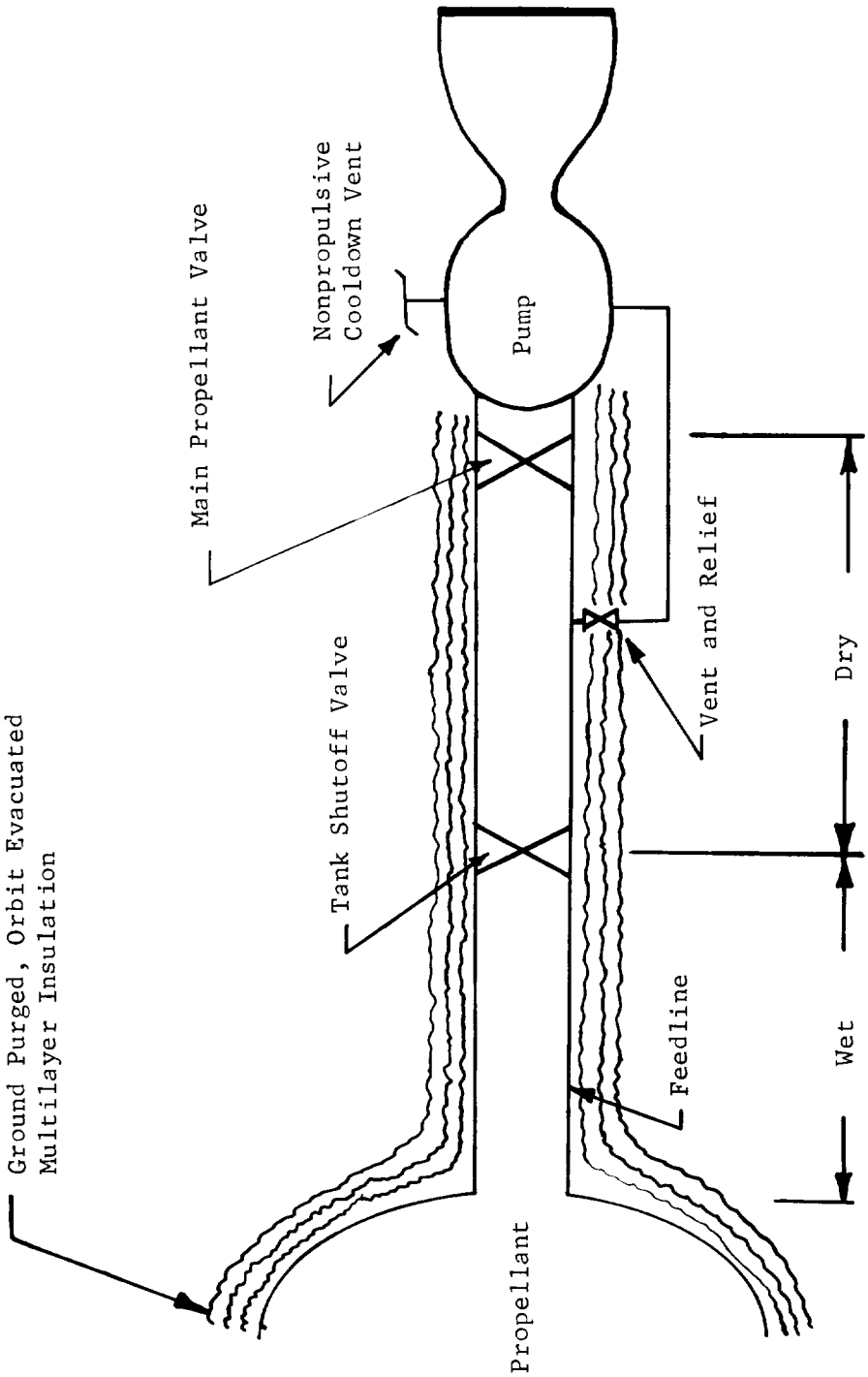

Figure 8. - Diagram of a Typical Cryogenic Propulsion Feed System

TABLE 5. - COMPARISON OF TOTAL PROPELLANT EXPENDED WITH FLOWRATE, COOLDOWN TIME, AND FEEDLINE TYPE - LOX

Flowrate		Feedline * Type	Cooldown Time (sec.)	Propellant Expended	
g/sec	lb/sec			kg	lb
1360	3.00	Stainless Steel	100	136	300
		Composite	10	14	30
		Mylar	1.7	2	5
590	1.30	Stainless Steel	200	118	260
		Composite	20	12	26
		Mylar	3.3	2	4
363	0.80	Stainless Steel	300	109	240
		Composite	30	11	24
		Mylar	5.0	2	4
136	0.30	Stainless Steel	600	82	180
		Composite	60	8	18
		Mylar	10	1	3
77	0.17	Stainless Steel	1000	77	170
		Composite	100	8	17
		Mylar	16.7	1	3

* 5 cm (2 in.) diameter vacuum jacketed feedline 1410 cm (556 in.) in length.

TABLE 6. - COMPARISON OF TOTAL PROPELLANT EXPENDED WITH FLOWRATE, COOLDOWN TIME, AND FEEDLINE TYPE - LH_2

Flowrate		Feedline * Type	Cooldown Time (sec.)	Propellant Expended	
g/sec	lb/sec			kg	lb
318	0.70	Stainless Steel	36	11.4	25.2
		Composite	3.6	1.1	2.5
		Mylar	0.6	0.2	0.4
168	0.37	Stainless Steel	60	10.1	22.2
		Composite	6.0	1.0	2.2
		Mylar	1.0	0.2	0.4
86	0.19	Stainless Steel	100	8.6	19.0
		Composite	10	0.9	1.9
		Mylar	1.7	0.1	0.3
27	0.06	Stainless Steel	250	6.8	15.0
		Composite	25	0.7	1.5
		Mylar	4.2	0.1	0.3
11	0.03	Stainless Steel	500	5.7	12.5
		Composite	50	0.6	1.3
		Mylar	8.3	0.1	0.2

* 5 cm (2 in.) diameter vacuum jacketed feedline 4310 cm (1397 in.) in length.

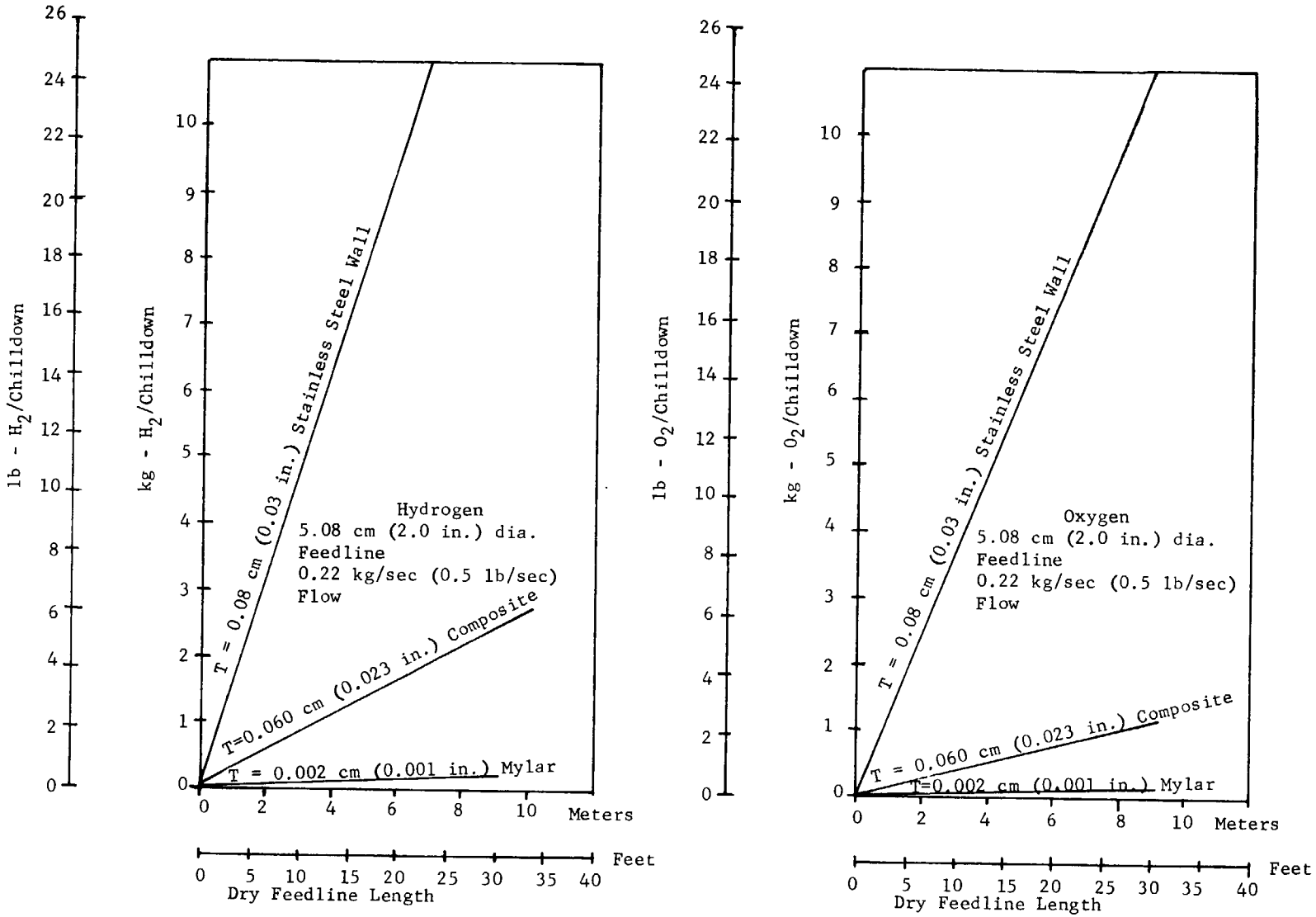

Figure 9. - Feedline Cooldown Propellant Requirement

TABLE 7. - MISSION DAYS REQUIRED TO CHANGE FROM WET FEEDLINES TO DRY FEEDLINES FOR A MISSION CONSISTING OF 10 COOLDOWNS

LINE STYLE	FEEDLINE WALL THICKNESS		HYDROGEN				OXYGEN		
			INSULATION CONDUCTIVITY	DAYS	BOILOFF WEIGHT		DAYS	BOILOFF WEIGHT	
	cm	in.	k		kg	lb		kg	lb
Stainless Steel	0.08	0.03	2×10^{-3}	18	104.0	230	290	592	2100
			9×10^{-4}	35			580		
			1×10^{-4}	175			2900		
Composite Liner Glass	0.008	0.003	2×10^{-3}	2	10.4	23	12	95	210
	0.051	0.020	9×10^{-4}	4			24		
			1×10^{-4}	18			120		
Mylar	0.003	0.001	2×10^{-3}	0.25	1.8	4	2	16	36
			9×10^{-4}	0.50			4		
			1×10^{-4}	2.5			20		

k values in Watts/m-K

Chilldown. - The purpose of the chilldown analysis on the OMS LOX and LH_2 feedlines was to predict the activity during the transient period and predict the total time and propellant required to obtain the pressure and temperature conditions at the engine or pump interface. Three different approaches were used to perform this analysis.

For the first approach the mist flow cooldown correlation proposed by Chi[7] was used. This correlation defines pipeline cooldown as a rate process, dependent upon the heat transfer coefficient. Mist flow occurs due to film boiling until a line cools down to a temperature permitting nucleate boiling and line wetting. The gaseous type of heat transfer coefficient of mist flow is low compared to a liquid type heat transfer coefficient found with the slug flow of nucleate boiling. Therefore, the dominant cooldown mechanism dictating total cooldown time and total propellant mass is mist flow. Mist flow was assumed to occur from an initial line temperature of 261 K (10°F) until nucleate boiling becomes possible at line wall temperatures of 35 K (-397°F) for LH_2 and 119 K (-245°F) for LOX. The cooldown time per unit length for various flowrates is shown on Figures 10 and 11. This analysis was performed on the flight configuration of the OMS LOX and LH_2 feedlines.

The second approach used the NERVA (FD 323 Transient Pipe and Pump Chilldown Program) computer program to perform the analysis. This program has the required thermodynamic subroutines, an energy equation, and considers friction factors and heat transfer film coefficients for two-phase flow. However, the program considers hydrogen only, so that a chilldown analysis of the hydrogen feedline was the only possibility.

The results of the analysis predicted the chilldown time of this line to be on the order of 2 seconds.

The third approach assumed that the chilldown liquid is converted to pure gas at saturated conditions at the feedline exit until chilldown is complete. All heat removed from the system is utilized in converting the flowing propellant to gas until the entire system reaches operating temperature. The technique involves calculation of the heat required to cool the entire system to operating temperature which is expressed as:

$$Z = WC_P \Delta T$$

where

Z = Total heat, in joules

W = Feedline weight, in kg

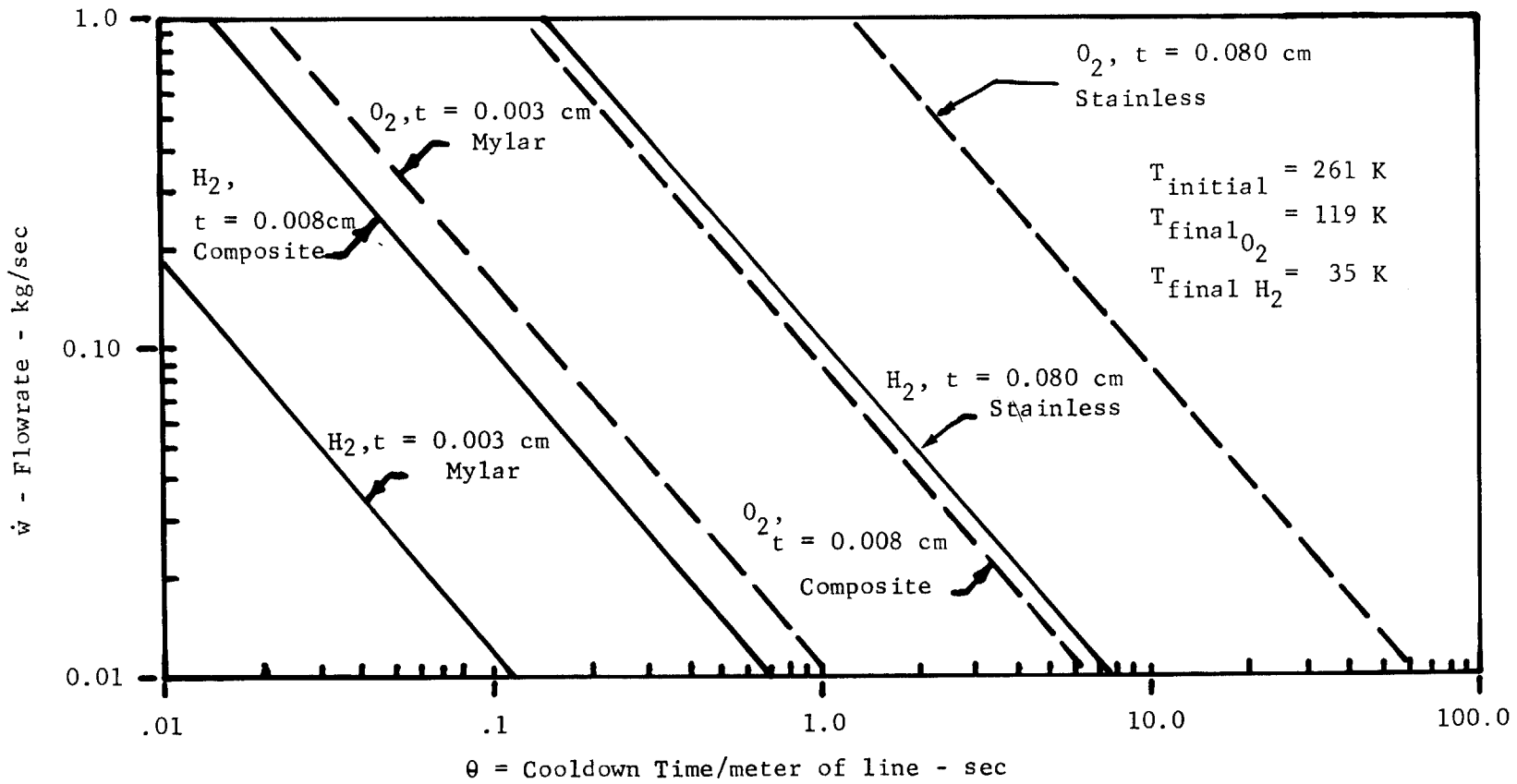

Figure 10. - Cooldown Time for Propellant Feedlines

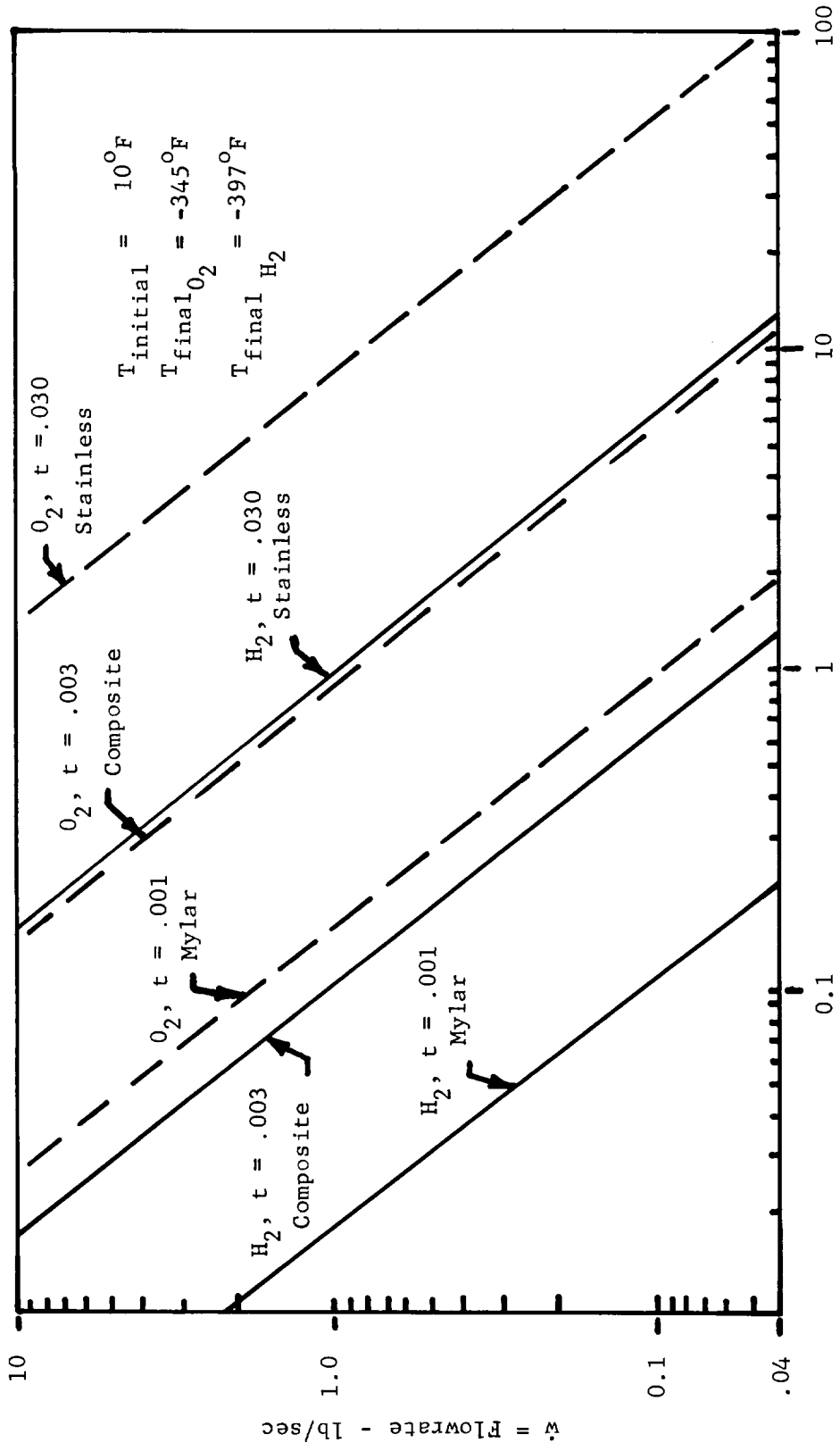

Figure 11. - Cooldown Time for Propellant Feedlines (U.S. Customary Units)

C_P = Material specific heat, in joules/kg-K

ΔT = Temperature change, in K.

Since the test system is composed of Inconel 718 liners, a glass-fiber overwrap and stainless steel fittings and flanges, the corresponding weights and specific heat for each material were used to determine the total heat for each material and then totaled to determine the total heat transferred to the chilldown propellant.

After the total heat was calculated, the weight of propellant converted to gas by this heat transfer was calculated as:

$$W_P = \frac{Z}{h_v}$$

where

W_P = Propellant weight boiled, in kg

h_v = Heat of vaporization, in joules/kg.

The chilldown time was then determined to be:

$$\theta = \frac{W_p}{\dot{w}}$$

where

θ = Chilldown time, in sec

$\dot{w}$ = Mean propellant flowrate, in kg/sec = $\frac{1}{\theta}\int_0^{\theta} d\dot{w}$.

This analytical method assumes there is no subcooling in the propellant. Since no losses or heat transfer film coefficients were considered, the time determined by this method represents the ideal absolute minimum chilldown time assuming the liner, end fittings, and overwrap all cool to operating temperature. It also reflects the relative validity of this method of analysis. The short chilldown time could have an error of 100% and would still be very satisfactory.

The results of this analysis indicated that the minimum chilldown time for the LOX OMS test configuration at the proposed flowrate would be approximately 0.3 seconds. Since the chilldown and flow testing of this line was

deleted from the program, these results were not verified by test. However, chilldown tests on the OMS LH_2 line using liquid nitrogen as the test medium gave a chilldown time of 2.0 - 2.5 seconds. The simplified analysis predicted a chilldown time of 1.1 seconds for this line using LN_2 as the test medium. These results indicate that the actual cooldown time for the OMS LOX test item would be approximately 0.68 seconds.

OMS/ACPS Flow Optimization. - The FLOWOPT computer program was used to optimize the diameter and configuration of the feedline for the Orbiter OMS and ACPS systems. This analysis optimizes the total required weight of non-usable materials (see Figure 12) so as to minimize on-orbit weight. The non-consumables are the basic system weights, including tankage, and propellants and gases expended without being used for thrust development. As the feedline diameter becomes larger, system pressure drops become smaller and pressure containing devices become lighter. The feedline (and vacuum jacket in some cases) becomes heavier. Additionally, the propellant required to cool the feedline will be increased and the boil-off of propellant in the feedline will also be increased due to larger surface areas. Using each component of the system as a variable, the optimum configuration based upon a specific mission profile can be selected.

For purposes of this analysis, the number of engine restarts per mission (4, 2 or 1) spread widely from the first start, the required propellant quality at engine start (single phase liquid), and overall feedline geometries were those used in the Phase B baselined Shuttle study.

To arrive at the optimum feedline design, the following variables were evaluated for their effect on the above weight and performance factors:

1) Feedline geometry including length using a two-dimensional study with a unit length of 30.5 cm (12 in.) the diameter being variable from 2.5 to 18 cm (1 to 7 in.) and configuration which was assumed straight;

2) Material, structural and thermal properties;

3) Valve placement at tanks;

4) Insulation properties of k = 0.000006 watts/m-K (0.0005 Btu/ft/^{o}F) and ρ = 80 kg/m^3 (5.00 lb/ft^3);

5) Boundary temperature of 289 K (60^{o}F).

These performance trades are presented in Appendix D of this report in a graphical presentation with accompanying clarifying tables.

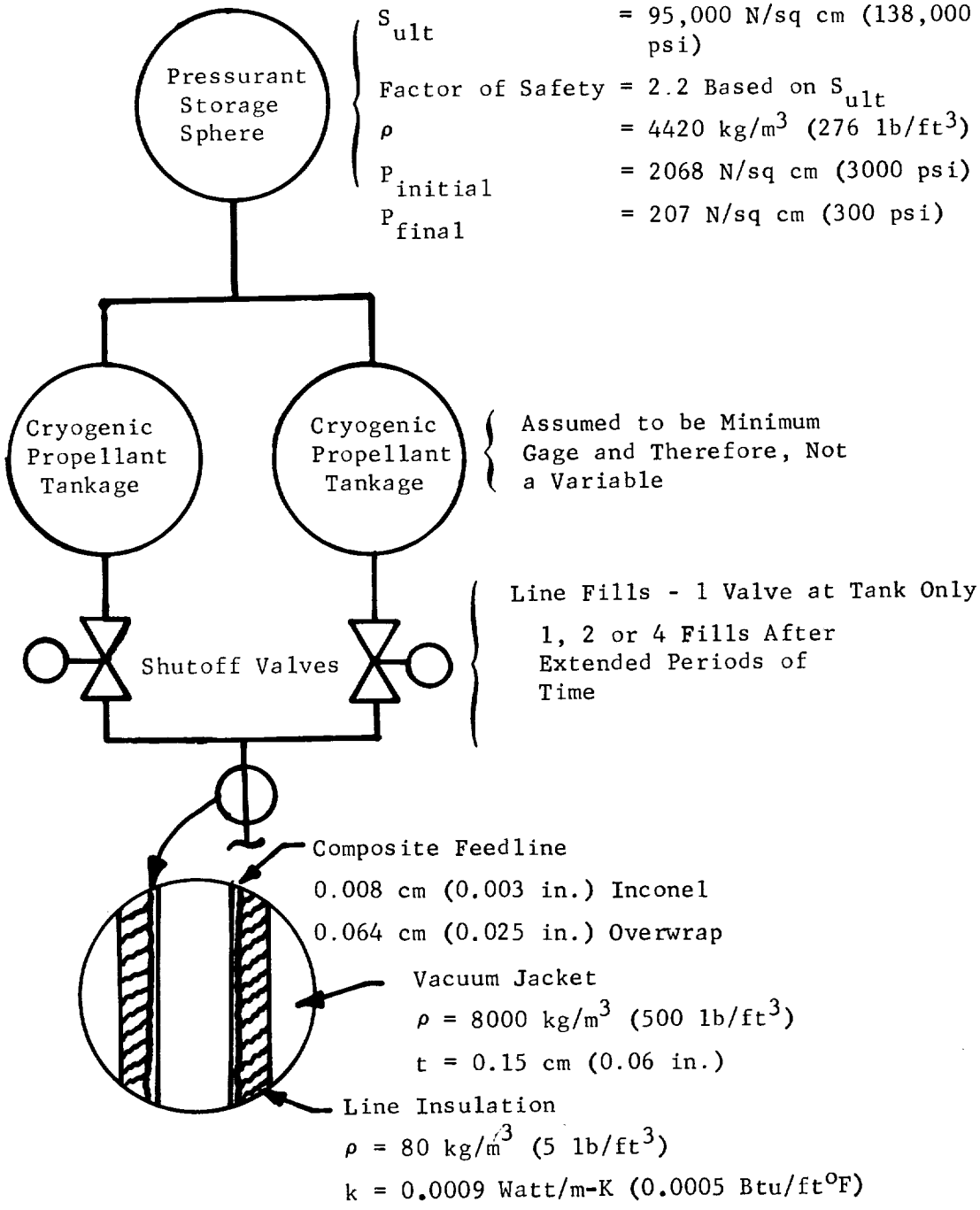

Figure 12. - Configuration of Optimized OMS and ACPS Systems for LOX or LH_2

The first of two optimization techniques set a feedline diameter ranging from 2.5 to 17.5 cm (1 to 7 in.) in increments of 2.5 cm (1 in.) and then optimized the configuration using the insulation thickness, vacuum jacket thickness, number of fills, flowrate of propellant, and boiloff of propellant as variables.

The second optimization technique utilized the simultaneous solution of two high order equations varying the insulating characteristics at the same time as the feedline diameter was varied over an infinite range. This resulted in an optimization of the total system weight which was plotted with the above data and shows the sensitivity of the system weight as a function of feedline diameter.

Thermal Coatings. - During the thermal analysis performed for the concurrent contract Vacuum Jacketed Composite Lines (NAS3-16762), the radiation heat transfer characteristics of conventional all-metal tubing was compared to the metal-lined glass-fiber composite tubing. The thermal performance of three all-metal and four composite configurations of vacuum jacketed lines were evaluated. Only one of the composite configurations (aluminum vacuum jacket liner) compares favorably with the all-metal configurations without modification of the emissivity of the outside of the inner line.

With a modification of the outside of the inner line to reduce its emittance to 0.035 or less all of the composite structures can be made to perform as well or better than the best all-metal configuration. This same result will be true of all line sizes and for lines without vacuum jackets. For emittance values of 0.02 and less the thermal performance of the composite tubing surpasses that of an all-aluminum tube. Emittance values of 0.035 or less can probably be achieved by vacuum depositing pure metal (silver, gold, aluminum or copper) films on the overwrap. Data relating to coating thickness and surface emittances for aluminum, gold, silver, copper, SiO/silver, and SiO/copper coatings are summarized in Reference 8. Initially the surface emittance decreases as the coating thickness increases. The emittance of aluminum and silver reach asymptotic values at /50-1000A. The emittance of gold achieves its asymptote at about 1500 A thickness.

For any given thickness, silver gives the lowest emittance surface. Although emittance data for copper is available over a limited range, it appears to have the next lowest emittance; gold and aluminum follow next in order. Further, the data indicates that significant lowering of the emittance value is obtained as the coating thicknesses are increased from 250 to 1000 A. A thickness of about 250 A is that normally available from commercial suppliers of metalized polyester film.

The protective coatings of silicon monoxide applied over the silver and copper coatings result in degrading the emittance of the basic surfaces by approximately 40%. Therefore, these composite coatings have emittance values generally comparable to that of gold.

The most practical method of reducing the emissivity of the overwrap surface is to wrap the feedline with one layer of double aluminized mylar. This would add no significant cost or weight to the vehicle. For those installations where the mylar cover might be damaged during operation, a coating of silver, gold, aluminum or copper may be required.

Internal Insulation. - Martin Marietta has developed an internal cryogenic insulation system based on a unique, pressure-equalized, capillary barrier concept. This system has been evaluated empirically and its feasibility has been demonstrated for application to cryogenic storage tanks, including Space Shuttle type hydrogen tanks.

A limited study has also been performed to determine the thermal performance of the insulation system in a feedline application. This effort was reported in MMC report number D-71-48774-004 entitled Capillary Insulation Feedline[9]. The following information was taken from this report.

A short section of simulated feedline was insulated with the Martin capillary (MARCAP) insulation. The feedline section is shown in Figure 13. It was formed by wrapping a flat sheet of half-inch thick MARCAP insulation into a cylinder 7 cm (2.75 in.) in outside diameter and 56 cm (22 in.) long. Low thermal conductance transition sections were attached to each end to provide mounting flange attachment. The particular structure shown was chosen to admit a floating carry-through for mating feedline sections. The MARCAP insulation consists of a honeycomb structure backed by a gas tight exterior wall and faced on the inside with a thin, flexible sheet. Each honeycomb cell communicates with the pipe volume through a small hole in the interior facesheet. Each cell is filled with opacified fiberglass insulation as an anti-convectant and an anti-radiant. There is no communication directly from cell to cell. The feedline weight per unit length is 460 g/m (0.311 lb/ft) exclusive of flanges.

The test goals were to measure the amount of propellant required for initial chilldown and for boiloff at equilibrium. Initial chilldown was found by plugging the line section with an insulated stopper and rapidly filling the vessel with liquid nitrogen to a specified level. Liquid nitrogen was continually added to hold the level until the amount added per unit time became constant. When the exterior temperatures were stabilized, the amount of liquid nitrogen added per unit time was taken to be the boiloff rate.

Initial chilldown data indicates that the MARCAP line has a volume heat capacity of 1820 joules/kg-K (0.434 Btu/lb^{o}F) and a linear heat capacity of 8.4 joules/cm-K (0.135 Btu/ft^{o}F).

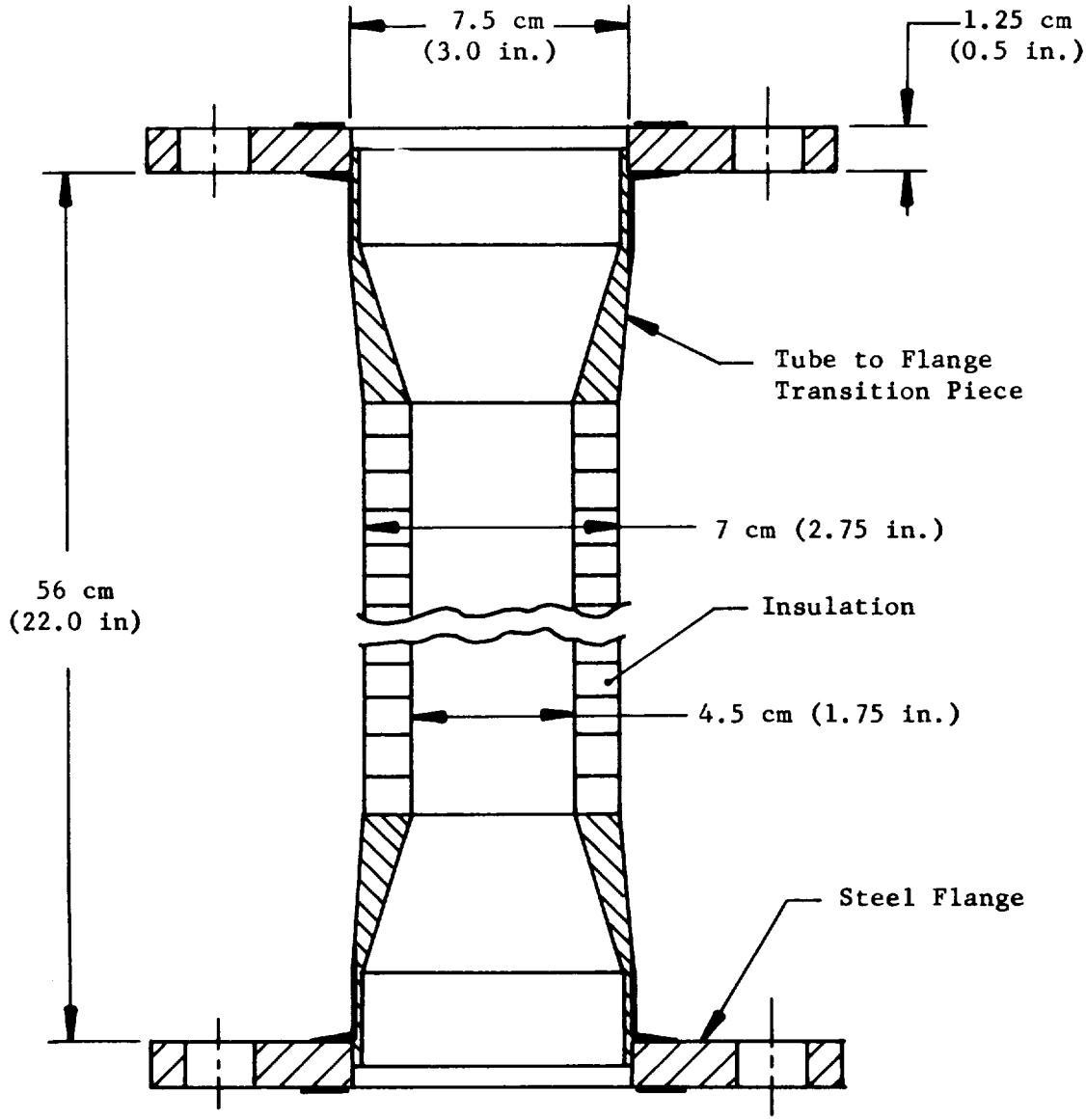

Figure 13. - Cross Section View of 4.5 cm (1.75 in.) Diameter Feedline -- MARCAP Insulation

Equilibrium boiloff data indicates liquid nitrogen boiloff per unit length of 577 g/m (0.39 lb/ft) and a radial wall thermal conductivity of 0.087 Watts/m-K (0.05 Btu/hr ft^{o}F). All cryogen tests were performed in air with accompanying heavy exterior frost and large convective transfer.

Additional Weight Reduction Analysis. - Several modifications can be applied to the tubing which will assist in obtaining additional weight reductions from the established baseline. Some of these would not require any substantial additional development including:

- o Axial pressure limitations;
- o Use of lower density overwrap material;
- o Addition of knurls on the end fittings.

Other modifications may be feasible but require additional development as discussed in a later section of this report. These optimizations include:

- o Addition of aluminum end flanges (page 41), and
- o Overwrapping with a large angle which can obviate the need for the axial 1/2 layer of cloth in the overwrap (page 41).

A composite feedline, in what can be considered the baseline configuration includes the following components:

- o Liner Material: Stainless steel or Inconel 718;
- o Composite: S/HTS glass-fibers in a 58-68R resin system overwrapped as 2 layers of hoop direction fiber separated by 1/2 layer of axial cloth;
- o End Fittings: Stainless steel or Inconel 718 with the tube designed to burst at the joint between the end fitting and the liner;
- o Metal Strengthening: The Inconel 718 liners can be heat treated before or after joining to the end fittings. The stainless steel liners can be strengthened by cold working the material before connecting fittings;
- o Liner Thickness: 0.008 cm (0.003 in.) for tubing up to 25 cm (10 in.) diameter in weight critical systems 0.013 cm (0.005 in.) for tubing over 25 cm (10 in.) diameter and for all diameters where weight is not critical and operating pressure does not dictate a thicker liner;

o Joint Methods: Fusion welding, resistance welding, or explosive bonding of the liner to end fittings. The resistance weld method will retain the strength of the heat treated liner.

Axial pressure limitations: The tubing is designed to withstand the internally applied pressure in both the hoop and axial directions. This concept facilitates testing and provides a tube capable of service without bellows in the system. Actual pressure requirements in the axial direction will usually be satisfied by bellows and support techniques. If the tube can be designed solely for hoop direction loading the liner can frequently be selected as a thinner gage. This design concept would be applicable only to high pressure systems where axial loads may dictate a liner thicker than the minimum gage.

Lighter composites: The selection of S/HTS glass-fiber, as the overwrap fiber was based primarily upon cost. Other candidate overwrap fibers include graphite, boron, and PRD-49-III.

The total tube weight per linear foot for four overwrap materials is shown as a function of line diameter on Figure 14. The curves are based on a propellant feedline designed for an operating pressure of 69 N/sq cm (100 psi) at liquid hydrogen temperature. The liner material for all cases was Inconel 718. A liner thickness of 0.008 cm (0.003 in.) was used for line diameters up to 25 cm (10 in.) and a thickness of 0.013 cm (0.005 in.) was used for line diameters above 25 cm (10 in.). The overwrap properties used for the weight study are shown in the following tabulation.

Fiber with 58-68R Resin System	S Glass	Graphite	Boron	PRD-49-III
Thickness/Layer, cm	0.020	0.010	0.013	0.020
(in.)	0.008	0.004	0.005	0.008
Minimum Wrap Thickness, cm	0.050	0.050	0.0445	0.050
(in.)	0.020	0.020	0.0175	0.020
Configuration[1]	H,1/2L,H	H,L,H,H,H	H,H,1/2L,H	H,1/2L,H
Density of Composite g/cm^3	2.35	1.52	1.9	1.38
(lb/in^3)	0.085	0.055	0.072	0.050
E N/sq cm	3.8 (10^6)	17 (10^6)	21 (10^6)	9 (10^6)
(psi)	5.5 (10^6)	25 (10^6)	30 (10^6)	13 (10^6)
Cost (prepreg), $/kg	29	550	550	77
($/lb)	13	250	250	35
% Resin	25	45	50	25

[1]H is a layer of hoop wrap; L is a longitudinal layer.

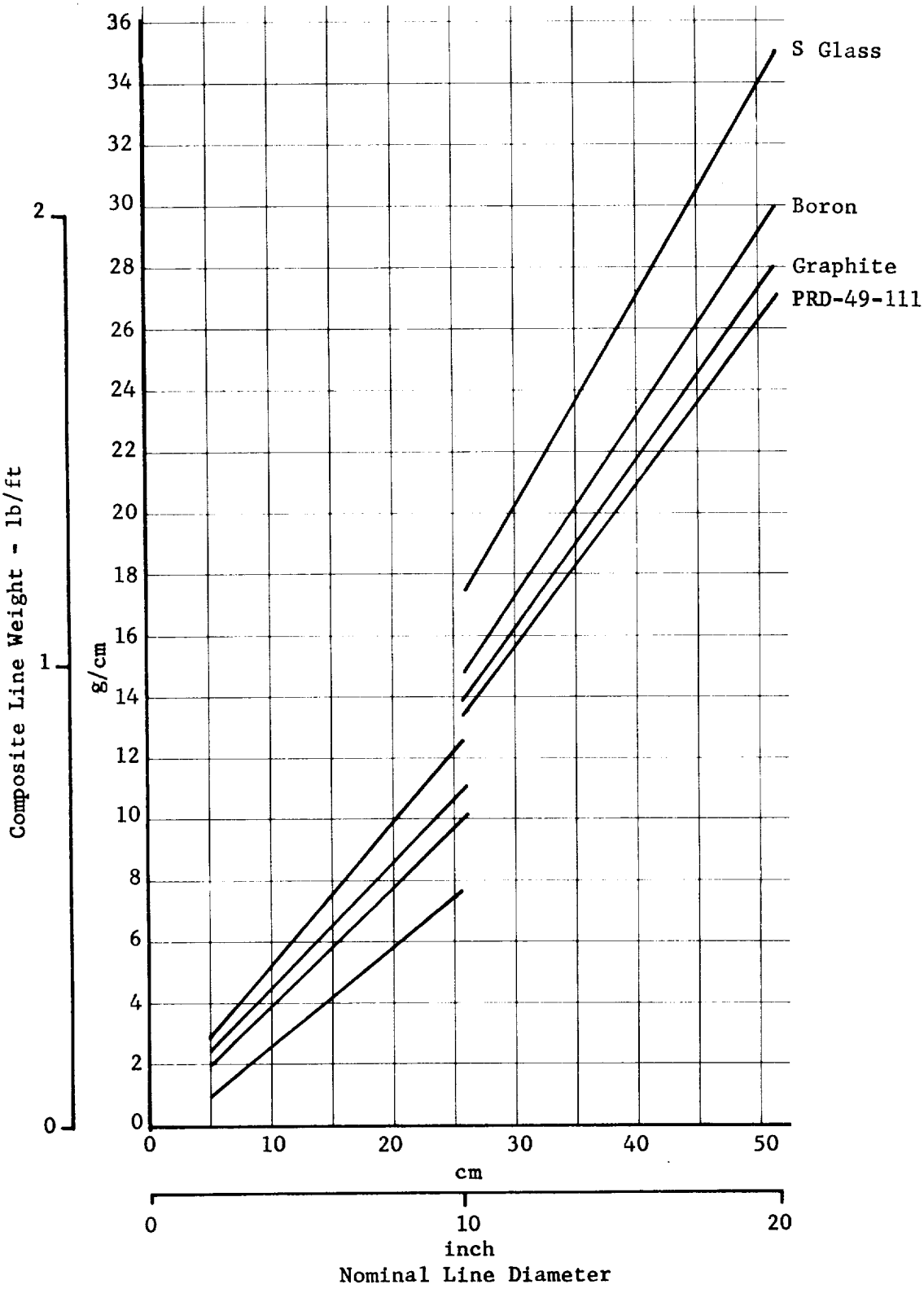

Figure 14. - Overwrap Weight of Candidate Materials

Figure 15 relates the cost of S-glass, boron, PRD-49-III and graphite as a function of line diameter. The selection between the heavier, less expensive S-glass and the lighter, more expensive PRD-49-III, graphite or boron will be a function of the allowable dollar expenditure per unit of weight saved for any specific vehicle being considered.

Addition of knurls on the end fittings: In the case where axial loads due to pressure must be considered, the addition of a knurl, as discussed in the proposed modifications section of this report (page 149), can facilitate load transfer to the overwrap and provide a considerable increase in load carrying capability. The 1/2 layer of axial glass cloth 0.02 cm (0.008 in.) thick with a tensile allowable of 52,000 N/sq cm (75,000 psi) can offset 390 N/sq cm (570 psi) internal pressure for a 5.1 cm (2 in.) diameter tube and 41 N/sq cm (60 psi) internal pressure for a 38 cm (15 in.) diameter tube.

Addition of aluminum end flanges: The development of explosive bonding techniques which will permit lightweight aluminum flanges to be attached to the liner cannot be considered safisfactorily completed. The fabrication of several very high quality joints has proven the feasibility, but the inability to repeat the success leaves the process in a state of development and reliability less than that required. The joint, when perfected, will be capable of reducing the feedline weight considerably. For example, a 56 cm (22 in.) diameter stainless steel conoseal flange weighs 10 kg (22 lb) and an aluminum conoseal flange for the same service weight 2.4 kg (7.5 lb).

The costs associated with this style joint, in production quantities, are not presently determined. The low value assigned to the external tanks will most likely not justify the further development and subsequent use of this concept. A longer life, reusable or weight critical vehicle will most likely benefit significantly from the concept.

Overwrapping with a larger angle: The currently used wrap pattern includes two layers of hoop oriented fibers and strips of longitudinal oriented fibers constituting an additional 1/2 layer. The axial oriented layer was added to assure the low strength resin did not fail during loading due to internal pressure, resulting in a gap in the overwrap. Since the liner is often not designed to withstand the entire hoop loading without strength from the overwrap, this gap in the overwrap may permit the liner to fail in the hoop direction.

For a 38 cm (15 in.) diameter tube, the wrap angle, at 6.3 wraps per linear centimeter (16 wraps per linear inch), is 0.0018 radians (0.1^{o}). By increasing this angle to approximately 0.088 radians (5^{o}) the axial loadings can be transferred to the stronger fiber and separation will not occur. This will result in a slight buildup at the tube ends but will result in a savings of about 680 grams (1.5 pounds) for the same 38 cm (15 in.) diameter, 300 cm (120 in.) long tube.

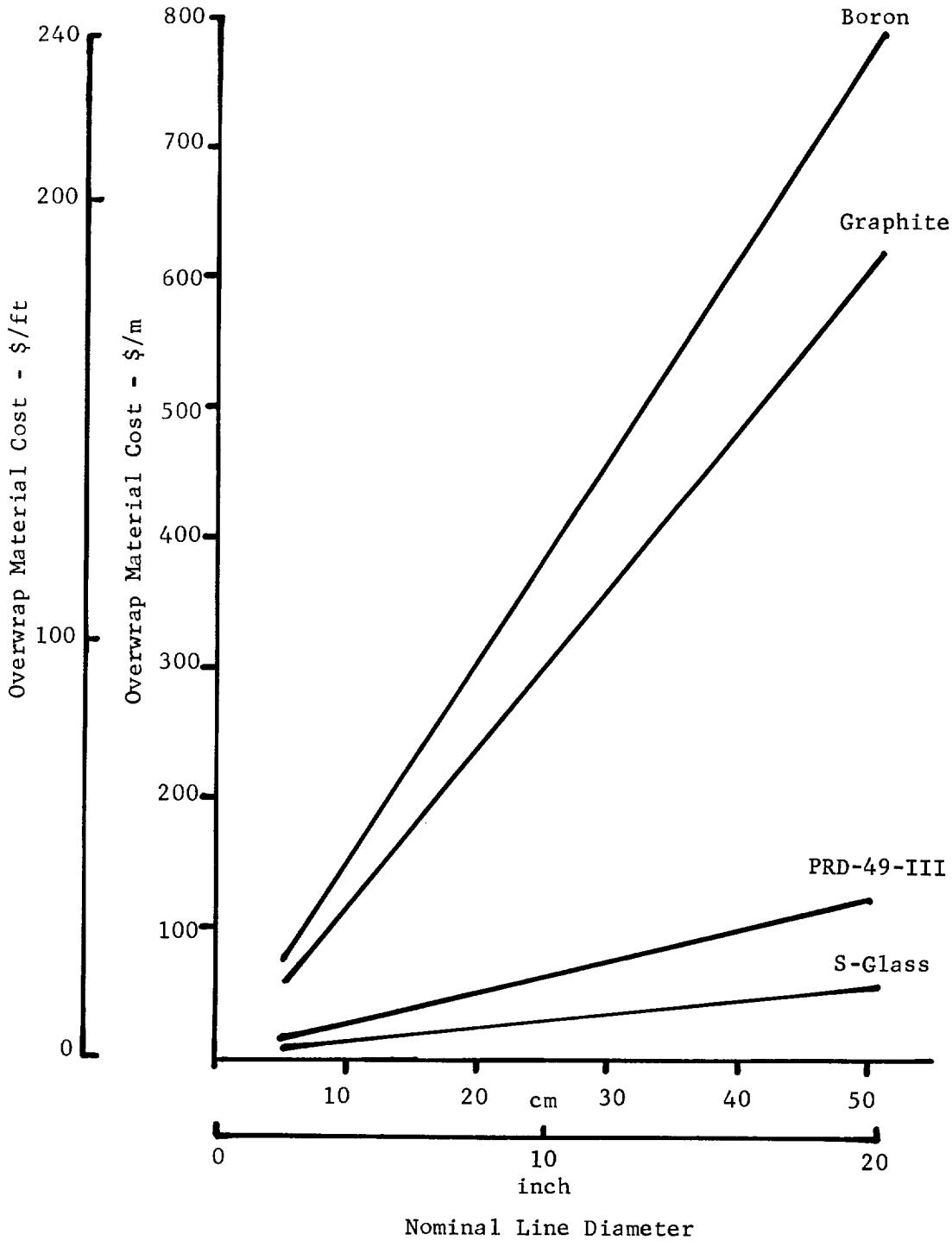

Figure 15. - Overwrap Material Cost

Weight Analysis. - The Phase B Space Shuttle configuration used as a baseline for this program locates the main LOX tank forward and the main LH_2 tank aft in both the booster and orbiter vehicles. This location necessitates extremely long feedlines for the main engine LOX feed systems. In the Phase B configuration these feedlines, from the tank to the manifold, are 2219-T87 aluminum. The LOX manifolds on the booster and orbiter and the rest of the candidate propellant systems are fabricated from Armco 21-6-9 stainless steel (21% Cr, 6% Ni, 9% Mn).

An analysis was performed to determine the optimum weights of the selected propellant feed systems using composite sections where practical. The results of the feedline weight optimization studies show that the optimum weight feedline would be an all-welded assembly. The glass-fiber composite sections in this assembly would be equipped with aluminum buttweld end fittings attached to the Inconel liners by an explosive bonding process. For small diameter systems the all-welded concept may be achievable, but it is unlikely for systems of the size required by the Shuttle main engines. For these systems tubing routing and component locations would have to be arranged such that access could be provided for welding equipment. However, disconnectable aluminum flanges could be bonded to the Inconel liners with very little weight penalty

In a vehicle mounting, the composite feedlines would require the same gimbal joints, bellows, sliding joints and structural supports as an all-metal feedline. These components are necessary to absorb bending, torsional and thermal contraction loads imposed on the feedlines. The structural supports should be designed to include a thermal barrier between the support and the feedline to eliminate heat leaks into the feedline.

The weight of the composite tubing designed for the candidate propellant systems is compared to the weight of the Phase B all-metal tubing in Appendix E of this report. A summary of this comparison is shown in Table 8. The section code used in column 2 of the table refers to the descriptive code indicated on the drawings of the candidate systems included in Appendix B of this report.

The Phase B design used aluminum and stainless steel conoseal flanges extensively in the assembly of the propellant systems. Several composite configurations are included in the table for the booster main engine LOX feedline. These configurations include either Inconel, 21-6-9, 304L or aluminum as the liner material and similar metal end fittings. Since the optimum weight composite feedlines use Inconel or 21-6-9 steel as the liner material, the table indicates the weight savings using stainless steel flanges. The table also indicates the weight savings that may be realized if aluminum flanges can be explosively bonded to the Inconel or stainless steel liners. Where the Phase B designed systems use buttweld joints, the table indicates buttweld joints for the composite lines.

TABLE 8. - WEIGHT SAVINGS OBTAINABLE BY USE OF COMPOSITE LINES IN THE SPACE SHUTTLE

DESCRIPTION	SECTION CODE	DIAMETER cm (in.)	LENGTH cm (in.)	PHASE B CONFIGURATION				COMPOSITE CONFIGURATION					WEIGHT SAVINGS/ SECTION kg (lbs)	NUMBER OF SECTION	TOTAL WEIGHT SAVINGS kg (lbs)
				MATERIAL	WALL THICKNESS cm (in.)	END FITTING	SECTION TOTAL WT. kg (lbs)	LINER MATERIAL	LINER THICKNESS cm (in.)	END FITTING	END FITTING TOTAL WT. kg (lbs)	SECTION TOTAL WT. kg (lbs)			
Booster Main Engine LOX Feedline	3A	56 (22)	305 (120)	2219-T87 Aluminum	0.203 (0.080)	Conoseal-Al	34 (75)	Inconel	0.0165 (0.0065)	SS Conoseal SS Buttweld Transition	10 (22) 1.13 (2.49)	26 (58)	8 (17)	2	16 (34)
	3A	56 (22)	305 (120)	" "	0.203 (0.080)	" "	34 (75)	21-6-9	0.0165 (0.0065)	" "	1.13 (2.49)	26 (58)	8 (17)	2	16 (34)
	3A	56 (22)	305 (120)	" "	0.203 (0.080)	" "	34 (75)	304L	0.0480 (0.0189)	" "	3 (7)	39 (87)	-5 (-12)	2	-10 (-24)
	3A	56 (22)	305 (120)	" "	0.203 (0.080)	" "	34 (75)	Aluminum	0.0655 (0.0258)	Al Conoseal Al Buttweld Tran.	2 (3.74)	23 (50)	11 (25)	2	22 (50)
	3A	56 (22)	305 (120)	" "	0.203 (0.080)	" "	34 (75)	Inconel	0.0165 (0.0065)	Al Conoseal Al Buttweld Tran.	2 (3.74)	17 (37)	17 (38)	2	35 (76)
Booster Main Engine LOX Manifold	6A	56 (22)	152 (60)	21-6-9 SS	0.318 (0.125)	Buttweld	67 (148)	Inconel	0.0445 (0.0175)	Buttweld Transition	23 (10)	18 (40)	49 (108)	2	98 (216)
Booster Main Engine LOX Feed Ducts	1 & 2 or 6 & 7	38 (15)	185 (73)	21-6-9 SS	0.203 (0.080)	Conoseal SS Buttweld	43 (94)	Inconel	0.0290 (0.0114)	SS Conoseal SS Buttweld Tran.	7 (15) 0.98 (2.16)	16 (36)	26 (58)	12	312 (696)
Booster Main Engine LOX Fill & Drain	1 & 2A	25 (10)	310 (122)	21-6-9 SS	0.089 (0.035)	Buttweld	18 (39)	Inconel	0.0180 (0.0071)	Buttweld Transition	0.60 (1.26)	9 (19)	9 (20)	1	9 (20)
Booster Main Engine LH_2 Feed Ducts	1 Eng. 2 & 3	30 (12)	94 (37)	21-6-9 SS	0.091 (0.036)	Conoseal SS Buttweld	12 (26)	Inconel	0.0076 (0.0030)	SS Conoseal SS Buttweld Tran.	5 (12) .35 (0.78)	8 (17)	4 (9)	2	8 (18)
Booster LH_2 Fill & Drain	1 & 2A	25 (10)	305 (120)	21-6-9	0.081 (0.032)	Buttweld	16 (35)	Inconel	0.0076 (0.0030)	Buttweld Transition	0.62 (1.36)	6 (13)	10 (22)	1	10 (22)
Orbiter Main Engine LOX Feedline	1A	46 (18)	808 (318)	2219-T87 Aluminum	0.127 (0.050)	Conoseal Al Conoseal SS	53 (116)	Inconel	0.0152 (0.0060)	SS Conoseal SS Buttweld Tran.	8 (17.3) .73 (1.62)	40 (89)	13 (27)	2	26 (54)
Orbiter Main Engine LH_2 Feedline	2	30 (12)	163 (64)	21-6-9	0.127 (0.050)	Buttweld	16 (35)	Inconel	0.0076 (0.0030)	SS Buttweld Tran.	1 (2.16)	4 (9)	12 (26)	1	12 (26)
Orbiter OMS LOX Feedline	2	7 (2.65)	381 (150)	21-6-9	0.041 (0.016)	Buttweld	3 (5.71)	Inconel	0.0076 (0.0030)	SS Buttweld Tran.	0.07 (0.15)	2 (3.94)	1 (1.77)	1	1 (1.77)
Orbiter OMS LH_2 Feedline	2	10 (3.9)	1460 (575)	21-6-9	0.050 (0.020)	Buttweld	18 (40.3)	Inconel	0.0076 (0.0030)	SS Buttweld Tran.	0.13 (0.28)	10 (21.63)	8 (18.67)	1	8 (18.67)
ACPS LOX Feedline	2A	3 (1.16)	79 (31)	2219-T87 Aluminum	0.07 (0.028)	Buttweld	0.15 (0.32)	Inconel	0.0076 (0.0030)	Buttweld Tran.	0.04 (0.12)	0.20 (0.44)	-0.05 (-0.12)	1	-0.05 (-0.12)
ACPS LH_2 Feedline	3B	4 (1.43)	56 (22)	2219-T87 Aluminum	0.07 (0.028)	Buttweld	0.13 (0.28)	Inconel	0.0076 (0.0030)	Buttweld Tran.	0.06 (0.14)	0.20 (0.44)	-0.07 (-0.16)	1	-0.07 (-0.16)

Undefined Variable Analysis. - Empirical data regarding the values of the following variables was either virtually non-existant or not developed for the proposed configuration.

- o Overwrap modulus of elasticity (limited investigation performed);
- o Effect of a doubler for the metallic liner in axial load transfer;
- o Effect of the overwrap in axial loading;
- o Gap size as a function of overwrap temperatures;
- o Thermal contraction properties of specific overwrap configurations;
- o Compressive hoop loads at ambient temperature.

The effect each of these ill-defined parameters would have on the total weight of a feedline was also not known.

The WEATOPT program was operated with each parameter varied through a selected range and also with a reasonable matrix developed by simultaneously varying several of them to determine the sensitivity of the tubing weights to these variables.

The results of this analysis show that the only undefined variable with any measurable effect on the feedline weight was the overwrap modulus of elasticity (E_o). The other variables had little effect on the weight of a section of feedline and no further investigation of these variables was performed. E_o was further evaluated by a review of the strain measurements made during the previous program (NAS3-12047) and by an empirical evaluation of the overwrap material which is reported in the following section of this report.

Empirical Evaluation During Analysis Phase. - In support of the analytical activity on the main engine feedlines, two, limited, empirical evaluations were performed. The first evaluated properties of two glass-cloth materials which were candidates for the axial overwrap. The second evaluated the gap between the liner and overwrap at cryogenic temperatures.

Determination of overwrap properties: A test program to provide an empirical evaluation of several properties of two overwrap cloth samples was performed. The specific properties to be verified by test included the modulus of elasticity (E_o) and the ultimate tensile strength (S_u).

Two laminates were fabricated; one laminate with style 143 glass cloth commercially impregnated by U.S. Polymeric with E78 epoxy resin and one laminate with style 1557 glass cloth hand-impregnated with 58-68R epoxy resin with 30% solids. The laminates were laid up so that the ends of the tensile specimens cut from these laminates would be reinforced with cross plies of the same material. Both laminates were oven cured under a vacuum bag for two hours at 339 K (150°F) followed by four hours at 422 K (300°F). Five tensile specimens were removed from each laminate so that the specimen length paralleled the warp threads in the laminate. Remnants of the laminates were used for resin content and density determinations.

The results of the testing tend to verify a modulus of 3.8×10^6 N/sq cm (5.5×10^6 psi) in the direction of the glass-fibers for a resin content of 30%. Variations from both unidirectionality and resin content limit the usefulness of the data for comparative purposes.

Gap determination: A limited test program was performed to empirically determine the gap between the liner and the overwrap when a composite tube is cooled to cryogenic temperature in an unpressurized condition. This gap is a result of the different coefficients of thermal expansion of the liner and overwrap material. The specimen for this testing was a 12.7 cm (5 in.) diameter 0.015 cm (0.006 in.) thick wall Inconel liner with explosively bonded stainless steel end fittings. The overwrap configuration consisted of one layer of hoop wound glass-fiber, one-half layer of longitudinal glass-fiber cloth and a second layer of hoop wound glass-fiber.

The test was performed by filling a cryostat and the test item with liquid hydrogen while maintaining the internal pressure in the test item at essentially zero psig. The output of bi-axial strain gages mounted inside of the liner was then recorded as the internal pressure was slowly increased. This data was then reduced and plotted versus the internal pressure to determine the point where the strain rate changes indicating that the gap has closed. The internal pressure in the tube when the gap was closed was found to be 4.5 N/sq cm (6.5 psi). The gap corresponding to this pressure was calculated to be 0.0005 cm (0.0002 in.). The predicted gap for this test item (assuming 0 stress in both the liner and the overwrap at room temperature) was 0.0048 cm (0.0019 in.). The test results indicate that the overwrap and cure process left a residual compressive load in the liner. The hoop strain gage became inoperative during the first pressurization so the repeatability of the data could not be established.

Cost Analysis and Effectiveness for Space Shuttle External Tanks. - As stated earlier the main engine feedlines and auxilliary lines for the Phase B study which formed the basis for this program are similar to the currently proposed configuration of the external tanks.

The external propellant tank will be carried into orbit but will then be expended rather than being reusable. This puts a high emphasis on both weight reduction and low per unit costs. An allowable expenditure of $55 to $66 per vehicle per kg saved ($25 to $30/lb) may be realistic in the external tank area. The propulsion plumbing on the orbiter will contain sections similar to those baselined in this study and allowable costs per pound saved will probably be approximately the same as for the external tanks.

Cost comparisons, based upon 449 vehicle tanks, are shown in Table 9. Cost estimates for both concepts were made by the same vendor, a reputable bellows and feedline manufacturer. Overwrapping of the liners was estimated by Martin Marietta using production facilities. The cost per kilogram reduced is also shown in the table. As an example of cost savings, the table shows a cost of $31/kg saved/vehicle ($14/lb saved/vehicle) for the LOX feedline. Based on an allowable expenditure of $66/kg saved ($30/lb saved) this indicates a cost savings of $35/kg ($16/lb) for this feedline which is a total savings of $9,800 per vehicle.

TABLE 9. - DROP TANK COST EFFECTIVENESS EVALUATION

Function	Sections/ Vehicle	All Metal Cost/ Section $	Composite Cost/ Section $	Weight Savings/ Section kg	$ Cost/kg saved/ Vehicle	$ Cost/lb saved/ Vehicle
LOX Feedline	7	890	2135	40	31	14
LOX Pressurization	18	92	595	7.5	67	30
LOX Recirculation	13	160	335	5.1	34	15
LH_2 Pressurization and Vent	15	535	677	4.1	35	13
LH_2 Tank Recirculation	3	221		6.5		47
Details of the orbiter feedline configuration are not presently available, however, this vehicle will be reuseable and the allowable cost per kg saved will be approximately the same as for the external tanks.						

TEST ITEM DESIGN

During the vehicle feedline design phase, critical portions of the various feedlines were determined and test items were designed to represent these portions in the testing program. Although these test items did differ from the actual feedlines, to facilitate testing, the critical areas were an exact simulation of the flight-configured design. Expansion joints, sliding joints, bellows and etc., were not included in the design of the test items since these components would be included in any feedline design and their performance is well known. In the OMS feedlines where the propellant flow is split to go to two engines, the flow characteristics of the feedline to one engine were simulated by the use of an orifice. Long straight sections were shortened and although all bends were included in the design the three-dimensional real world was reduced to essentially two dimensions to accommodate assembly and testing.

Selected Configurations. - OMS test item selection was based on a system which would lend itself most favorably to achieving all program objectives. Selected for the actual test item designs were the OMS LOX system and portions of the OMS LH_2 system as shown in Figures 16 and 17. With the use of orifices to simulate the flow characteristics of the split flow configurations, it was not necessary to fabricate the entire feedline system.

Selected configurations of the main engine test items represent both the LH_2 and LOX systems of the Phase B orbiter and booster. These items were selected to represent extreme conditions for the LOX and LH_2 main engine feedlines. The LOX configuration was based upon maximum working pressures in the system requiring the thickest metallic liner. The LH_2 configuration was based upon minimum system pressure to firmly establish the minimum gages suitable for fabrication.

Physical Dimensions and Properties. - The physical dimensions of the 12 subassemblies which comprise the selected configurations are shown in Table 10. Detailed engineering drawings were prepared for each test item and copies of the drawings were included in interim progress reports. The materials of construction and fabrication techniques closely paralled those used in the previous program and are summarized in the fabrication section of this report starting on page 55.

Design Objectives. - Design of the OMS test configurations was focused on duplicating actual baseline configured systems while staying within the constraints set by contract objectives and available facilities. The following items were considered during the OMS test item design:

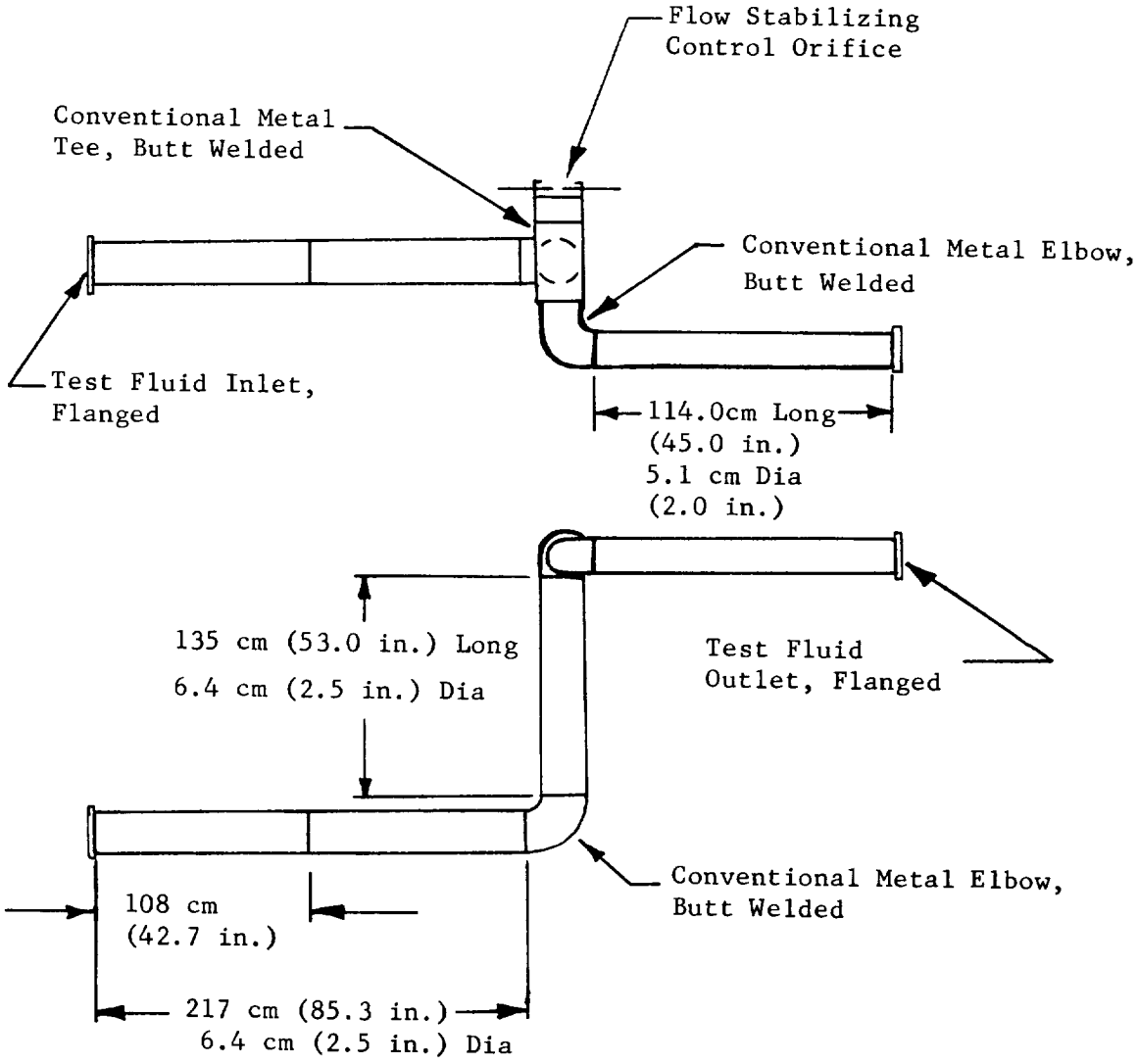

Figure 16. - OMS LOX Test Configuration

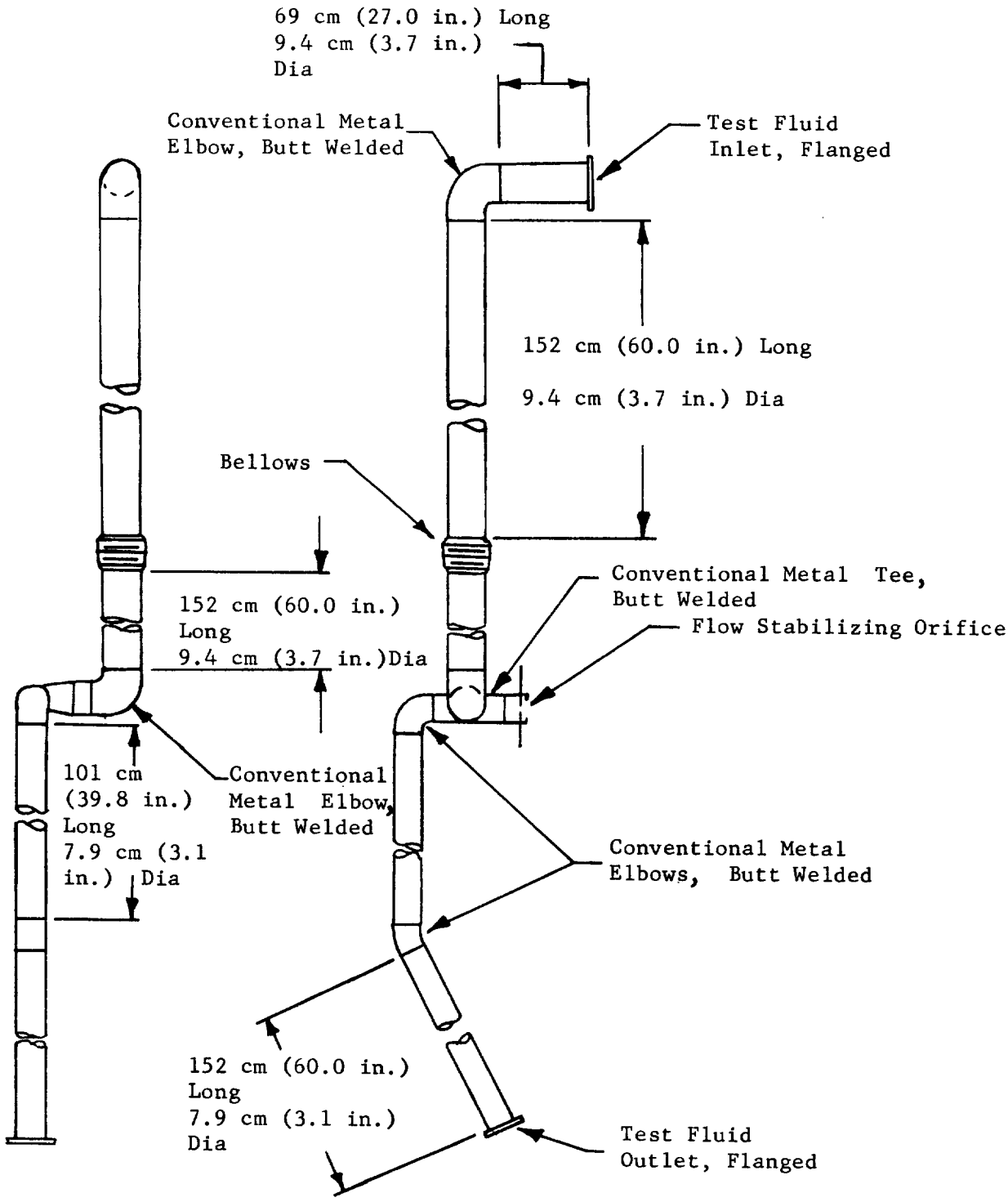

Figure 17. - OMS LH_2 Test Configuration

TABLE 10. - TEST ITEM PHYSICAL DIMENSIONS AND PROPERTIES

Test Item	Section Numbers	Diameter		Length		Material Thick.		Longitudinal Weld		Circumferential Weld		Heat Treat and Aging
		cm	(in.)	cm	(in.)	cm	(in.)	Quantity	Type	Quantity	Type	
OMS LOX	1, 2 & 3	6.4	2.5	104	41.0	0.008	0.003	1	Fusion	N/A	N/A	N/A
OMS LOX *	4	5.1	2.0	104	41.0	0.009	0.0035	1	Fusion	N/A	N/A	N/A
OMS LH_2	2, 3	9.4	3.7	152	60.0	0.008	0.003	1	Resistance	N/A	N/A	N/A
OMS LH_2	1	9.4	3.7	68.6	27.0	0.008	0.003	1	Resistance	N/A	N/A	N/A
OMS LH_2	4	7.9	3.1	152	60.0	0.008	0.003	1	Resistance	N/A	N/A	N/A
OMS LH_2	5	7.9	3.1	91.0	36.0	0.008	0.003	1	Resistance	N/A	N/A	N/A
Main Engine Preliminary	1 Assembly	38.0	15.0	91.0	36.0	0.015	0.006	1	Fusion	N/A	N/A	Heat Treated and Age Hardened
Main Engine LH_2	1 Assembly	38.0	15.0	305	120.0	0.008	0.003	4	Resistance	N/A	N/A	Heat Treated and Age Hardened
Main Engine LOX **	1 Assembly 4 Sections	38.0	15.0	305	120.0	0.028	0.011	2 each Section	Fusion	3 Joining the 4 Sections	Resistance	Heat Treated and Age Hardened

* This section of the OMS LOX line was helically wrapped, fusion welded, and redrawn. Diameter, length and material thickness dimensions shown are after redrawing.

** The main engine LOX line was made in 4 sections to enable heat treating. To preserve heat treat the sections were resistance welded together.

- Proper insulation material and thickness to simulate a vacuum condition heat leak (for the steady-state tests);
- Location and frequency of temperature measurements;
- Wet or dry analysis results;
- Ability to submit a section of the feedline to radial thermal conductivity testing;
- Ability to easily perform the thermal cycle testing of sections of the lines;
- Ability to easily leak check and burst test the test items;
- The three-dimensional real world was reduced to essentially two dimensions to accommodate assembly and testing since all elbows, bends, and other three-dimensional directional changes can be adequately simulated in a test item that can be fabricated in one plane. The fabrication advantages without elaborate tooling are apparent;
- The second leg of the OMS engine feedline was simulated with a flow-control device;
- A maximum diameter of 9.5 cm (3.75 in.) was used to facilitate fabrication from a single 30.5 cm (12 in.) wide Inconel sheet;
- Length constraints of various liner fabricators;
- Size of the vacuum chamber available for the cryogenic testing.

Structural requirements formed the design basis for the main engine test items. Emphasis was on minimizing weight. However, the effect of composite tubing on the following feedline requirements was considered:

- Desire to have a minimum number of joints;
- Requirements for 100 mission reliability;
- Ability to be fabricated at a reasonable cost;
- Varying the strength of the tubing as a function of location;
- Pressure drop stability during flow; and
- Ability to assemble large diameter composite lines into a propellant system.

A summary of the design boundaries, which formed the baseline for the design is shown in Table A-1 for the OMS systems and Table A-2 for the main engine systems of Appendix A to this report. The weight and performance of the composite systems were compared with the baselined all-metal system.

End fitting design. - The criteria used for design of end fittings was based upon results of the previous contract[1] and included:

- The capabilities of the various liner fabricators to weld thin foil to a relatively thick section of flange;
- The capabilities of the explosive bonding vendor to join thin foil to the main engine LOX flange;
- Ease of connecting composite tubes to other composite sections and to metallic tubes or elbows;
- To optimize the system weight and provide higher reliability through leak-free performance, butt weld fittings were chosen over flanges.

The thickness of the main body of the end fitting is controlled by three factors including, a) the minimum thickness to withstand the internal pressure, b) the maximum thickness permitted by the welding process which is generally three times the liner thickness, and c) the desired thickness to join the tube to an adjacent component. The tapered portion of the end fitting is provided as a transition to the overwrap.

Schematic diagrams of the end fittings designed for the various test items are shown in Figure 18.

The end fitting selected for the LH_2 OMS feedlines is designed for use when the liner-to-end-fitting-joint is a resistance weld. The end fitting selected for the LOX OMS feedlines is identical to the LH_2 fitting except for the weld prep area which is shaped to provide an approximately equal area for effective weld heat buildup during welding. This style of end fitting is designed for use when the liner-to-end-fitting-joint is a fusion weld.

The end fitting selected for the main engine LH_2 feedline is designed to be resistance welded to the liner. The end fitting selected for the main engine LOX feedline is designed to be explosively bonded to the liner.

The test item design effort was concluded by preparing engineering drawings from which liners and end fittings could be fabricated.

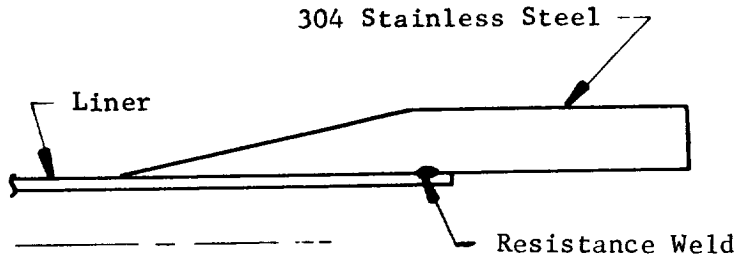

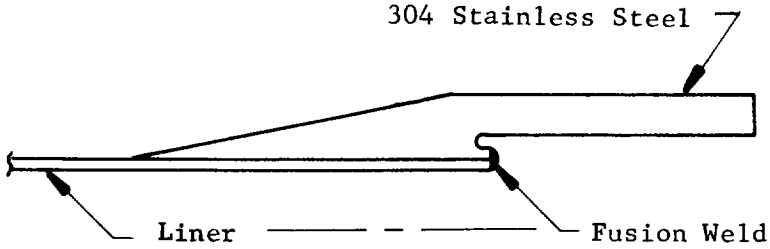

OMS LH_2 End Fitting Design

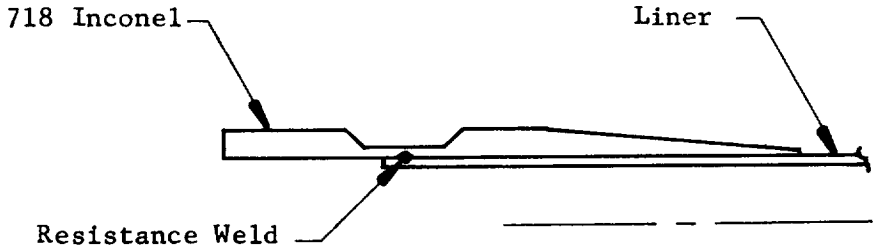

Main Engine LH_2 End Fitting Design

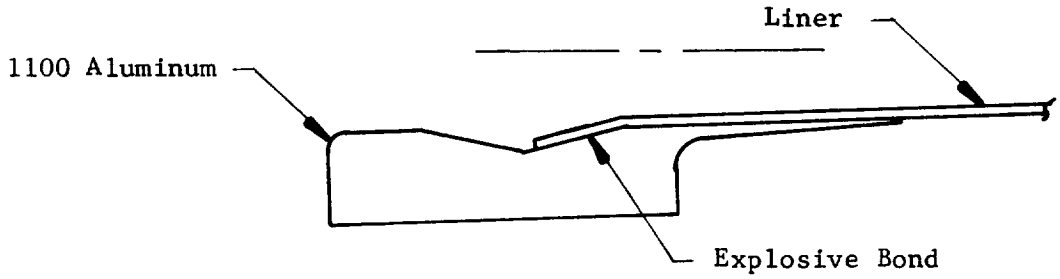

Main Engine LOX End Fitting Design

Figure 18. - End Fitting Configurations

FABRICATION

After completion of the analysis and design effort, fabrication of test items was started. The fabrication effort consisted of the following major functions:

- Evaluating and selecting vendors;
- Fabricating the liners;
- Fabricating the end fittings;
- Joining the liners and end fittings;
- Mounting the instrumentation;
- Installing the end closures;
- Overwrapping and curing the assembly;
- Performing the various in-process leak checks.

The materials, manufacturing and welding techniques, along with fitting fabrication and fitting attachment processes used to produce the test items, were developed during the NAS3-12047 program. The larger diameter main engine test items presented several new fabrication problems, therefore prior to committing to the 38 cm (15 in.) diameter fabrication program, a 90 cm (30 in.) long preliminary tube was fabricated to check out several unproven fabrication techniques.

In addition to this preliminary test item, other fabrication quantities were as follows:

- Four pieces of OMS LOX feedline;
- Five pieces of OMS LH_2 feedline;
- One representative section of main engine LOX feedline;
- One representative section of main engine LH_2 feedline.

The flow charts, Figure 19 and 20, show the general fabrication steps used for the test items.

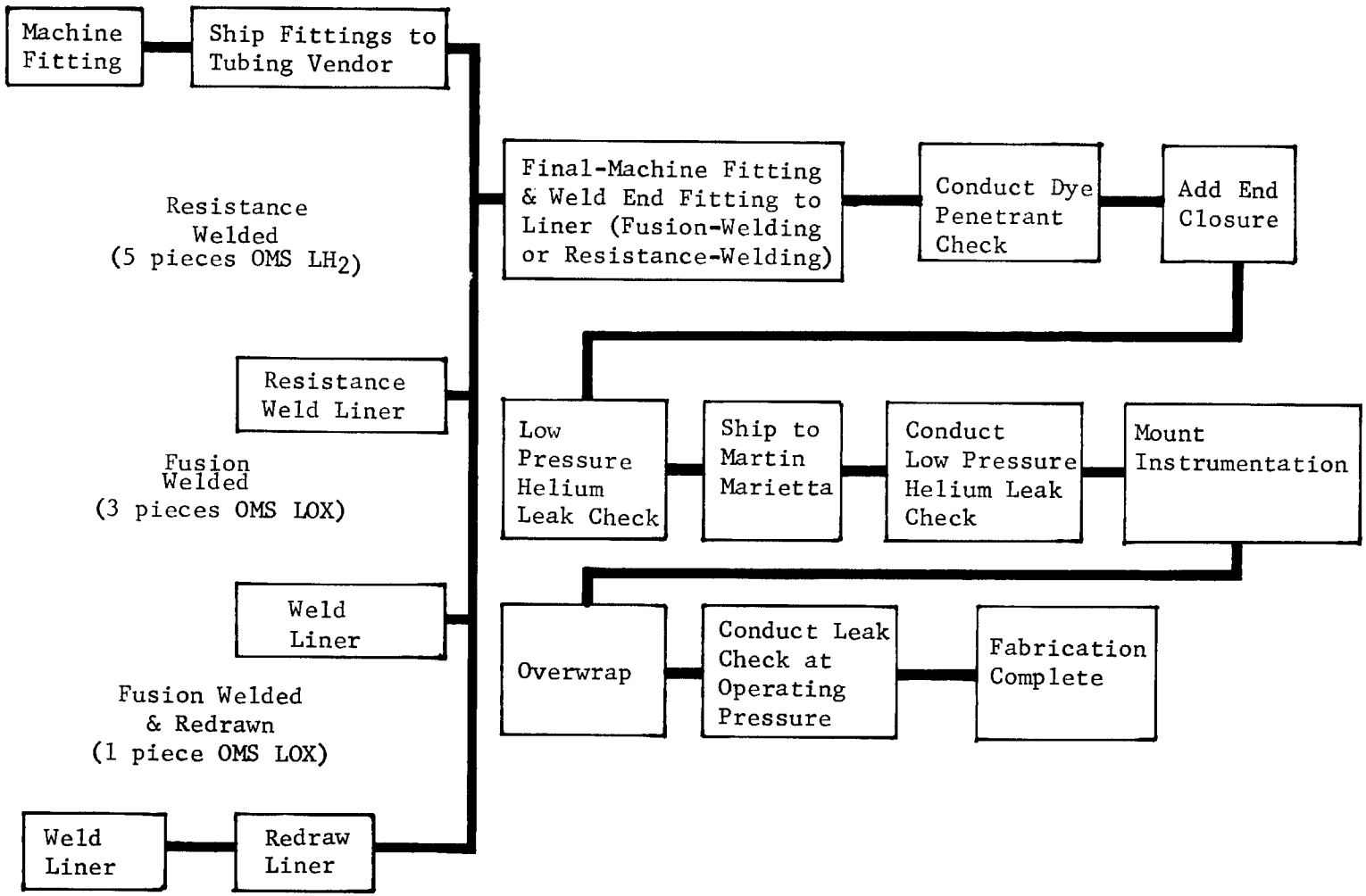

Figure 19. - Generalized Fabrication Flow Chart for OMS Feedlines

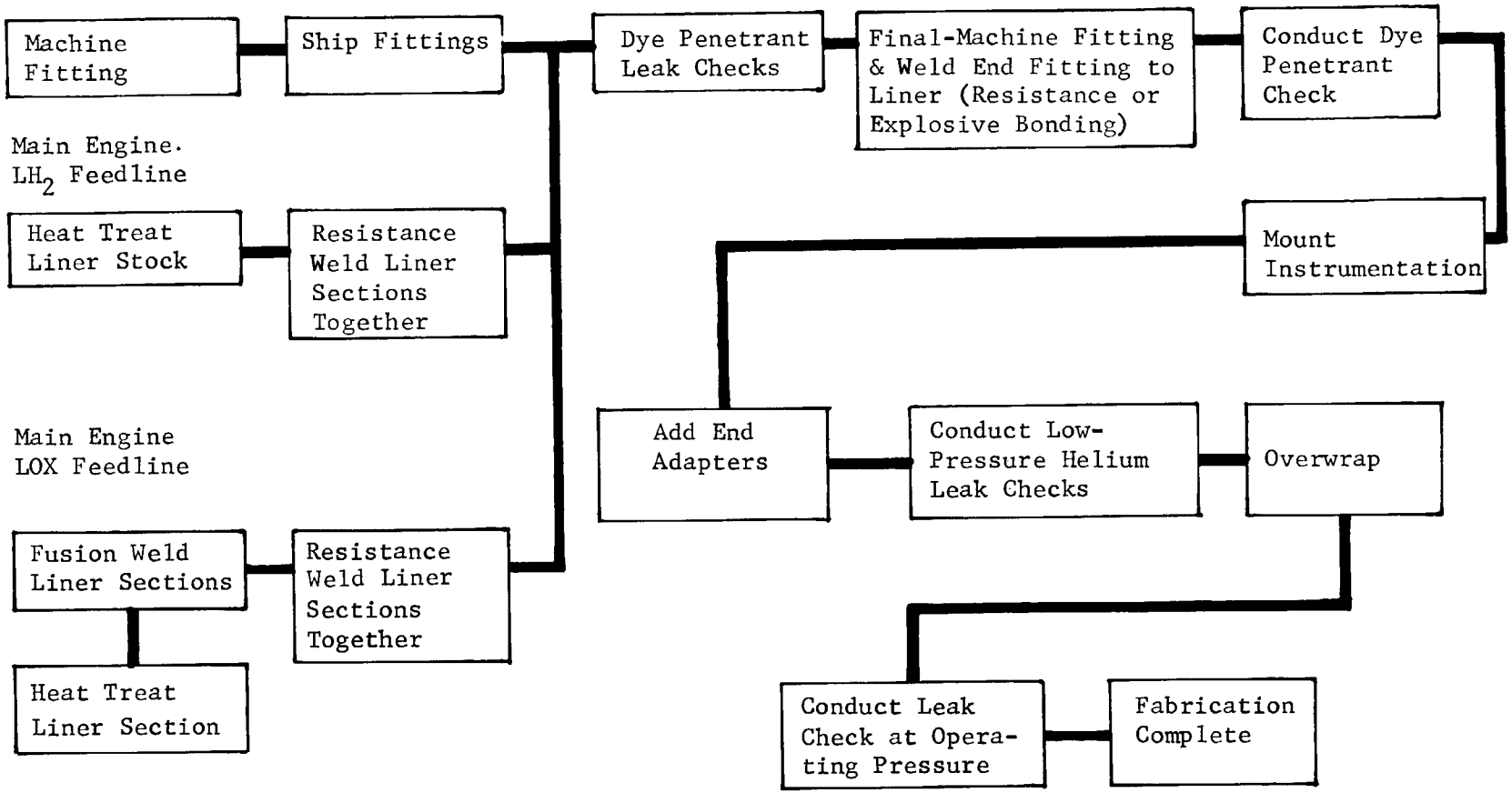

Figure 20. - Generalized Fabrication Flow Chart for Main Engine Feedlines

End Fitting Fabrication. - The requirements of the program dictated that flightweight fittings be used on the test specimens providing either weldable or mechanically connectable joints. The end fittings chosen were the butt-welded style. The internal configurations of the end fittings, where the liner welds or bonds to the end fitting, were set forth by the liner fabricators, or explosive bonder.

The OMS test item end fittings were configured to allow welding on end closures so a helium leak check could be performed by the liner fabricator. After overwrap and final leak checks, the end closures were removed. The end fittings were of sufficient length to allow joining the sections into an assembly or to another flange without having weld-heat effect the liners or overwrap.

The LH_2 main engine test item end fittings were fabricated from Inconel 718. The fitting is of a weight and strength optimized design. The end fitting design was affected by the vendors welding capabilities. Difficulties were encountered while machining these fittings, since the dimensions of the end fittings would change when removed from the lathe chuck as a result of residual stresses of the parent material from which the ring was machined. This problem was solved by annealing, heat treating and age hardening prior to machining the material. The end fittings were then shipped to the liner fabricator where they were resistance welded to the liner.

The main engine LOX test item end fittings were fabricated from 1100 aluminum. The end fittings were designed over-thick and hence over-strength since they were to be explosively bonded to the Inconel liner and the extra thickness could be used to prevent end fitting deformations during bonding. After bonding and overwrapping, the fitting can be machined to reduce its weight. The internal configuration of the end fitting was established by the explosive bonding vendor during the series of explosive bonding development tests (see page 64). The end fittings initially used on the actual test item were machined from a solid billet of 1100 aluminum to eliminate the weak area created by a weld seam. As a result of subsequent failure of one of the explosively bonded joints, it was necessary to salvage one of the previously used, rolled and welded fittings for use on the test item. The test item final configuration included one end fitting machined from a solid billet and one end fitting machined from a rolled and welded bar.

Liner Fabrication and Joining the End Fittings. - The three different methods of liner fabrication which were used include resistance welded, fusion welded from stock of desired final thickness, and helically wrapped and fusion welded followed by redrawing to the final thickness. The type of weld used to form the liner was also used to attach the end fitting (either resistance or fusion) except for the main engine LOX test item and one end of the preliminary test item which had explosively bonded end fittings.

Resistance welding technique: This tube fabrication technique required the liner to be roll-formed to the desired diameter with a slight overlap at

the mating surface as shown in Figure 21. An anode was placed in the liner and a resistance weld run down the length of the tube. The excess overlap on both the inside and outside of the tube was then peeled away from the weld. After peeling, the end fittings were installed on the liner using the same welding technique. This process was used for the OMS and the main engine LH_2 test items. This technique was also used to join the sections of the LOX main engine line. A major benefit of this weld method is the heat treating and age hardening can be performed prior to resistance welding and the low heat and small heat-affected-zone do not degrade heat treat.

The liner fabrication of the 38 cm (15 in.) diameter main engine feedline varied from the smaller diameter OMS liner fabrication since the smaller diameter liners could be fabricated from one piece of Inconel 718 stock. The larger diameter lines required welding several pieces of the stock together prior to making the close-out weld, forming the desired diameter liner. Table 10 shows the test item liner welds. Figure 22 shows the main engine LH_2 test item (with end fittings installed). The wrinkles which are clearly visible in the figure were caused by this process change and are analyzed in a later section of this report (page 86).

Fusion welding technique: The liner was formed by rolling a tube of the final thickness material to the proper diameter and preparing each of the butting edges with a slight curl. The seam along the length of the liner was then fusion welded. The fusion welded seam was then polished and planished, thus making the weld area conform to overall tube size with no weld buildup inside or outside the tube. Next, when appliable, end fittings were installed on the liner using the same welding technique. Heat treating and age hardening, if required for strength, was performed after fusion welding.

This welding process was used for three of the four OMS LOX lines. Figure 23 shows a typical liner and end fitting assembly prior to overwrap. This assembly includes sections 1 and 2 of the OMS LOX feedline butt-welded together with end closure flanges installed. The fusion weld process was also used to form the liner sections of the main engine LOX line and on the preliminary test item for both the longitudinal weld and one end fitting. The main engine LOX line without end fittings is shown in Figure 24.

Helically wrapped, fusion welded and redrawn: This technique for forming a liner required wrapping a 7.6 cm (3 in.) wide strip of metal around a mandrel in the form of a helix and fusion welding the edges. The liner formed by this process is then redrawn to the proper thickness and diameter also accomplishing the planishing and polishing of the weld in one operation. In this process, the vendor can weld thicker material and still meet the minimum gage requirements of 0.008 cm (0.003 in.). The strength of this tube is enhanced by the cold reduction process and it does not require heat treatment. This process as shown in Figure 25 was used on one of the OMS LOX feedline sections. By controlling the area which is redrawn, the vendor was able to maintain the original material thickness in the area adjacent to the end fitting which was installed by fusion welding. This technique was selected to enhance the reliability of the critical liner to end fitting weld without sacrificing weight.

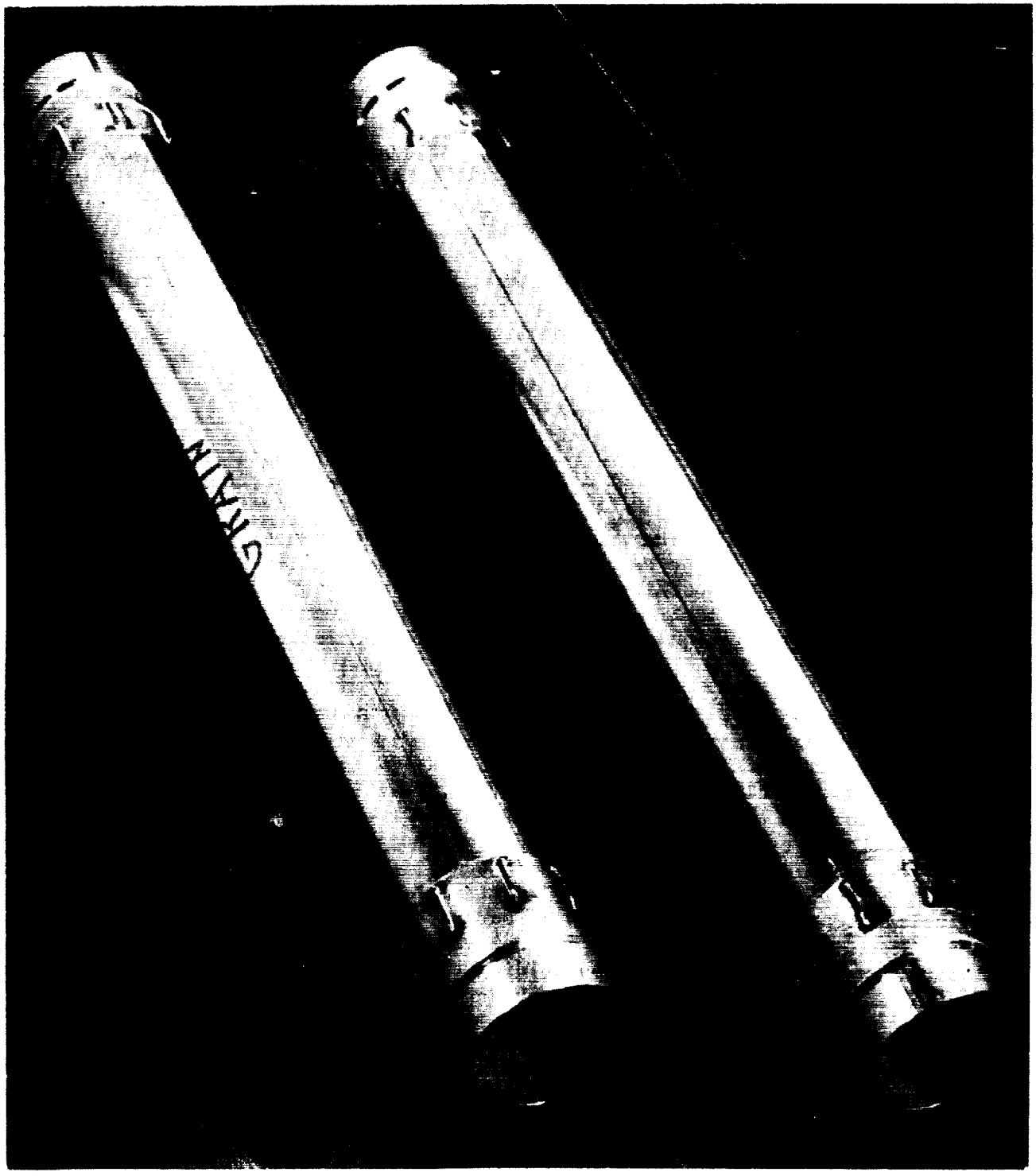

Figure 21. - Peeled and Unpeeled Resistance Welded Liners, 5 cm (2 in.) Diameter

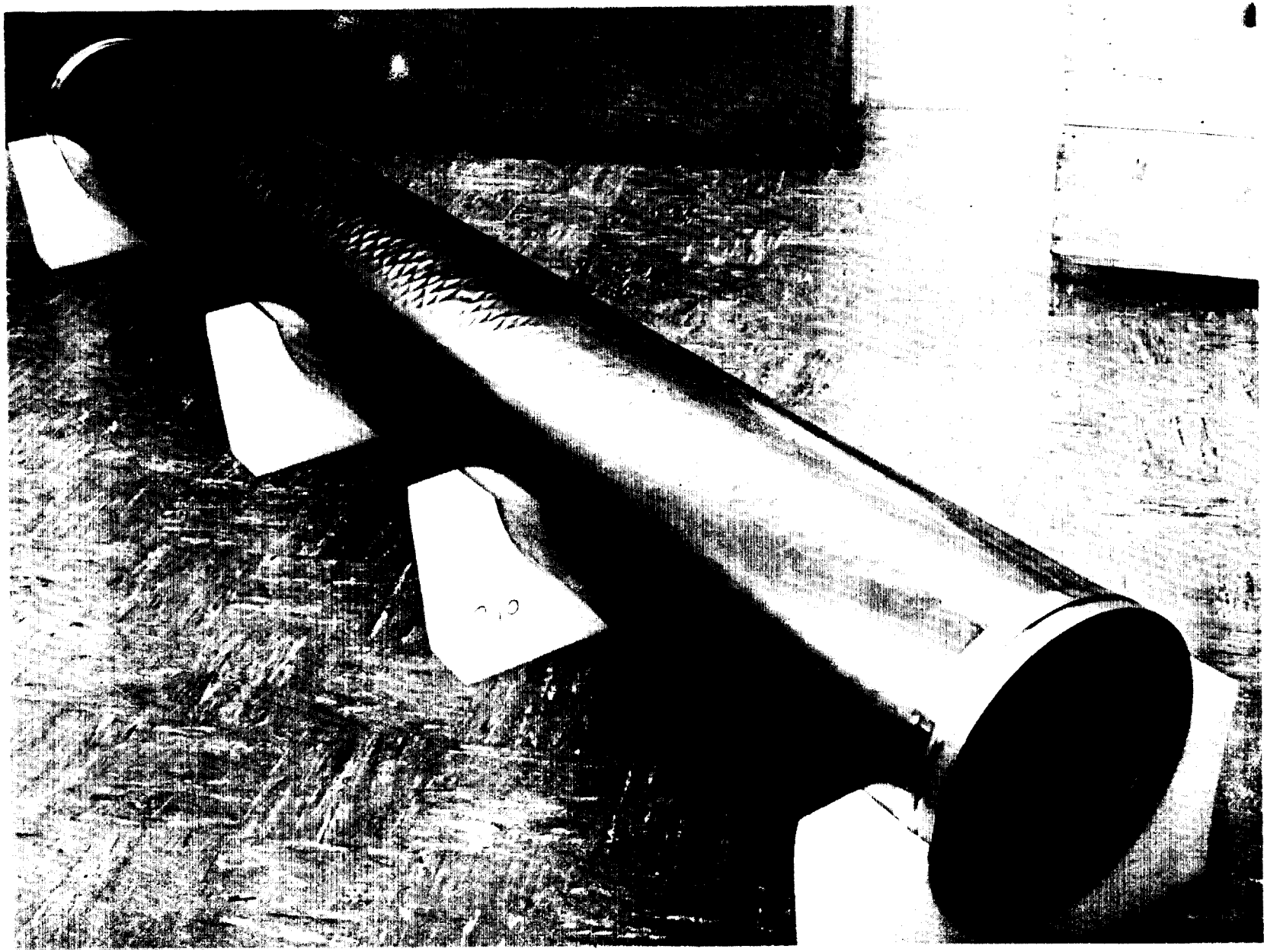

Figure 22. - LH_2 Test Item Liner Upon Receipt From Vendor

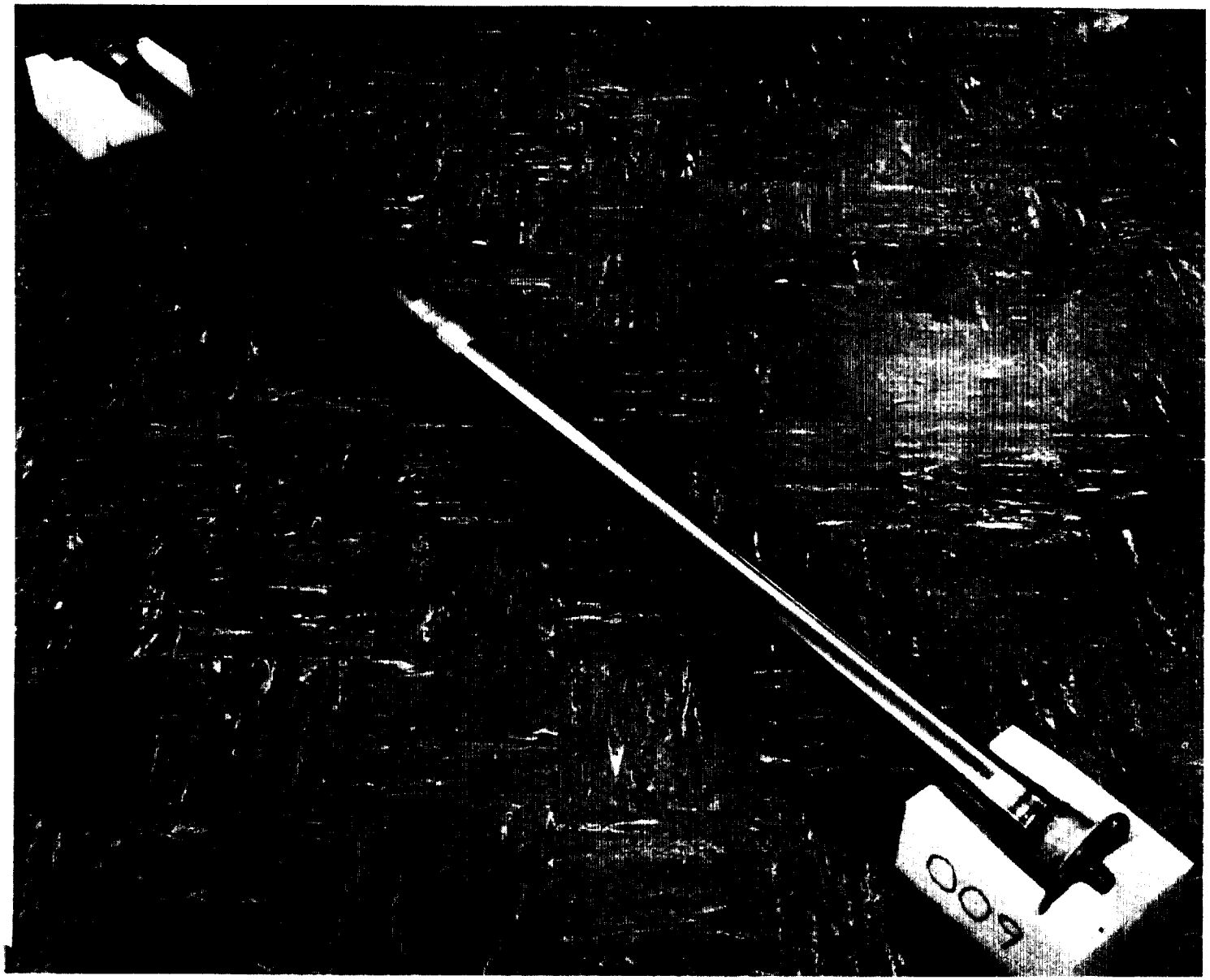

Figure 23. - OMS LOX Feedline Sections 1 and 2 Prior to Overwrap -- 6.4 cm (2.5 in.) Diameter

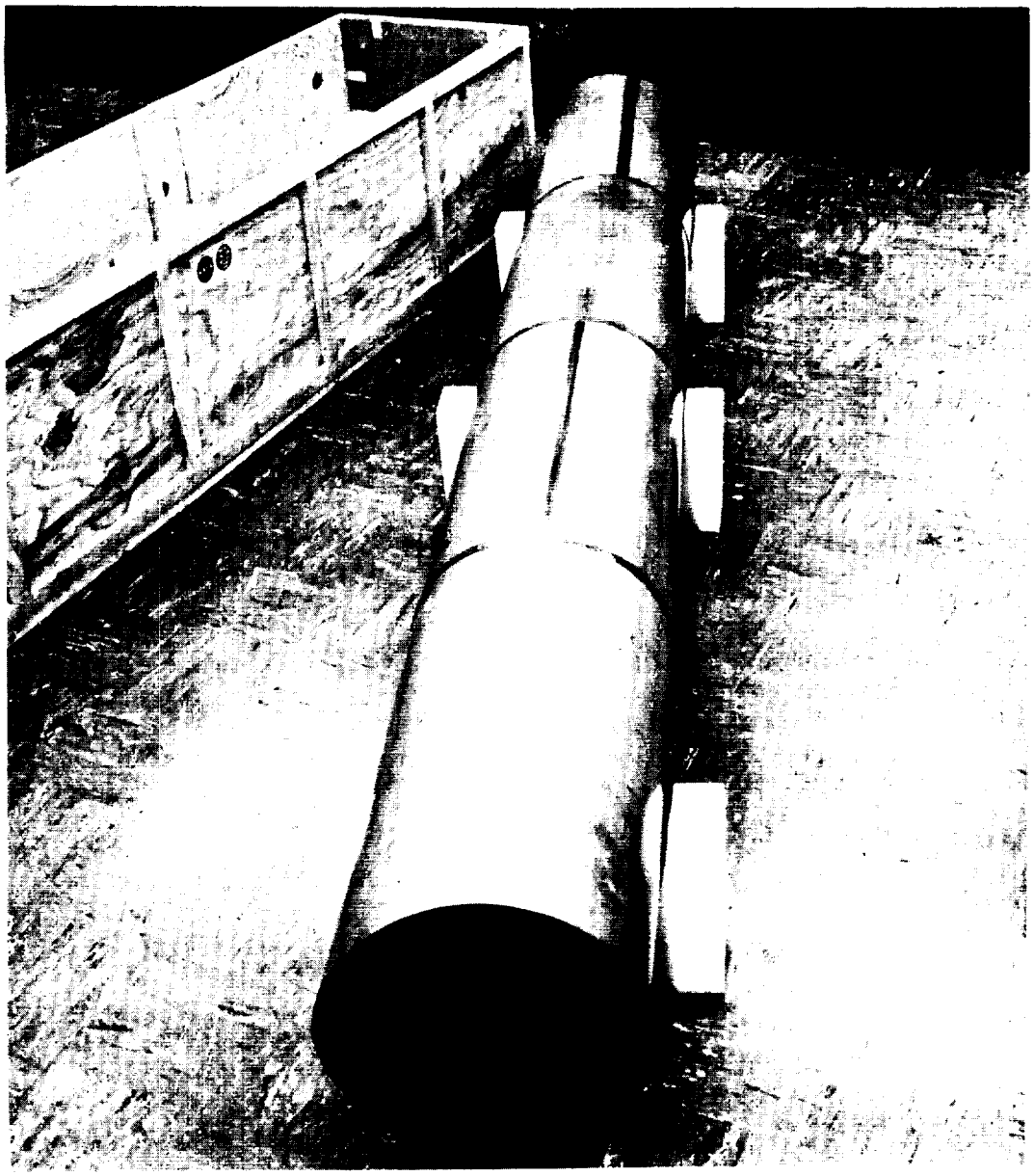

Figure 24. - LOX Main Engine Test Item Upon Receipt From Vendor

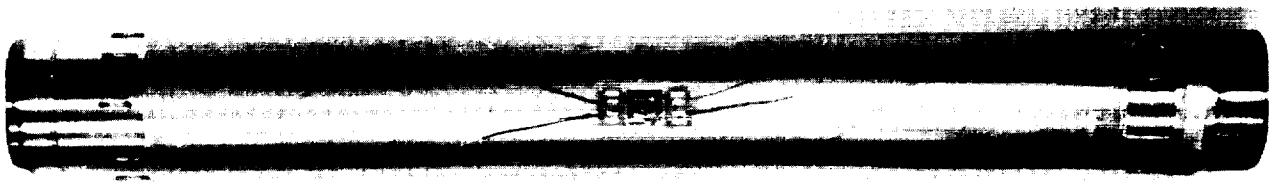

Figure 25. - Helically Welded Redrawn Liner

Explosive bonded end fitting installation: The preliminary test item was provided with one explosively bonded stainless steel end fitting. The LOX main engine feedline included two explosively bonded aluminum end fittings. Details of this process and of the LOX feedline bonding are discussed in the next section.

The preliminary test item explosive bond was considered successful although leakage did exist at several points. The leaks were attributed to an improper fit between the liner and the end fitting; i.e., the difference in the outside diameter of the liner and the inside diameter of the end fitting was too large although a visual prebond inspection seemed to show a good fit. A photograph of the joint resulting from the explosive bonding process is included as Figure 26. Figure 27 shows a closeup of the bonded area. Leaks in the joint can be repaired by bonding a patch over the leaking area in the manner shown in Figure 28 which is an example of a successful leak repair. The patch has been peeled back to inspect the bond.

Explosive Bonding. - Explosive bonding may be defined as the use of an explosive charge to develop heat and force to create a mechanical bond between two materials.

The initial development of explosively bonding fittings to thin metal liners was first performed on NASA Contract NAS3-12047. Under that development, the limited work done indicated that the joint was stronger than the base metal. It was also learned that dissimilar metals could be explosively bonded together with the bond being stronger than the weakest of the dissimilar metals.

Development program: The goal of the work to be performed under this contract was to begin with the successful result (achieved in bonding stainless steel to Inconel) from the prior program and successfully bond 38 cm (15 in.) diameter aluminum end fittings to an Inconel liner.

With limited funds and time allotted to the development of the explosive bonding techniques, the following program was set up in an attempt to achieve a successful large diameter aluminum to Inconel bond on the LOX main engine feedline.

1) Flat stock bond 0.015 cm (0.006 in.) thick Inconel to stainless steel plate;

2) Bond a 12.7 cm (5 in.) diameter, 0.015 cm (0.006 in.) thick Inconel liner into a stainless steel end fitting;

3) Bond a 38 cm (15 in.) diameter, 0.015 cm (0.006 in.) thick Inconel liner into a stainless steel end fitting;

4) Flat stock bond 0.025 cm (0.010 in.) thick silver to an aluminum plate;

Figure 26. - 38 cm (15 in.) Diameter, Stainless Steel to Inconel Explosive Bonded Joint

Figure 27. - Explosive Bonded Joint - Closeup View

Figure 28. - Leak Repair by Explosive Bonding a Patch Over the Leak Area

5) Bond a 12.7 cm (5 in.) diameter, 0.015 cm (0.006 in.) thick Inconel liner onto an aluminum end fitting;

6) Bond a 38 cm (15 in.) diameter, 0.027 cm (0.011 in.) thick Inconel liner onto an aluminum end fitting; and concluded by

7) Bonding aluminum flanges to the LOX test item.

Details of each of these steps, resulting in partially successful bonding of the aluminum fitting to the LOX main engine test item, are included in the following paragraphs.

The sketches below are used to clarify standoff and buffer nomenclature.

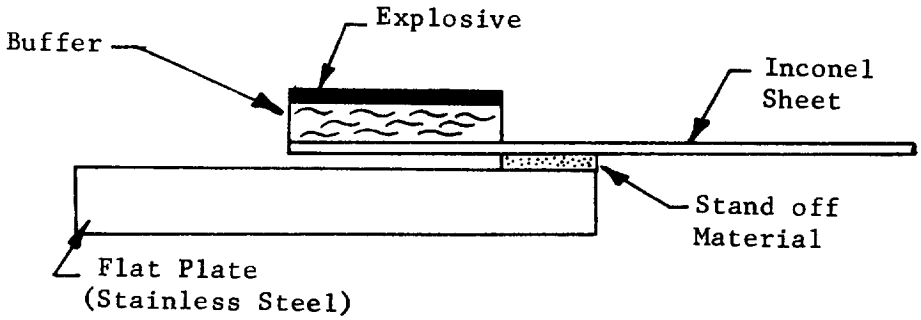

Parallel Standoff

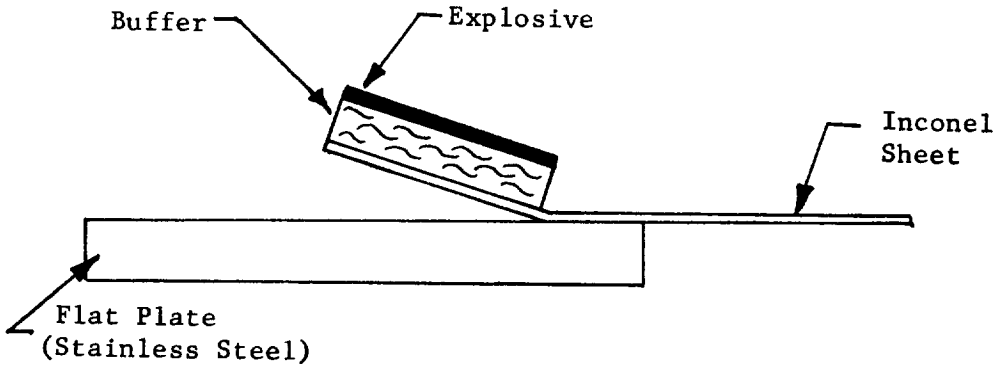

Angle Standoff

The buffer serves to reduce the heat and melt on the material to be bonded. The buffer material is generally a non-metallic soft material (i.e., cardboard, mylar, tape, etc.), does not adhere to the bond and is destroyed by the force and heat of the explosive charge.

The standoff serves to set the Inconel sheet at some distance from the material it is bonded to. The purpose of this precisely set distance is to allow the liner to gain velocity and force necessary to create a good

bond. The parallel standoff uses the same types of material as the buffer (i.e., cardboard, mylar, tape, etc.). The standoff literally stands the materials to be bonded away from each other while maintaining parallelism between the pieces. The parallel standoff material is always positioned out of the path of the bond. The bond path is considered to be the width of the explosive.

The angle standoff stands the materials to be bonded away from each other at a predetermined angle. The angle is formed by bending one of the materials to be bonded at the selected angle.

Flat stock bonds: Several approaches were used to develop the bond. The initial attempts were focused on bonding an Inconel liner to a stainless steel plate. Various combinations of explosives, explosive size, parallel and angle standoffs, and buffers were used. Eight attempts were made to bond 0.015 cm (0.006 in.) thick 718 Inconel sheet to 0.63 cm (0.25 in.) thick stainless steel plate. Specifics of these attempts are shown in Table 11. Test #5 gave the best results. A photo-micrograph (Figure 29) of the bond showed good bond waves which were fairly regular.

Bonding an Inconel liner into a stainless steel end fitting: Eleven attempts were made to achieve a successful bond of an Inconel liner onto a circular stainless steel 12.7 cm (5 in.) end fitting. Specifics of these attempts are shown in Table 12 using a continuing sequence to avoid confusion with the first eight tests. The final test in this series was used to bond the end fitting to the 38 cm (15 in.) diameter preliminary test item.

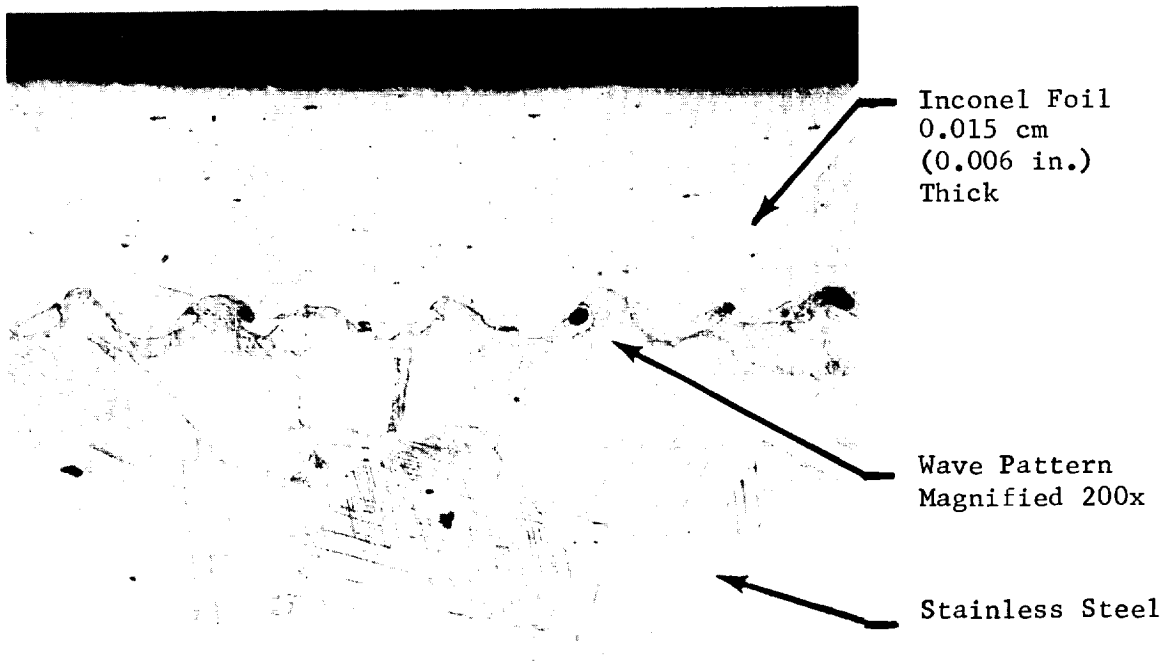

Figure 29. - Photomicrograph of Inconel to Stainless Steel Bond

TABLE 11.- FLAT PLATE BOND DEVELOPMENT

+Explosive	grams/cm^2	grams/in^2	Standoff	Buffer
Test #1 .025 Detasheet	0.09	0.60	0.38 cm (0.15 in.) Parallel	0.076 cm (0.030 in.) Cardboard
Test #2 .042 Detasheet	0.16	1.00	0.38 cm (0.15 in.) Parallel	0.076 cm (0.030 in.) Cardboard
Test #3 .042 Detasheet	0.16	1.00	0.175 rad (10°) Angle	0.076 cm (0.030 in.) Cardboard
Test #4 .063 Detasheet	0.23	1.50	0.175 rad (10°) Angle	0.076 cm (0.030 in.) Cardboard
Test #5 .025 Detasheet	0.09	0.60	0.175 rad (10°) Angle	0.076 cm (0.030 in.) Cardboard
Test #6 SWP-2	0.93	6.00	0.10 cm (0.040 in.) Parallel	0.076 cm (0.030 in.) Cardboard
Test #7 SWP-2	0.93	6.00	0.165 cm (0.065 in.) Parallel	0.076 cm (0.030 in.) Cardboard
Test #8 .042 Detasheet	0.16	1.00	0.175 rad (10°) Angle	0.089 cm (0.035 in.) Vinyl*

+The difference between explosives, other than grams/cm^2 is the rate of burn which alters the velocity of the moving piece. The burn rates are: Detasheet 6,800 m/sec (22,310 ft/sec) and SWP-2 2,743 m/sec (9,000 ft/sec).

*Vinyl was used because cardboard of sufficient size was not available.

TABLE 12.- CIRCULAR BOND DEVELOPMENT

+Explosive	grams/cm^2	grams/in^2	Standoff *	Buffer
Test #9 .025 Detasheet	0.09	0.60	Conical 0.088 rad (5°) Angle	0.020 cm (0.008 in.) Mylar
Test #10 .025 Detasheet	0.09	0.60	Conical 0.088 rad (5°) Angle	0.020 cm (0.008 in.) Mylar
Test #11 SWP-2	0.93	6.0	0.076 cm (0.030 in.) Parallel	0.020 cm (0.008 in.) Mylar
Test #12 SWP-2	0.93	6.0	0.025 cm (0.010 in.) Parallel	0.020 cm (0.008 in.) Mylar
Test #13 .042 Detasheet	0.16	1.0	Conical 0.088 rad (5°) Angle	0.025 cm (0.010 in.) Mylar
Test #14 .063 Detasheet	0.23	1.5	Conical 0.088 rad (5°) Angle	0.020 cm (0.008 in.) Mylar
Test #15 .042 Detasheet	0.16	1.0	Conical 0.175 rad (10°) Angle	0.020 cm (0.008 in.) Mylar
Test #16 .025 Detasheet	0.09	0.60	0.14 rad (8°) Recessed Angle	0.025 cm (0.010 in.) Tape
Test #17 .025 Detasheet	0.09	0.60	0.14 rad (8°) Recessed Angle	0.018 cm (0.007 in.) Mylar
Test #18 .025 Detasheet	0.09	0.60	0.14 rad (8°) Recessed Angle	0.018 cm (0.007 in.) Mylar
Test #19▲ .025 Detasheet	0.09	0.60	0.14 rad (8°) Recessed Angle	0.018 cm (0.007 in.) Mylar

+The difference between explosives, other than grams/cm^2 is the rate of burn which alters the velocity of the moving piece. The burn rates are: Detasheet 6,800 m/sec (22,310 ft/sec) and SWP-2 2,743 m/sec (9,000 ft/sec).

▲This test was performed on the 39 cm (15 in.) diameter preliminary specimen.

*See following sketches for definition of conical & recessed standoffs.

During this phase of the development, two new standoff styles were developed, a conical and a recessed angle.

The conical standoff is metal and uses the same principle as the previously defined angle standoff. The buffer and explosive are placed on the angle as before to meet different test requirements. As shown in Table 12, test #9, #10, #13, #14, and #15 used conical standoffs.

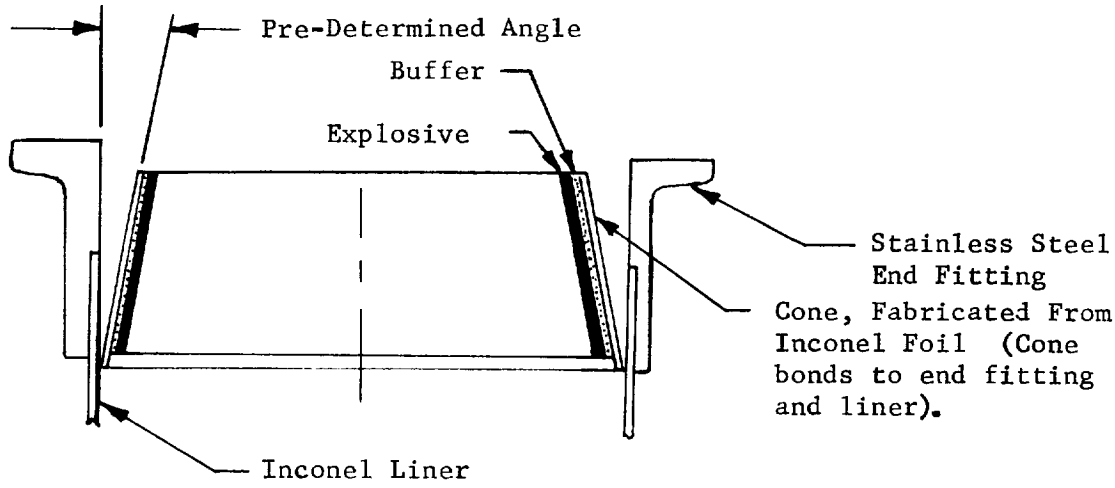

The recessed angle style involves machining the desired angle into an end fitting and proceeding with the tests as before, using different explosives or buffers as required. Tests #16, #17, #18, and #19 used the recessed angle style.

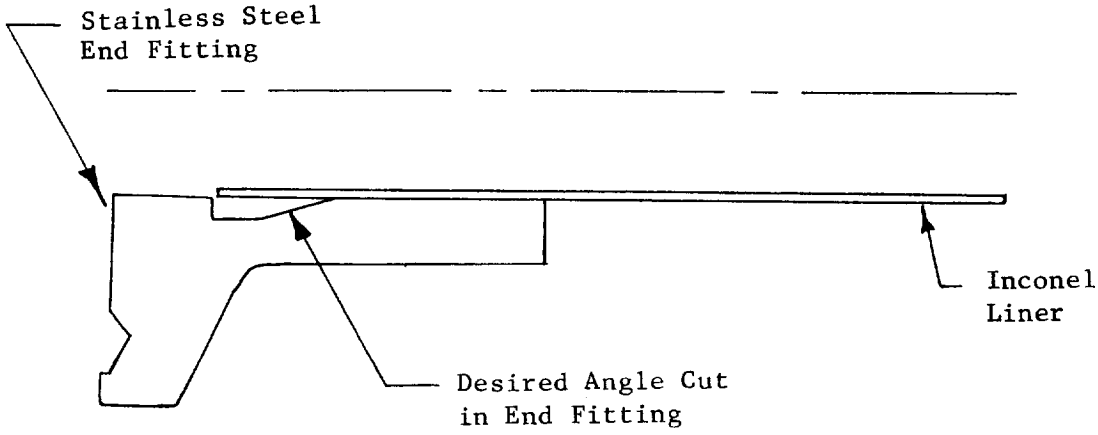

Patching: Because of the cracks and shear areas developed on Test #19, it was decided to attempt to patch these cracks using explosives and the concepts developed in earlier tests. The four patching attempts used the same explosive charge and buffer used in Test #19. The standoff was 0.015 cm (0.006 in.) Inconel set at 0.14 radians (8^{o}) angle. The standoff was cut to a size which would fit over the defective area. Of the four attempts at patching, one was successful. The other three took on the characteristics of the bad areas they attempted to patch.

Resolution of testing thru Test #19 including patches: It was determined that it is possible to achieve a good bond between thin Inconel liners and stainless steel end fittings up to 38 cm (15 in.) diameter. It was also determined that patching of defects in a bonded joint was practical depending on the seriousness of the defect. To assure a good bond in large diameter assemblies it was recommended that the tolerance of the end fittings and liner should be such that a minimum clearance fit always exists while staying away from an interference fit. To assure proper fit, the liner should be swaged into the end fitting with the use of an expanding mandrel.

Aluminum to Inconel bonding: To further develop the concepts used in the first nineteen tests, attempts were made to explosively bond 0.015 and 0.027 cm (0.006 and 0.011 in.) thick Inconel to an aluminum end fitting.

A test for test account will not be given in this report since most test set ups were repetitious of Test #19, with varying explosives and buffers. The major difference was the use of a sterling silver intermediate between the Inconel and aluminum, which becomes a part of the bond. The development of this tri-metal bond was done by the vendor on previous work in a different configuration when they determined that a bond of Inconel directly to aluminum was not practical.

The approach was to bond a 0.025 cm (0.010 in.) thick silver collar into the recessed angle bond area of the aluminum fitting. Then the Inconel was bonded to the silver collar. The first seventeen tests were used to bond the silver into the recessed angle. The successful test set up is shown in the following sketch. The transfer adhesive allowed the 1100-0 aluminum plate to be removed without degrading the silver to aluminum end fitting bond.

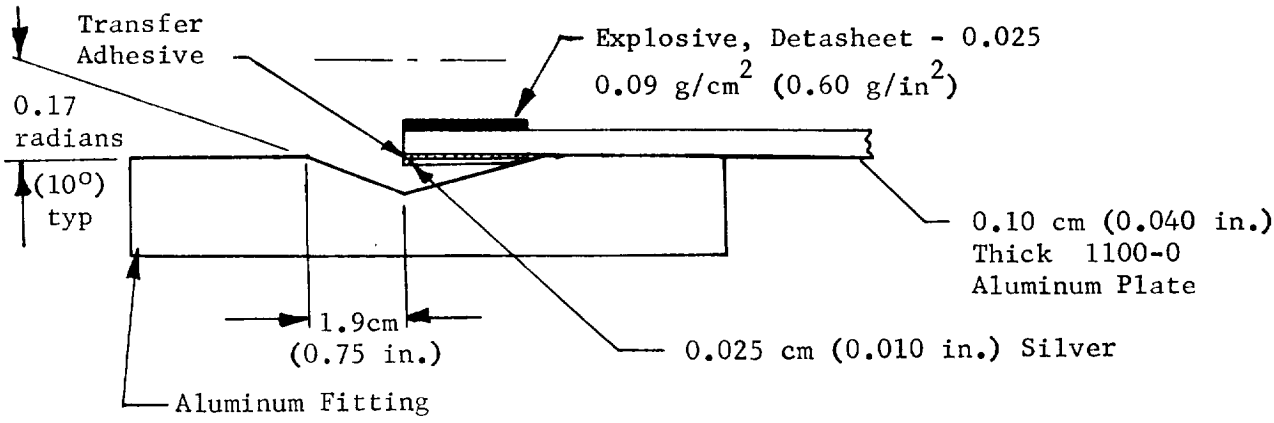

It is important to note that the recess angle is cut from both edges of the fitting. The reason for cutting the angle from both edges, versus cutting from one edge, as developed earlier, was because of high pressure air erosion of the fitting. Figure 30 shows both fitting concepts. The erosion is severe in aluminum as compared to stainless steel because of its material characteristics. It may be theorized that the single recess angle cut in a stainless steel fitting, even though erosion of the fitting was not evident, may have caused back pressure which could have been involved in the failure of the 38 cm (15 in.) diameter inconel to stainless steel fitting test (Test #19). However, more tests would be needed to substantiate this theory.

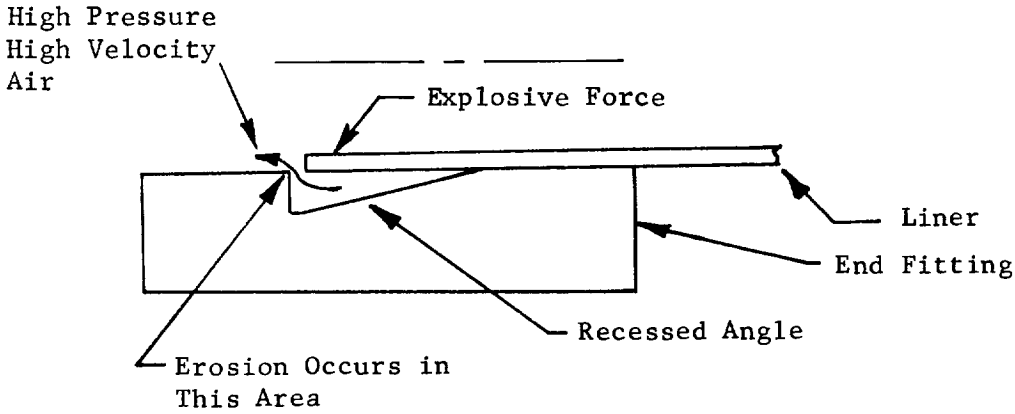

Single Recessed Angle

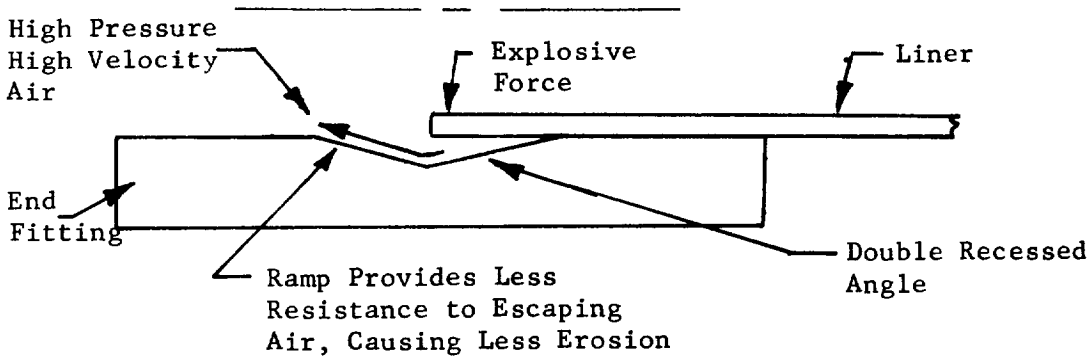

Double Recessed Angle

Figure 30. - End Fitting Recessed Angle Configurations

After successfully bonding the silver into the aluminum fitting the next step was to bond the Inconel into this assembly. The successful set up used a 12.7 cm (5 in.) diameter 0.015 cm (0.006 in.) thick Inconel liner bonded into an aluminum end fitting. The charge was Detasheet 0.025, 0.09 grams/cm^2 (0.60 grams/in^2). Tape was used as a charge cover, and 0.018 cm (0.007 in.) thick mylar was used as a buffer as shown in the sketch.

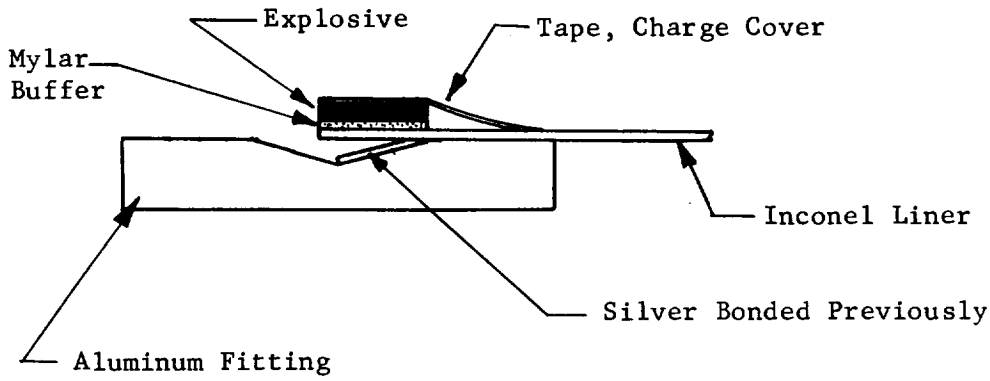

The result of the above was a leak-free bond, which appeared to have the structural integrity explosive bonds are noted for as well as a smooth transition area which will cause as little flow disturbance as possible.

Full scale aluminum to Inconel bonding: The next step in the explosive bonding procedure was to bond an aluminum fitting to a 38 cm (15 in.) diameter Inconel liner 0.015 cm (0.006 in.) thick. The procedure used to bond this fitting was identical to that used on the successful aluminum to Inconel 12.7 cm (5 in.) diameter bond including the charge, buffers, and angle. A split mandrel was used to assure a good fit between the fitting and liner. The result of the test was a good bond in all areas except above the weld line of the aluminum fitting which was made from a rolled and welded bar where there was an approximate 0.6 cm (0.25 in.) width of unbonded area. The failure of the explosive bond was attributed to the fusion weld in the aluminum fitting which had improper weld penetration. One solution of this problem is to use aluminum fittings machined from a billet. Since an aluminum fitting which was rolled and

and welded from a bar still existed, an attempt was made to salvage it by re-welding the ring to get 100% penetration. This fitting was used for the next explosive bonding test.

The next step in the explosive bonding development was to bond an aluminum fitting to a 38 cm (15 in.) diameter Inconel liner which was 0.027 cm (0.011 in.) thick which represented the thickness of the LOX test item liner. The procedure used to bond this fitting was identical to that used on the successful aluminum to Inconel 12.7 cm (5 in.) diameter bond including the charge, buffers and angle. The bond was successful and showed no dye penetrant leaks.

The photomicrographs in Figures 31 and 32 illustrate some of the bonds developed during this test program, specifically the aluminum to silver and the aluminum to silver to Inconel.

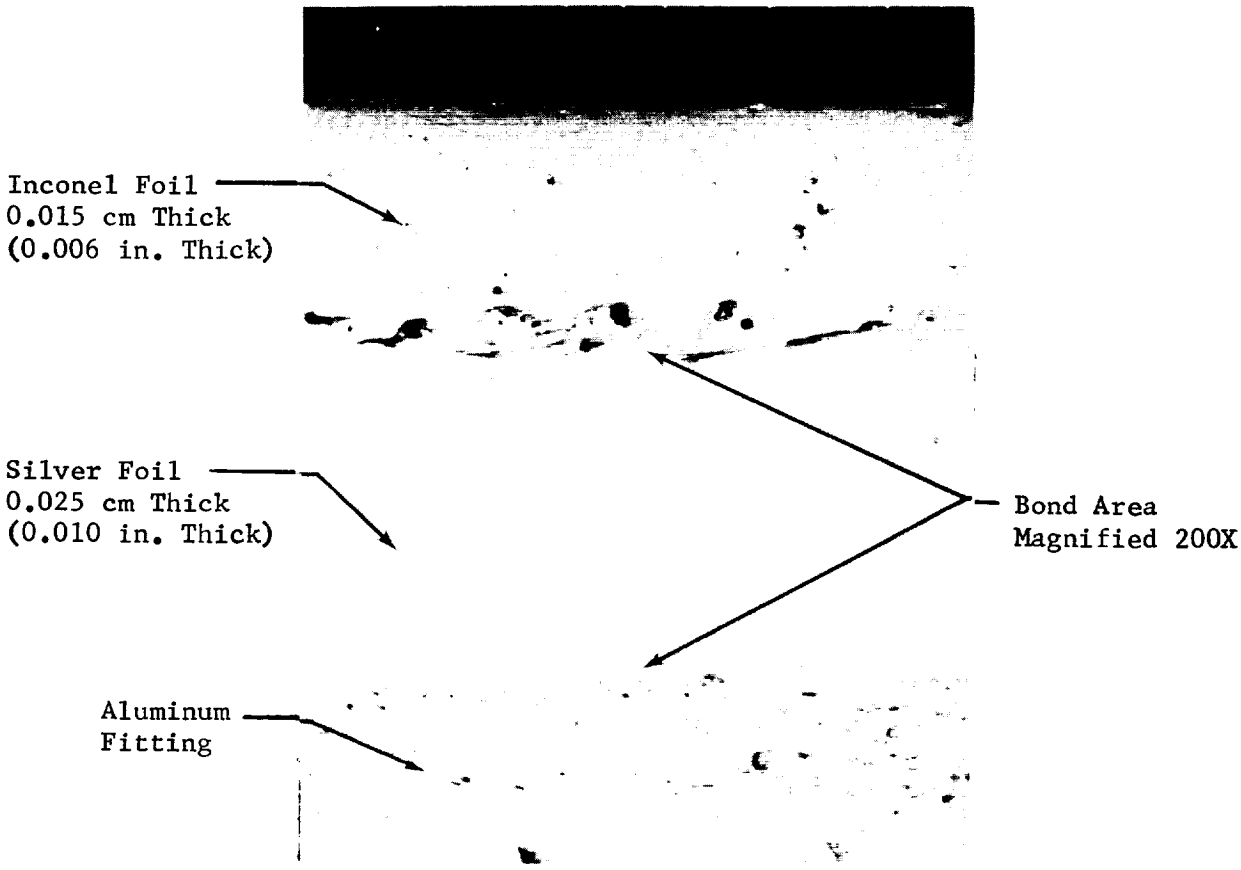

Figure 31. - Photomicrograph, Aluminum to Inconel Bond

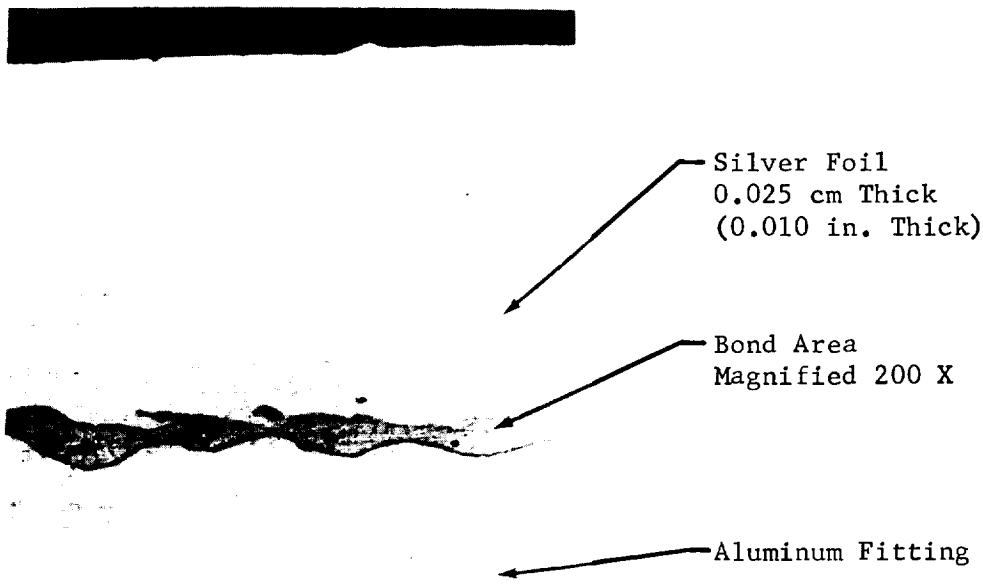

Figure 32. - Photomicrograph of Aluminum to Silver Bond

Cold shock test: The 38 cm (15 in.) diameter assembly, formed above using the 0.015 cm (0.006 in.) thick liner, was subjected to a liquid nitrogen cryogenic shock test. The item was immersed into an open liquid nitrogen cryostat and allowed to remain submerged until the surface of the liquid became quiesent indicating stabilized temperature. The item was quickly removed from the LN_2 and during the warm-up period the liner buckled.

Considering the difference in coefficient of thermal expansions of the two metals, the buckling of the liner can be explained. The thin wall liner, with very little mass, reached ambient temperature within three minutes time. The aluminum end fitting with a much larger mass, required 25 minutes time to reach ambient temperature. During this time the aluminum flange induced compressive loads in the hoop direction sufficient to fail the liner in compressive hoop buckling. The liner hoop buckling can be prevented by increasing the liner thickness or overwrapping with fiberglass.

The assembly using the 0.027 cm (0.011 in.) liner was also cryogenically shocked in the same manner as the previous 38 cm (15 in.) diameter assembly. The thicker liner prevents buckles from developing in this assembly.

LOX main engine test item bonding: The bonding of aluminum end fittings to the LOX main engine test item was performed using the experience gained in the development program. The fittings were machined from a billet of solid aluminum. The bonds were successful and exhibited no leakage when checked with dye-penetrant.

One of the aluminum end fitting bonds failed while attempting to weld an aluminum cap to the assembly. This failure is discussed later in this report (page 88), but it required the bonding of another joint. At this time, the fitting selected had been used previously and included a seam weld.

Conclusions: Successful bonds were made at each level of the development. The lightweight characteristics of this joint style should provide impetus to the resolution of the remaining problems.

Overwrap. - After end fittings were attached and end closures were installed to permit test item pressurization, the test items were overwrapped. Prior to overwrap, all test items were coated with Dow-Corning DC-20 silicone release agent.

The overwrap consisted of three distinct layers: Hoop, longitudinally laid, and hoop, applied in that order. The hoop roving was applied under a predetermined wrap tension. The longitudinal cloth was laid the length of the test item and consisted of equal widths of cloth separated by equal width gaps. The hoop wound glass-fiber roving was 20 end S/HTS-901 fibers preimpregnated with 58-68R resin. The longitudinally laid cloth was 1557 glass, hand impregnated with 58-68R resin. The resin content was specified to be between 20 and 25%. The hoop wound roving is applied at a rate of 6.3 turns/cm (16 turns/in.). Required instrumentation was installed on the longitudinal cloth and secured in place when the final hoop layer of overwrap was applied. Table 13 shows various specifics of the overwrap.

The 58-68R resin matrix and cloth mat require a cure cycle at elevated temperatures. Several combinations of time and temperature are acceptable. Figure 33 shows the cure temperature profile used for all test items except the main engine LOX test item. Constant positive internal pressure was maintained during cure.

The failure of an explosively bonded joint on the main engine LOX line made it necessary to extend cure time and lower cure temperature. The overwrap cure cycle for the main engine LOX line is shown in Figure 34. [The early failure of an explosive bonded joint, as discussed later in this report (page 88) was attributed to thermal expansion.] The new cure cycle eliminated the explosive bond thermal failure problem.

TABLE 13.- TEST ITEM OVERWRAP PARAMETERS

Test Item	Section No.	Liner Internal Pressure		Overwrap Tension/20 Ends		Longitudinal Cloth Width & Gap	
		N/cm^2	(psi)	kg	(lb)	cm	(in.)
OMS LOX	1,2,& 3	17.2	25	1.4	3.0	2.0	.78
	4	17.2	25	1.4	3.0	1.6	.62
OMS LH_2	1,2,& 3	17.2	25	1.7	3.75	1.5	.58
	4 & 5	17.2	25	1.7	3.75	1.2	.48
Main Engine Preliminary One Assembly		17.2	25	1.8	4.0	3.5	1.38
Main Engine LOX One Assembly		27.6	40	1.4	3.0	3.5	1.38
Main Engine LH_2 One Assembly		10.3	15	1.8	4.0	3.5	1.38

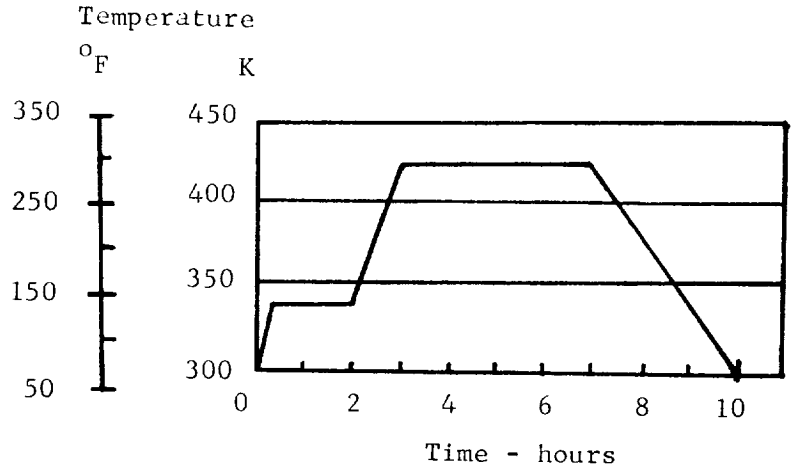

Figure 33. - Overwrap Cure Cycle

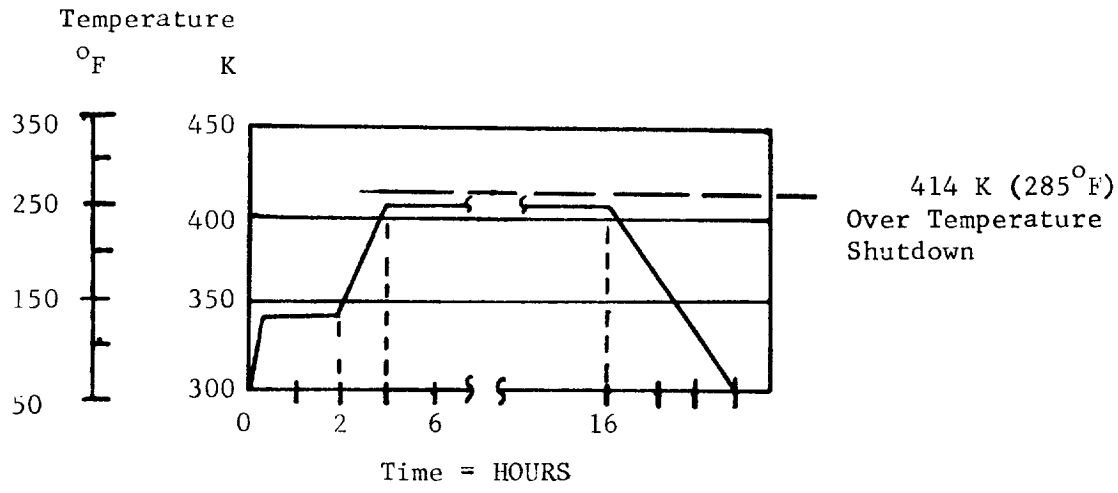

Figure 34. - Overwrap Cure Cycle for Explosive Bonded Joint

Figure 35 shows a test item being overwrapped. Figure 36 and 37 show typical overwrapped tubes.

Leak Tests - In-Process Verification. - During various stages of the test item fabrication leak tests were performed to determine the quality of the various test items at each fabrication level. Two types of leak checks were performed on the test items at various steps. These were helium mass spectrometer and dye penetrant leak checks.

As an in-process verification, the weld which forms the liner, prior to welding on end fittings, is dye penetrant leak checked. After welding or explosively bonding end fittings to the liner the end fitting attachment weld or bond was also dye penetrant leak checked serving as another in-process verification. After end fitting closures were welded in place, permitting internal pressurization of the tube, the assemblies were subjected to a low pressure helium leak check which completed the final in-process verification of the metal assemblies. Safety restrictions and/or material yield strength precluded leak checks at operating pressure until the overwrap system was installed and cured.

Upon receipt of the test articles from the tubing vendor, the liner assembly underwent another low pressure helium leak check to determine if any damage occurred during shipping. The final in-process leak check occurred after the assembly had been overwrapped and cured. This was also a helium leak check, but at system operating pressure. The results of the test item leak checks are covered in the testing section of this report (page 94).

Insulation Installation. - The OMS LOX system was insulated with 20 layers of double aluminized 1/4 mil mylar separated by 20 layers of 10 mil thick nylon net. The insulation was used only on one of the steady-state heat input tests for the OMS LOX system. The joints were of a lap joint butt-style as shown in the following sketch.

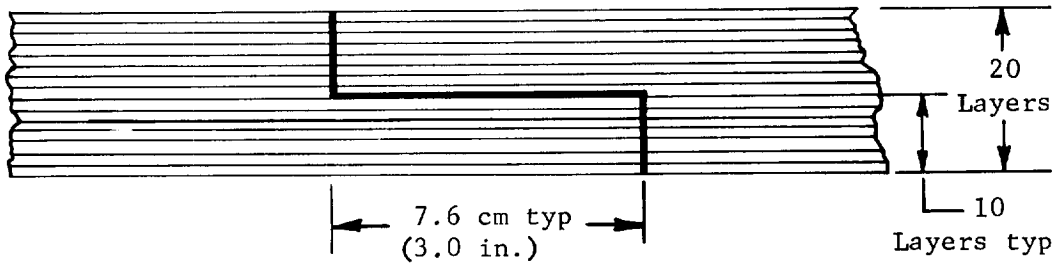

Figure 35. - LH_2 Test Item Installed in En-Tec Winder

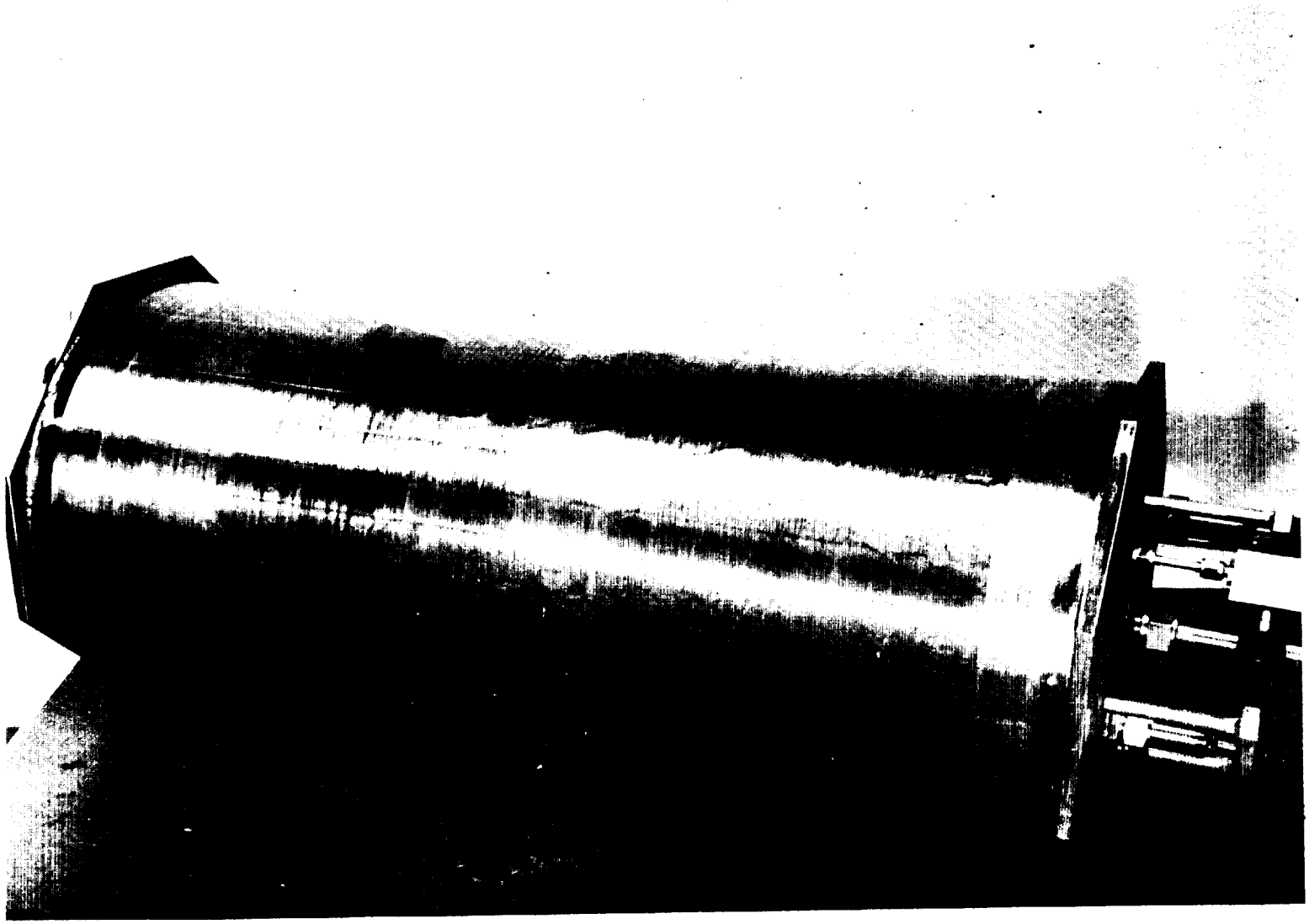

Figure 36. - Completed, 15" Diameter Preliminary Test Specimen

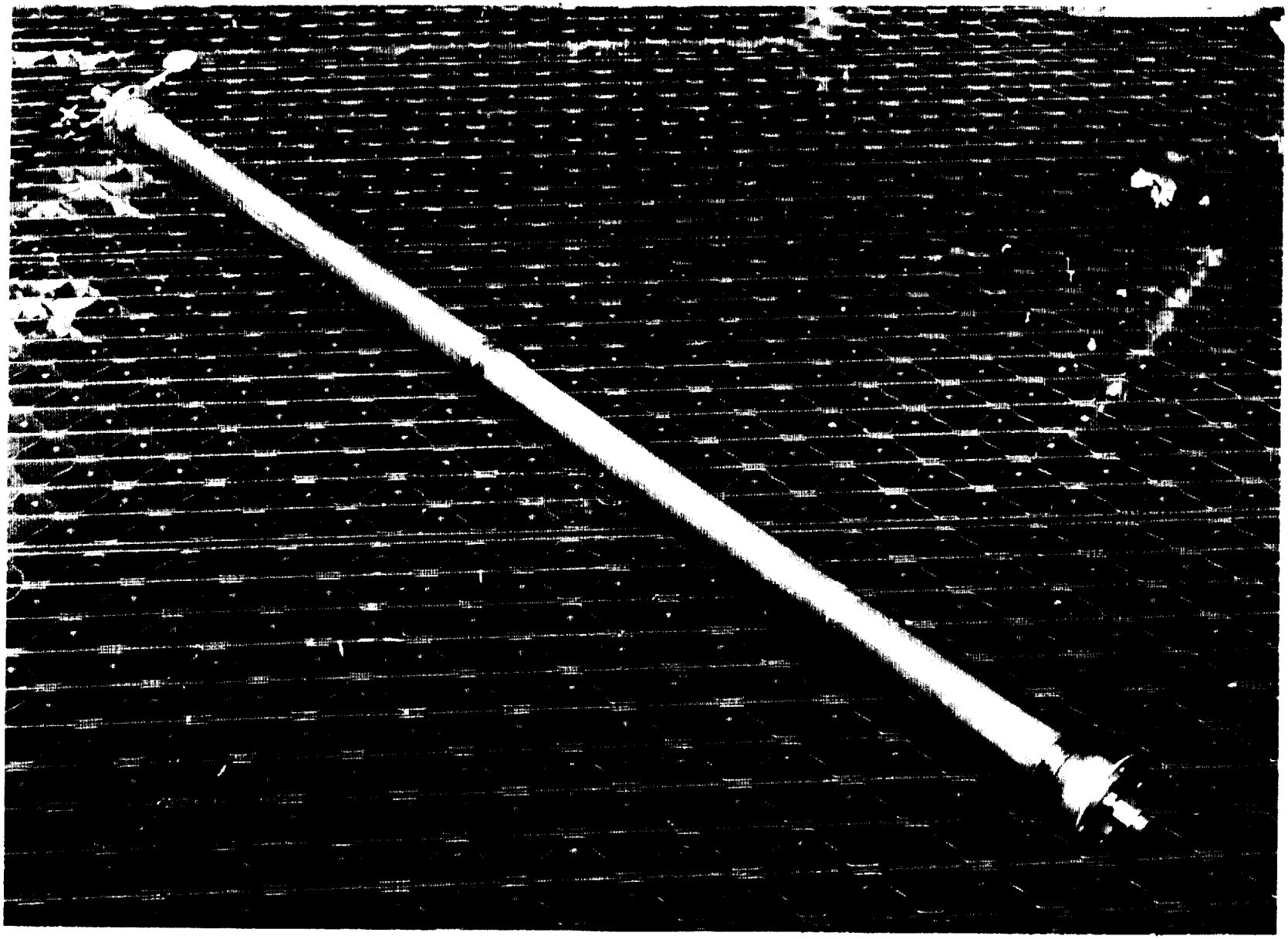

Figure 37. - OMS LOX Feedline Sections 1 and 2 After Overwrap -- 6.4 cm (2.5 in.) Diameter

The LH_2 OMS system had one layer of double aluminized 1/4 mil mylar installed for emissivity purposes. This same technique was used for the LOX OMS system for one run of the steady-state heat input test.

The LH_2 OMS tube used for the radial thermal conductivity testing was insulated per the sketch with 60 layers packed to a total thickness of 2.5 cm (1 in.).

The main engine LH_2 test item was insulated with a quick setting, spray on, closed cell urethane foam. Foam depth was 15 cm (6 in.). The insulation was added to conserve liquid hydrogen and prevent the formation of liquid air during testing. The main engine LOX test item was not insulated since the test cryogen was liquid nitrogen, which is a less costly commodity and presents no safety hazard as result of liquid air formation.

Test Fixture Design and Fabrication. - Test fixtures were either modified from those used in Contract NAS3-12047 or specifically designed for this program. A single test fixture was designed and fabricated for use on the thermal cycle, pressure cycle, bending, and torsion tests of the main engine test items. The fixture consisted of a liquid hydrogen, liquid nitrogen, and hot gas supply, structural support and the test item. Modified test fixtures were used to perform the OMS test item cycle testing, leak testing, and burst testing. New fixtures were designed to perform the OMS test item flow tests, radial thermal conductivity, heat capacity and vibration tests. Details and schematics of these fixtures are shown in the test section of this document (page 94).

The designs incorporated the necessary safety considerations and provided predictable and controllable operation without compromising technical objectives. Established design practices for cryogenic and high-pressure gas systems were employed to ensure adequate safety factors for all fixtures.

The major effort of the test fixture design and fabrication was centered around the vacuum chamber used for the OMS test item flow testing and steady-state heat input testing. The use of the vacuum chamber allowed the testing to be performed in a more realistic environment.

Required Modifications and Fabrication Problems. - During fabrication of the various test items, several problems were encountered which required some modification of the design criteria. The problems encountered and the design changes or corrective actions taken for each problem are discussed in the following paragraphs.

Main engine preliminary test item: Throughout the overwrap and cure process, the test item was pressurized internally to approximately 14 N/sq cm (25 psi). A visual inspection of the test item, after completing the cure process, showed indications of liner buckling. An inspection of the test item interior confirmed that buckling existed, but due to the limited field of view of the borescope, the type of buckling could not be determined. One closure plate was removed from the test item to allow a closer inspection. This inspection

showed that the buckling, shown in Figure 38, was characteristic of a compressive failure in the longitudinal direction and it was suspected that the failure occurred during the cure cycle. After completing the overwrapping, the glass-resin composite is cured at elevated temperatures by placing the test item in an oven and increasing the temperature to 340 K (150°F) for two hours. The temperature is then increased to 420 K (300°F) and maintained for a period of four hours. The oven temperature is then linearly decreased to ambient over a three hour period. When the over temperature is initially increased, the temperature of the thin metal liner will increase rapidly and the liner will attempt to grow. The temperature of the solid support rods will not increase as rapidly due to the mass and location of the rods in a quiescent atmosphere, so the support rods will not grow at the same rate. The support rods would, therefore, restrain the expansion of the liner and force the liner into compressive buckling.

An analysis of the liner stress condition during the initial temperature increase, assuming no growth in the steel restraining rods, which is only slightly conservative, shows the stress in the liner to be approximately twice the allowable buckling stress. The allowable stress of 5200 N/sq cm (7500 psi) was determined using the equation for buckling stress found in Reference 1.

The preliminary test item test program was abandoned at this point, although considerable information was gained about the critical fabrication parameters. The 38 cm (15 in.) diameter fusion welded and explosively bonded joints were both acceptable. No hoop buckling occurred during or after the overwrap process providing confidence in the internal pressure level selected. The axial support rods were deleted in favor of end fitting closure designs which could withstand the operating pressure levels. The buckles in the tube have since disappeared as creep of the liner within the unbonded overwrap occurred.

LH_2 main engine test item: The significant discovery during fabrication of this test item was the undesirability of 0.008 cm (0.003 in.) thick metal liners for large tubes. Liners of this thickness are not practical for large diameter, long tubes due to the extreme care that must be exercised during fabrication before the overwrap is applied. A thickness of 0.013 cm (0.005 in.) is considered more practical.

The liner of this test item was received with a rather severe waffle pattern. This was caused by improper preparation of the Inconel foil edges before welding the sheets together. Removal of 1 cm (0.4 in.) from each edge of the sheet will alleviate most of this problem by providing a straight edge of uniform thickness. The tube was considered acceptable since no compressive loading was planned, and the wrinkles had been proven to have little or no effect in performance when the tubes were used as pressure vessels [1]. All test systems were modified to provide a minimum of 10 N/sq cm (15 psi) pressure in the test item at all times. This pressure was required to remove the buckles or waffle patterns which existed in the liner at ambient pressure.

Figure 38. - Interior View of Preliminary Test Item Showing Support Rods and Post-Overwrap Buckles

LOX main engine test item: The original design of the LOX main engine test item permitted a maximum of two sections joined together by a single hoop weld. The final item was made of four sections joined together by three hoop welds. The variance was a result of the resistance welder's capability to extend tooling into the test item to the depth of the shorter section seams. The hoop weld had to be a resistance weld to preserve the heat treat performed on the liner after the longitudinal seam welds. The liner length was also controlled by the oven size available for heat treating the Inconel.

Several problems occurred during the bonding and welding of the end fittings of the LOX main engine test item. The explosive bonding of the aluminum end fittings to the Inconel liner was successful on the first attempt (no dye penetrant leaks were detectable). After receipt of the assembly at Martin Marietta, while the end fittings were being prepared for welding, one end fitting was subjected to a heat of approximately 450 K (350°F) and while at this temperature a disbond occurred. The fitting was salvaged and an unsuccessful attempt was made to rebond it to the liner (dye penetrant leakage existed). Another salvaged fitting was bonded to the liner, but again dye penetrant leakage was evident. A decision was made to proceed with the test item with the known leakage and a cryogenic adhesive was used in an attempt to seal this leakage. To preclude a disbond of another fitting, a weld development program was undertaken. During the development program, it was determined that end fitting closure plates could be joined to the aluminum end fitting with sufficient strength while using finely chopped solid carbon dioxide to maintain the explosive bond area at or below 365 K (200°F) during the welding of the end caps.

Prior to installing the LOX main engine test item in the test fixture, a proof test was performed. The suspected weak explosive bond failed at 174 N/sq cm (253 psi). The failure of the bond prohibited the use of the test item to perform many of the planned tests.

OMS LH_2 test items: A design change was required during the fabrication process to accommodate the length constraints requested by the liner fabricator. An expensive tooling charge would have been required to make the original design length. In a production phase, the tooling for longer tubes can be amortized and not result in any significant cost impact per unit.

The leakage requirement on the test items was also changed. The capability of the vendor to achieve leak free welds, to some degree of repeatability, was proven in the previous program. When leaks did result in some of the test items it was concluded that to refabricate the test items would create a significant schedule impact, so the test items were accepted with the leakage. Upon receipt of the test items from the vendor, an attempt was made to repair the leaking items by use of a cryogenic adhesive. Although all leaks were not sealed, the leakage was reduced to a level where all

items were considered useable. A tare leakage was performed on each item so any degradation during tests would be noted by subsequent leak checks.

Overwrap constraints and provisions: An inspection of the LH_2 main engine test item, after completion of the overwrap cure cycle, revealed a significant displacement of the Inconel liner from the overwrap. This displacement could not be attributed to the waffle pattern and suggested that allowable hoop buckling limits had been exceeded in the liner at some point in the fabrication process.

A failure analysis was conducted to estimate stress levels occuring in the liner so an estimate of different factors that contribute to the liner buckling could be made. The very conservative assumptions made in this analysis included:

- No resin is present between liner and the first overwrap layer, after layup, but before cure;
- Each circumferential wrap contributes its full compressive load to the liner, that is, the addition of a second circumferential layer does not relieve the tension in the initial layer but adds an equal amount so that the compressive load in the liner is doubled;
- Axial overwrap layers do not contribute to the hoop strength of line;
- Resin does not contribute to wrap strength until after 340 K ($150^{o}F$) cure;
- No axial loads are transmitted between the liner and overwrap;
- Effective wrap thickness:

  Before cure 0.023 cm (0.009 in.) which is the thickness of 2 layers of glass-fibers.

  After cure 0.04 cm (0.016 in.) which is the thickness of 2 layers including resin.

Based on these assumptions the following conclusions were reached:

- A major contributor to liner buckling could be the initial wrap tension;
- Gas pressure during wrapping and curing was too low to prevent compressive hoop stress in the liner;
- Liner buckling was due to excessive hoop stress and possibly uneven axial stresses along liner seams;
- The fabrication process should be conducted to avoid compressive loads.

Since the assumptions employed in the analysis were conservative, a re-evaluation of the assumptions was made to define more reasonable choices. The first two assumptions listed above were modified as follows:

- A resin layer of 0.0025 to 0.005 cm (0.001 to 0.002 in.) would be present between the liner and the overwrap; and
- The wrap compressive load is 75% of the sum of the loads produced by two independent circumferential layers.

With these modified assumptions, it was concluded that the liner should not have buckled.

As a result of this analysis, the wrapping and curing of the LOX line was accomplished according to the following criteria:

- Use 1.4 kg (3 lb) per 20 ends wrap tension which was down from the planned 1.8 kg (4 lb) per 20 ends;
- Increase internal liner pressure to offset compressive loads during both wrapping and curing based upon the conservative approach. This would require approximately 28 N/sq cm (40 psi) in the tube as internal pressure; and
- Cure at 408K (275°F) maximum temperature, instead of the previously used 422 K (300°F).

It was also decided to monitor a series of strain gages during the overwrap and cure processes. Strain gage readings taken at intervals during the overwrap process are shown in Table 14. The location of the strain gages are discussed in the test item instrumentation portion of the following report section (page 94).

These strain gage data do not correlate well with the expected results. The strains (ϵ) due to pressurizing the tube to 28 N/sq cm (40 psi) can be expressed as:

$$\epsilon_H = \frac{\frac{Pr}{t} - .3\,\frac{Pr}{2t}}{E} = 800 \quad \mu cm/cm$$

$$\epsilon_A = \frac{\frac{Pr}{2t} - .3\,\frac{Pr}{t}}{E} = 188 \quad \mu cm/cm$$

TABLE 14. -
STRAIN GAGE READINGS - LOX LINE - DURING OVERWRAP AND CURE (IN MICRO IN./IN. OR MICRO CM/CM)

Operation Step	Pressure		Temperature		Hoop Readings				Axial Readings			
	N/sq cm	PSI	K	°F	A	B	C	Mean	A	B	C	Mean
Start	0	0	294	70	0	0	0	0	0	0	0	0
Pressurized	27.6	40	294	70	635	668	625	643	132	140	100	128
After 1st Wrap	27.9	40	294	70	605	630	605	613	152	195	130	159
After 2nd Wrap	27.9	40.5	294	70	560	595	565	573	152	190	160	167
Installed in Oven	27.6	40	294	70	585	610	555	583	172	210	140[a]	174
At 340 K (150°F) Cure	27.6	40	340	150	555	570		562	122	200		161
At 408 K (275°F) Cure	27.6	40	408	275	545	540		542	152	300		176
After 6 hours at 408 K (275°F)	27.6	40	411	280	550	520		535	152	290		221

NOTE: a Method of resting the line in the oven may change readings. Gage C became inaccurate.

The data, which was all temperature compensated, shows

ϵ_H = 643 μcm/cm or 11.1 μcm/cm/(N/sq cm)

and

ϵ_A = 128 μcm/cm or 2.2 μcm/cm/(N/sq cm)

This discrepancy has not been explained by data analysis and may indicate a built-in factor should be utilized in explaining other data. Significantly, all delta strains from this starting measurement were fairly low which tends to minimize the significance of any built-in error.

After the first overwrap the average hoop strains decreased by 30 μcm/cm and the average axial strains increased by 31 μcm/cm. This would translate to less than 1.4 N/sq cm (2 psi) pressure required to offset the overwrap. The second overwrap layer caused the average hoop strain to decrease by 40 μcm/cm, requiring about 1.8 N/sq cm (2.6 psi) to offset this change. Using an established equation for the required internal pressure to offset wrap tension:

$$P = \frac{Tnm}{r}$$

Where P = line pressure in N/sq cm, unit stress

T = overwrap tension in N

n = No. of overwrap layers

m = No. of turns per cm

r = tube radius, in cm

The required internal pressure for the LOX line would be 8.9 N/sq cm (13 psi). This is considerably higher than the total of 3.1 N/sq cm (4.5 psi) which was actually required. The overwrap system used was fairly old and should not have had any substantial resin migration. The total shift in strain during the cure cycle was 50 μcm/cm in the hoop direction which could be offset by less than 2.8 N/sq cm (4 psi) internal pressure.

Summarizing, the strains associated with overwrap and cure are about 30% of those predicted by the very conservative analysis. The gross discrepancies are identified as:

- o A built-in error in the strain reading during pressurization, probably caused by the strain gage proximity to the hoop stiffeners provided in the liner; and

- o A fairly substantial squeezing of the resin both during overwrapping and during curing, even at above 340 K (150°F) which was considered to be the resin set temperature.

Future overwrapping can be accomplished with less conservative numbers, if required to avoid overstress in the unreinforced liner. However, the failure in the LH_2 tube must not be overlooked when reducing this pressure.

Shipping Problems. - The original test items of both the LH_2 and LOX OMS systems were damaged in-route from the west coast vendors. In both cases, the damage was attributed to rough handling by the airlines. To prevent damage to the remade lines, a pressurization package was made available for each item. Since these items were to be air freighted to Denver from Los Angeles, a possible implosion of the lines could occur. To eliminate this problem, a custodian escorted the tubes during flight. The custodian had access to the test items and also the pressurization system capable of restoring test item pressure as required.

As a result of the knowledge gained during this program, the following suggestions are made for further tube shipments:

- o During the shipment of thin metal lines it is always desirable to maintain an internal positive pressure; or

- o If an internal pressure that lends both axial and hoop support is not possible, an air bag, balloon, or internal mandrel should be used to support the test item in the hoop direction; and finally,

- o Assure proper design and identification of the shipping container.

Many of the tubes fabricated on this and the previous program were shipped without any sign of damage. The tubes are adequately strong to be shipped with judicious handling practice and packaging techniques. The main engine LOX and LH_2 test items were not damaged in shipping. The thicker gage of the LOX test item contributed significantly to its strength and the main engine LH_2 test item was transported with an internal mandel which supported the test item adequately in the hoop direction.

The objectives of the test program were to determine the flow and thermal characteristics, and verify the structural integrity of the test items. To accomplish these objectives the test items were subjected to the test programs outlined in Figure 39 for the OMS LOX test items, Figure 40 for the OMS LH_2 test items and Figure 41 for the main engine test items.

Test Item Instrumentation. - For this test program each of the composite sections used in the assembly of the OMS LOX and LH_2 feedlines were instrumented to provide biaxial strain measurement of the liner during burst testing. The strain gages were bonded to the outside of the liner at the midpoint and near an end fitting prior to applying the overwrap. Two thermocouples were mounted on each composite section for temperature measurement. The location of the thermocouples and strain gages are shown in the sketch below. The thermocouples were installed during overwrapping prior to applying the last layer of glass fibers. For the flow and steady-state heat input testing, additional thermocouples were attached to the end fittings and to the metal elbows and tees. Thermocouples were also installed on the outside of the vacuum chamber walls for the steady-state heat input test.

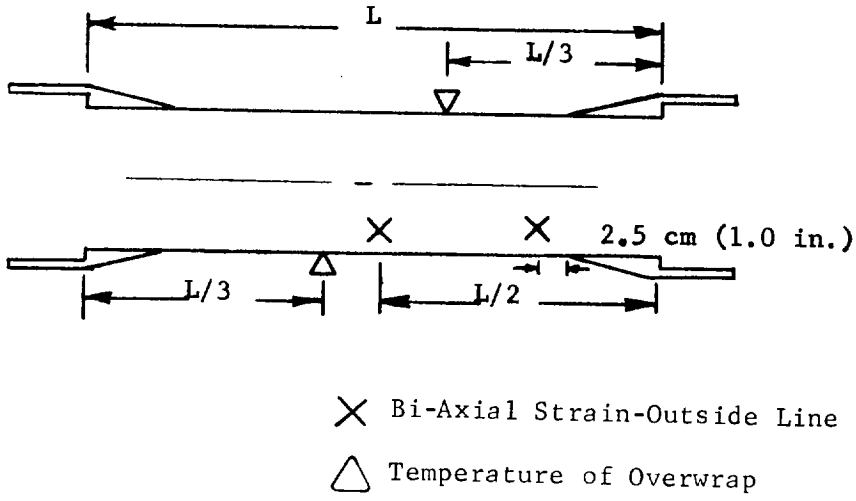

OMS Test Items Instrumentation

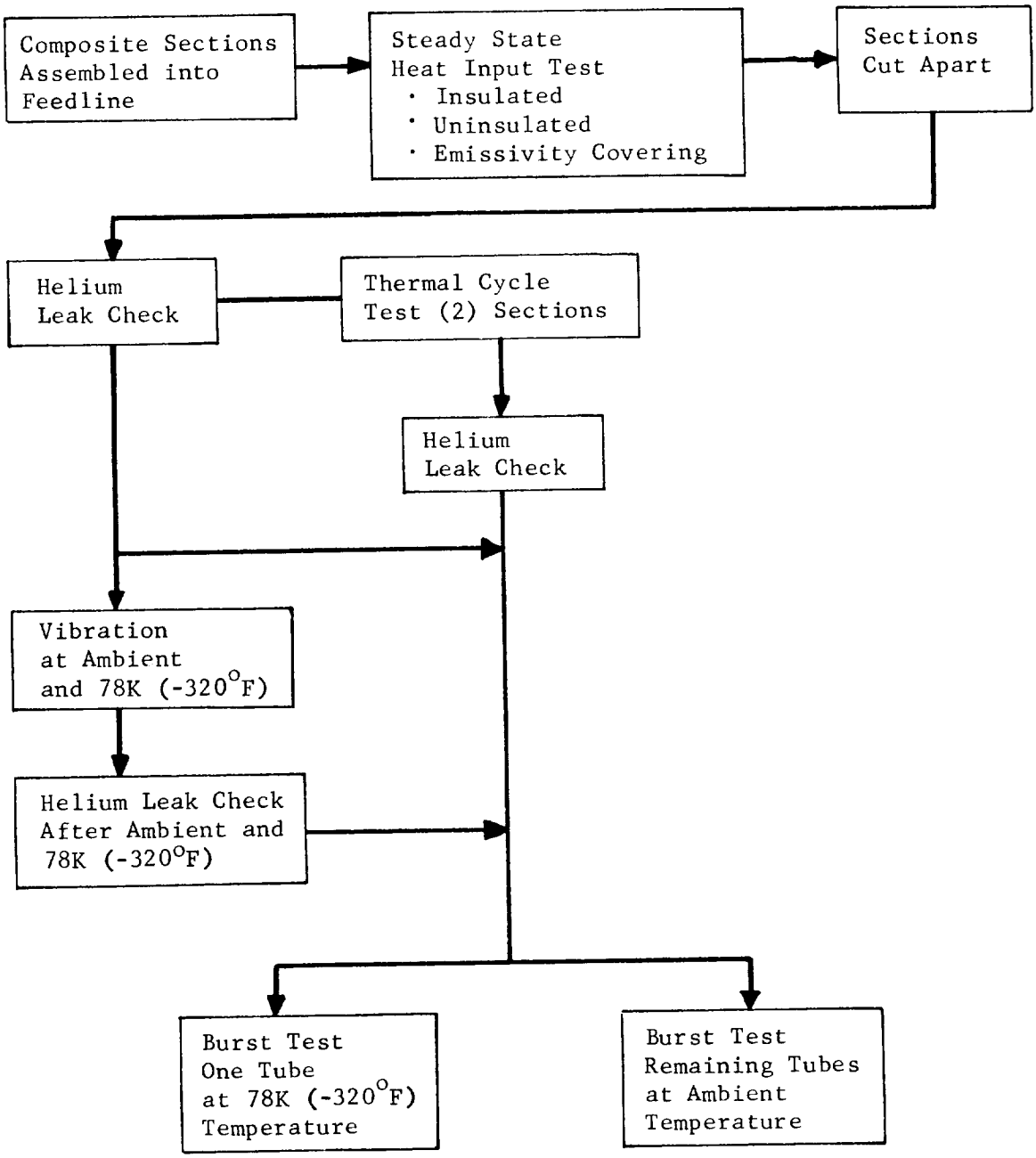

Figure 39. - OMS LOX Feedline Test Program

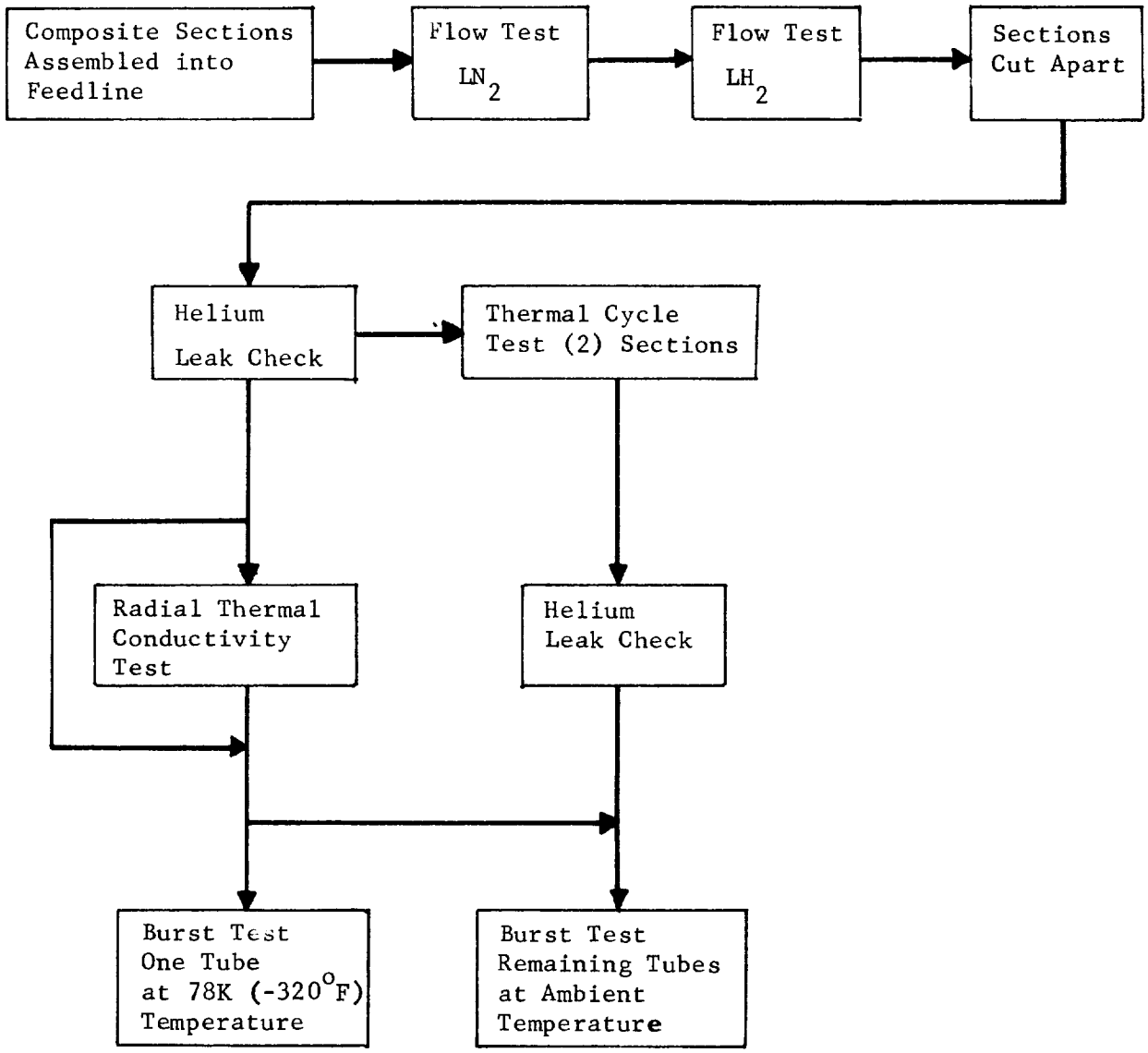

Figure 40. - OMS LH_2 Feedline Test Program

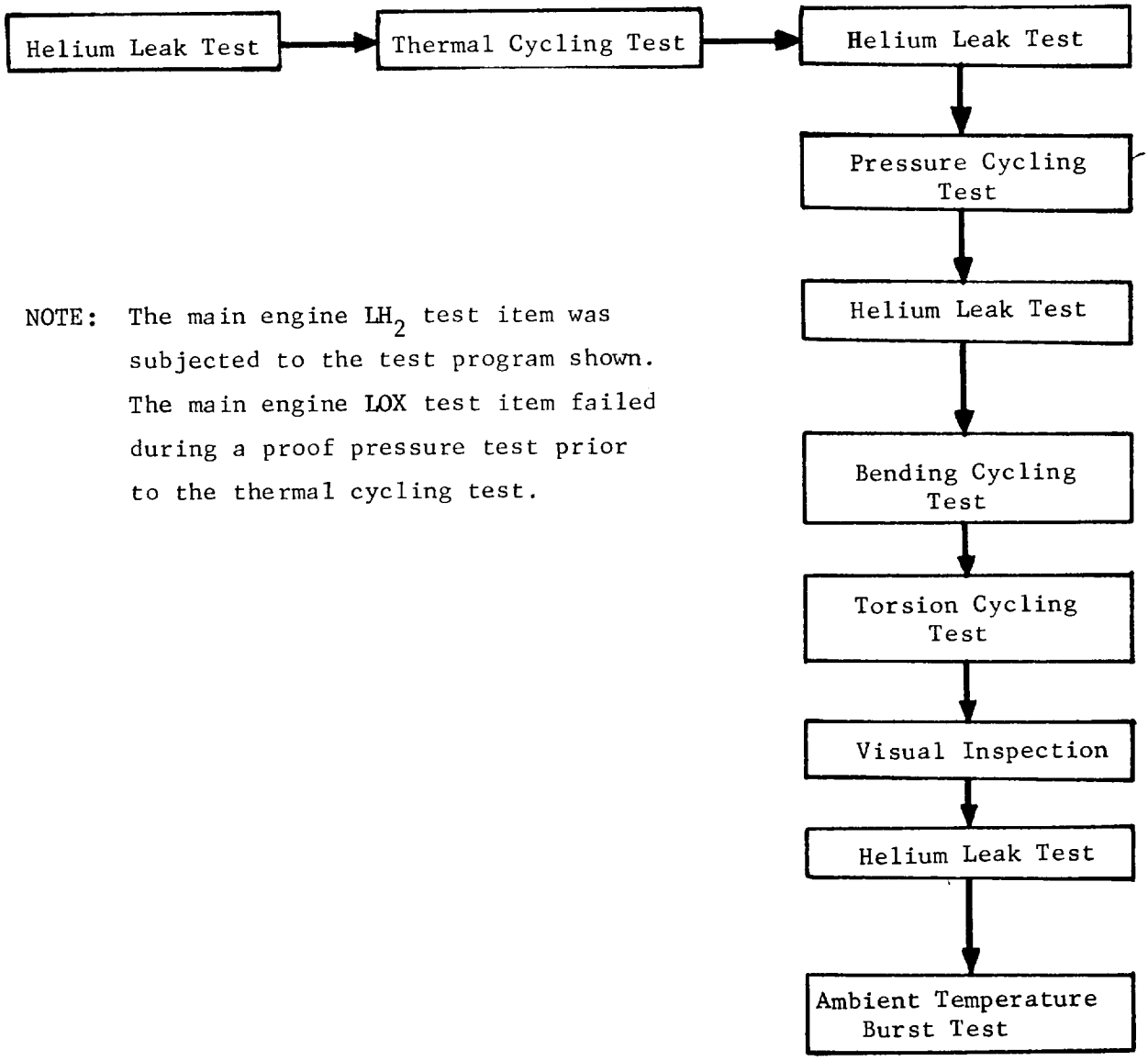

NOTE: The main engine LH_2 test item was subjected to the test program shown. The main engine LOX test item failed during a proof pressure test prior to the thermal cycling test.

Figure 41. - Main Engine Feedline Test Program

The instrumentation on the main engine test items also consisted of strain measurements and temperature measurements. The strain gages were bonded to the inside of the liner prior to installing the end caps and to the outside of the liner prior to overwrapping. The thermocouples were installed under the last layer of overwrap.

The location of the thermocouples and strain gages on the main engine LOX and LH_2 test items is shown in Figure 42. Two additional thermocouples were added to the LOX test item on the outside of the liner, under the overwrap, near the point where the thermocouples are installed under the final layer of overwrap to provide a ΔT at the locations shown on the figure.

During the burst and cycle tests the pressure in the test items was determined by continuously recording the output of a pressure transducer installed on the test item.

The output of the pressure transducers, thermocouples, and strain gages were recorded on direct writing recorders. A detailed description of the instrumentation and data acquisition system components is included as Appendix G.

Leak Tests. - The purpose of the leak tests was to verify the integrity of the test items prior to overwrap, after overwrap and cure, and after each test in the test program. After completing the overwrap and cure process, the tare leakage rate of the test items was determined by a qualitative leak test at the operating pressures listed below:

OMS LOX Test Items	45 N/sq cm (65 psi)
OMS LH_2 Test Items	31 N/sq cm (45 psi)
Main Engine LH_2 Test Item	69 N/sq cm (100 psi)

For leak testing the test item was encased in a plastic bag and the mass spectrometer probe was sealed into the bag as shown in Figure 43. The test item was then pressurized with gaseous helium to operating pressure, and the output of the mass spectrometer was recorded.

This method of leak checking, referred to as accumulation, is qualitative and is excellent if there are no leaks in the tube. The method is not considered to be quantitative in nature because the leaking helium will accumulate in the bag and replace the nitrogen gas or air that was originally in the bag.

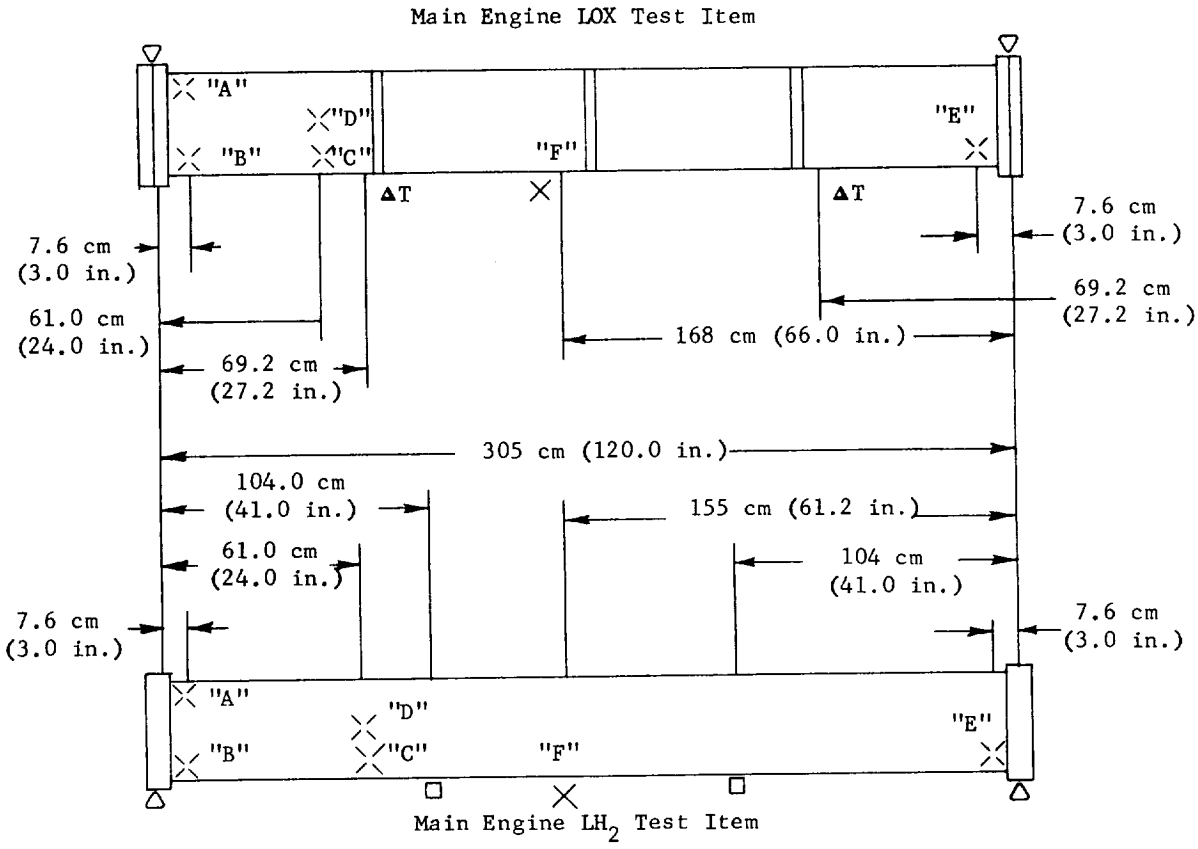

⤫	Bi-Axial Strain - Inside Liner
X	Bi-Axial Strain - Outside Liner
□	Temperature of Glass
△	Temperature of End Fitting
ΔT	Temperature Delta Between Glass and Liner

"A", "B", "C", "D", "E" and "F" Strain Gage Designators (TYP)

Figure 42. - Main Engine Test Items Instrumentation

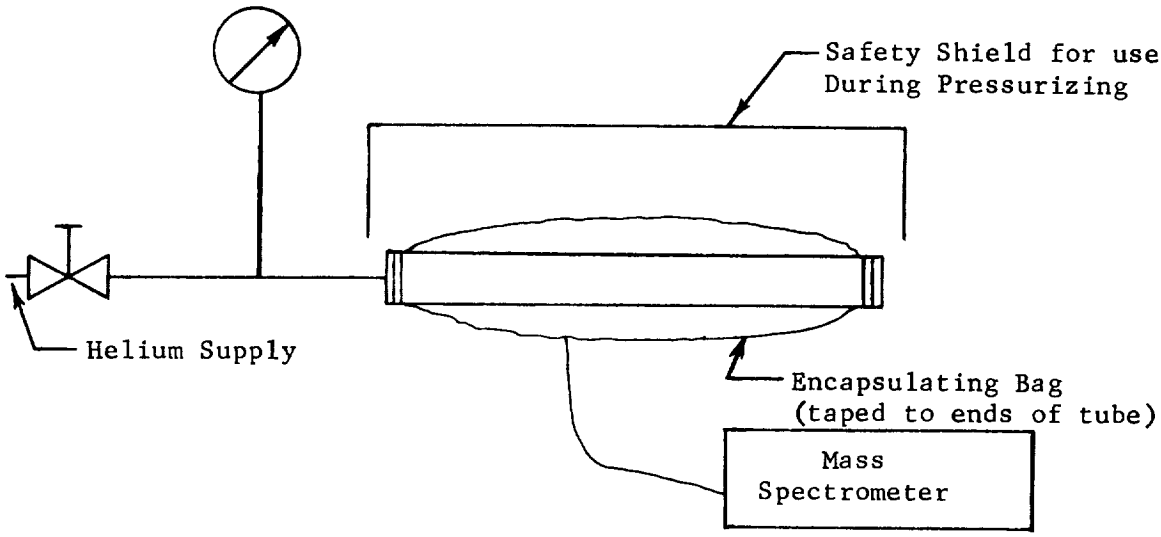

Figure 43. - Qualitative Helium Leak Check Method

The results of the pre- and post-overwrap leak tests on the OMS test items are summarized in Table 15. The results of the post-overwrap leak checks provided the baseline data for the subsequent leak checks performed during the test program. These leak checks are discussed in the individual test writeups for the OMS test items. The results of the leak tests on the main engine LH_2 test item are plotted in Figure 44.

After completing the overwrap and cure process the LOX test item was leak tested by the qualitative method. During this test the mass spectrometer was driven off scale at a test item pressure of 117 N/sq cm (170 psi). In view of the high leakage rate and the knowledge that the final explosive bonded joint was not entirely successful, a decision was made to proof pressure test the LOX test item to a pressure of 172 $\pm$ 3.5 N/sq cm (250 $\pm$ 5 psi). For this test the ends of the test item were sealed and the pressure was slowly increased. The suspect joint failed at a test item pressure of 174 N/sq cm (253 psi). The failure was attributed to the weakness of the unbonded portion of the explosive bond. A photograph of the failure is included as Figure 45.

TABLE 15. - OMS TEST ITEMS IN-PROCESS LEAK CHECK RESULTS

COMPOSITE SECTION INDENTIFICATION		PRE-OVERWAP 17 N/sq cm (25 psi) Helium Pressure	POST-OVERWRAP Operating Pressure Helium[b]
OMS LOX Sections	1 & 2	1.56 scc/sec [a, c]	1.5×10^{-6} scc/sec
	3	0	0
	4	2.3×10^{-6} scc/sec	2.5×10^{-6} scc/sec
OMS LH_2 Sections	1	0	2.7×10^{-7} scc/sec
	2	0	0
	3	0	0
	4	0	0
	5	0	0

a. This tube was repaired with a cryogenic epoxy after completing the overwrap and cure process.

b. 45 N/sq cm (65 psi) for LOX test sections.
31 N/sq cm (45 psi) for LH_2 test sections.

c. No leakage was noted by the dye penetrant method on any tube, except the OMS LOX Sections 1 and 2.

d. Zero leakage, as stated, means not detectable by a helium mass spectrometer.

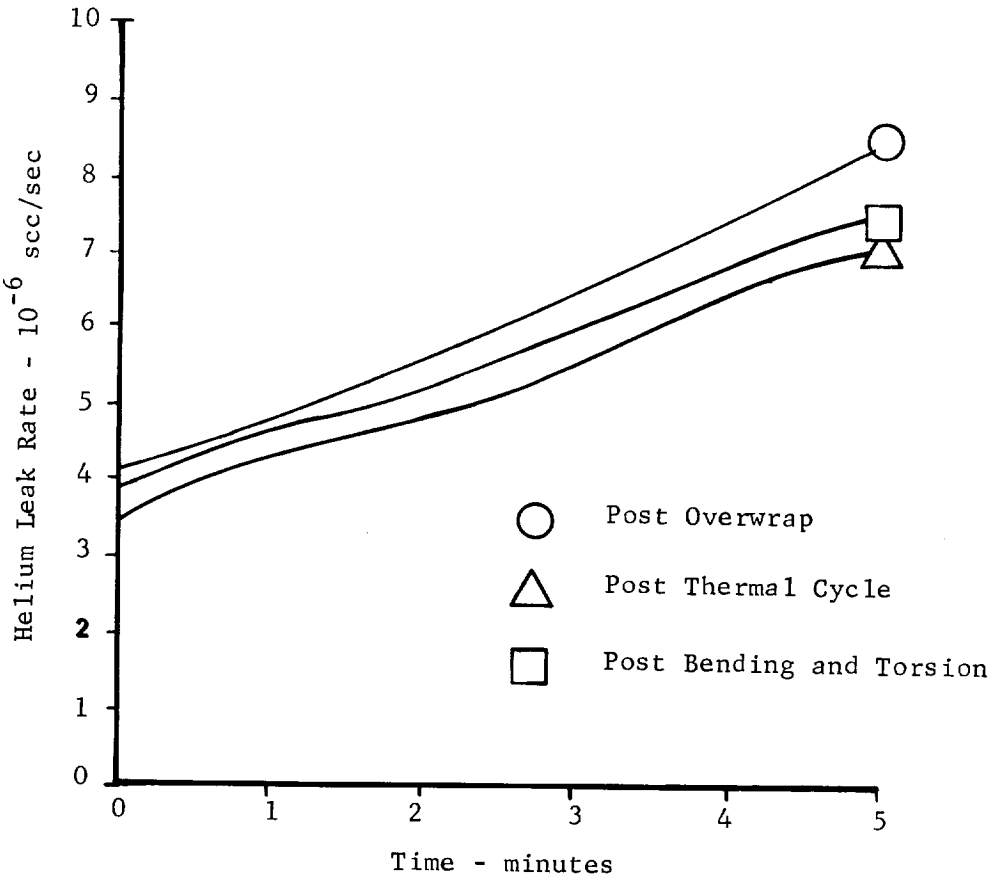

Figure 44.- Main Engine LH_2 Test Item
Leak Test Results

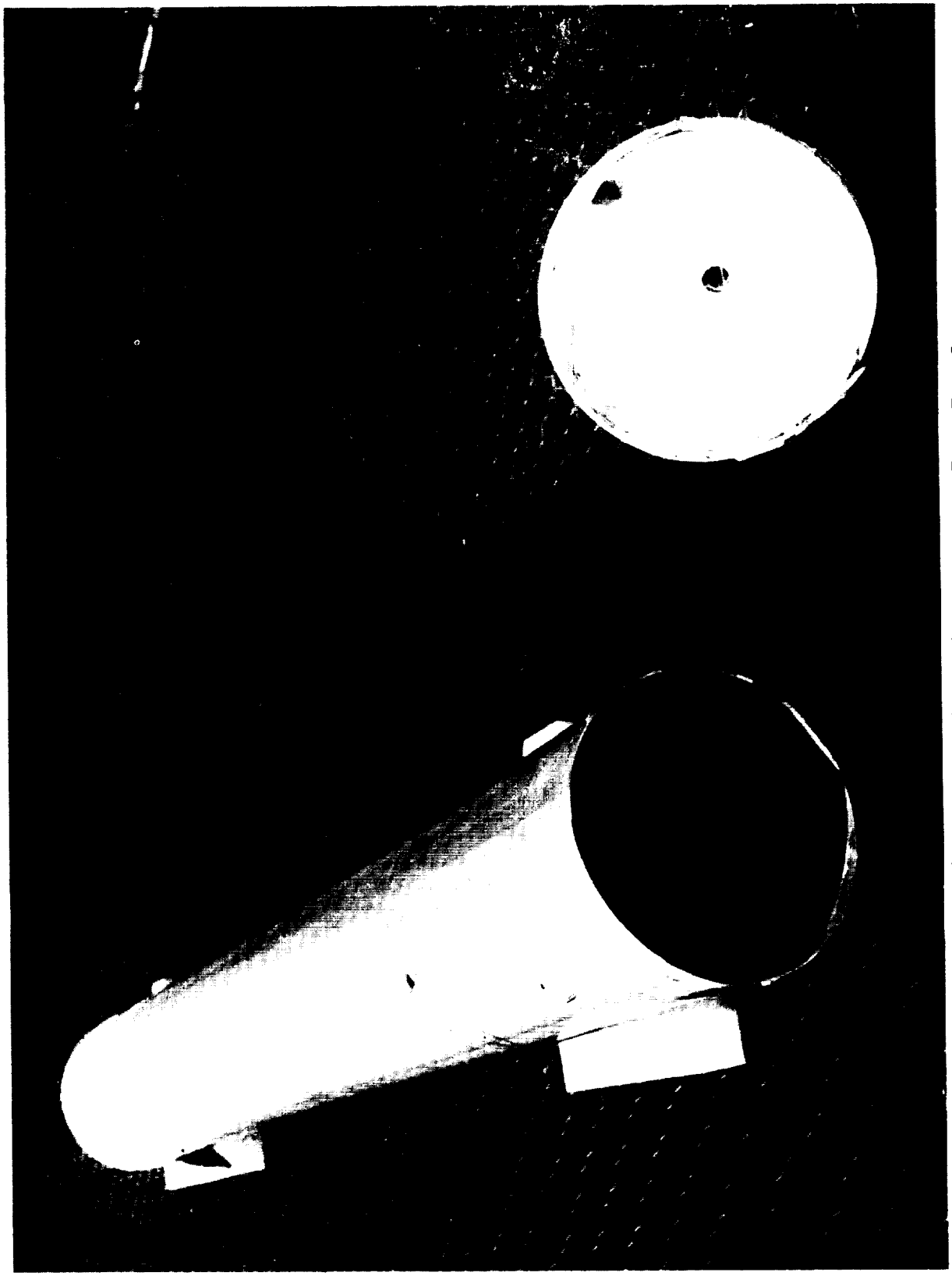

Figure 45. - LOX Main Engine Test Item Post-Proof Test Showing Failure Area

Since the remaining explosive bonded joint was still intact, it was decided to perform the thermal cycle testing on this joint. In order to verify the integrity of the joint after subjecting it to thermal cycling, a method of performing low pressure leak checks was devised. This consisted of inflating a plug in the end of the tube. The good end of the tube was then encased in a plastic bag and the test item was pressurized to 2 N/sq cm (3 psi) with gaseous helium. A sketch of the test setup is shown below.

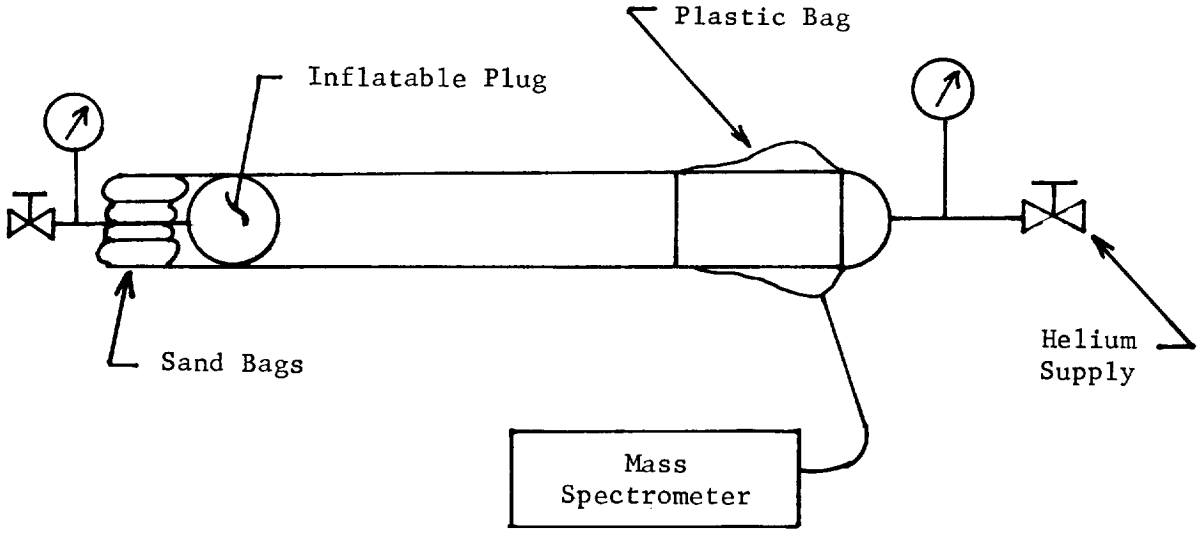

The output of the mass spectrometer was monitored for a period of one hour while the tube was pressurized. This test was performed prior to starting thermal cycles, after completing 10 cycles and after completing 50 cycles. The results of these leak tests showed no leakage through the joint on any of the tests.

LH_2 OMS Flow Tests. - Outflow tests were performed on the LH_2 OMS test item to determine the chilldown, transient, and steady-state flow characteristics. The initial tests used liquid nitrogen as the working fluid while the last test in the program used liquid hydrogen. Discussions of system geometry, instrumentation, test procedures, and results are presented. A schematic of the test installation is shown in Figure 46.

System description: The test item was installed in a vacuum chamber that was capable of operating at 10^{-5} torr to simulate the heat transfer to the feedline in a space environment. The test item which simulated the OMS LH_2 feedline from the tank outlet to one engine, is shown in Figure 47.

The test fluid was supplied from a pressurized, insulated tank through a short insulated line to the test section. The insulated line contained a flow metering orifice and a flow control valve jacketed with the test fluid. The cryogenic jacket assured that zero quality liquid was contained in the line above the flow start valve.

Temperature instrumentation used during the test is shown in Figure 47. Pressure measurements of primary concern in evaluating chilldown were the tank top pressure and the pressures at the inlet to the engine and simulated leg orifices. In addition, the pressure drop across the orifice in the insulated line between the supply tank and the test item inlet was used to compute mass flow in the system. Other pressure drop measurements recorded were engine and simulated leg orifices and across line sections.

Test description: In general, each test consisted of the following sequence of events: 1) evacuate test chamber; 2) propellant loading; 3) tank pressurization; 4) hold; and 5) outflow. Variations in these events were made in specific tests to evaluate their effect on the chilldown process. Table 16 is presented to compare these events for two liquid nitrogen and one liquid hydrogen outflow tests. The storage dewar conditions have also been included in the table.

During LN_2 Run 1, propellant loading was conducted with the tank vented to assure saturated propellant at 8.3 N/sq cm (11.7 psia) absolute pressure. The loading process took approximately 12 minutes. After loading, the tank was pressurized to approximately 28.3 N/sq cm (41 psi) and held for 3.5 hours. The pressurized hold period was employed to allow warming of the propellant. However, since the supply tank insulation was designed for use with liquid hydrogen, the heat leak into the tank was extremely low. As a result, only a 2 K (3°F) rise in temperature was noted on the orifice inlet temperature measurement. Outflow for this run was initiated by manual opening of the flow control valve in approximately

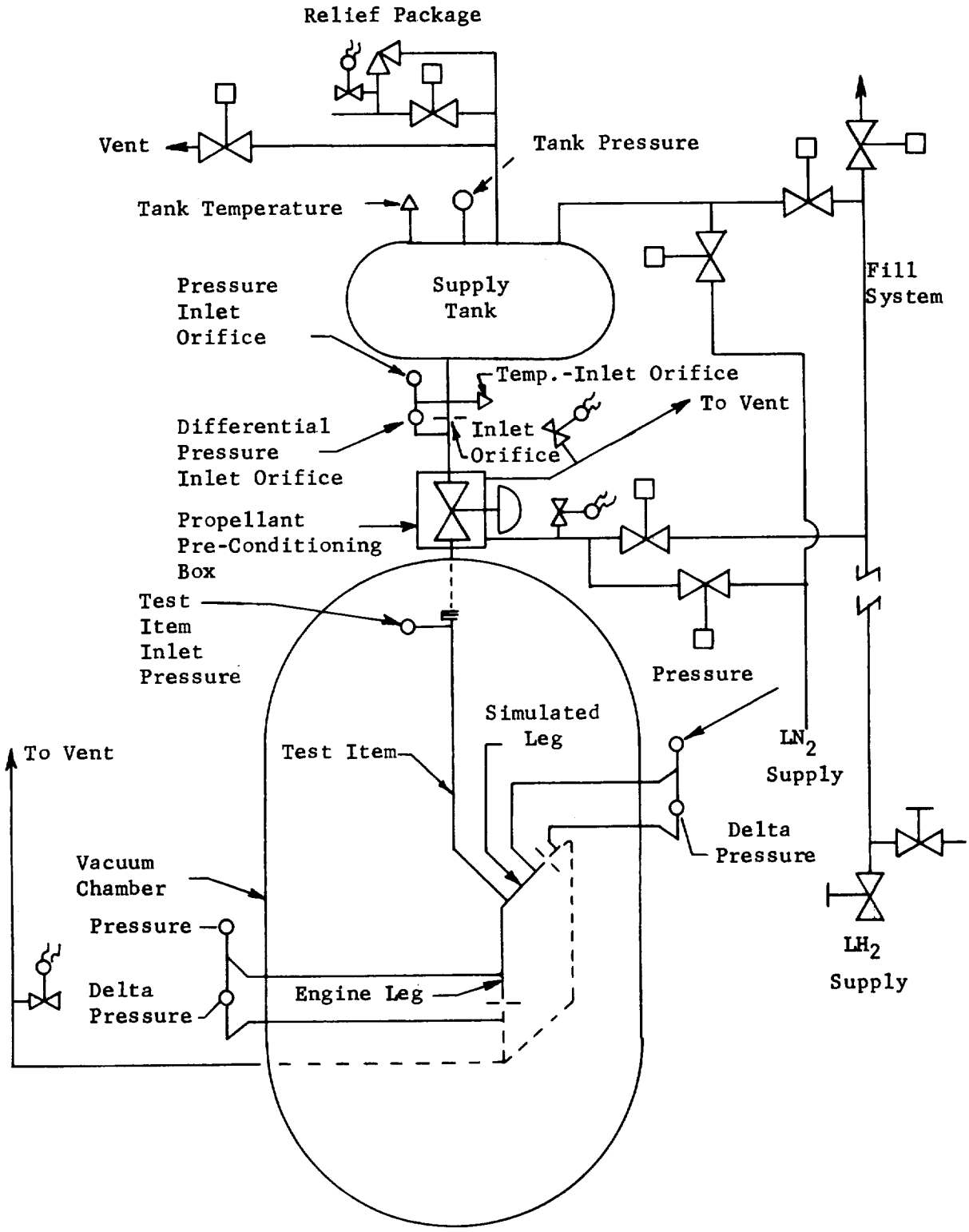

Figure 46. - LH_2 OMS Flow Test Installation Schematic

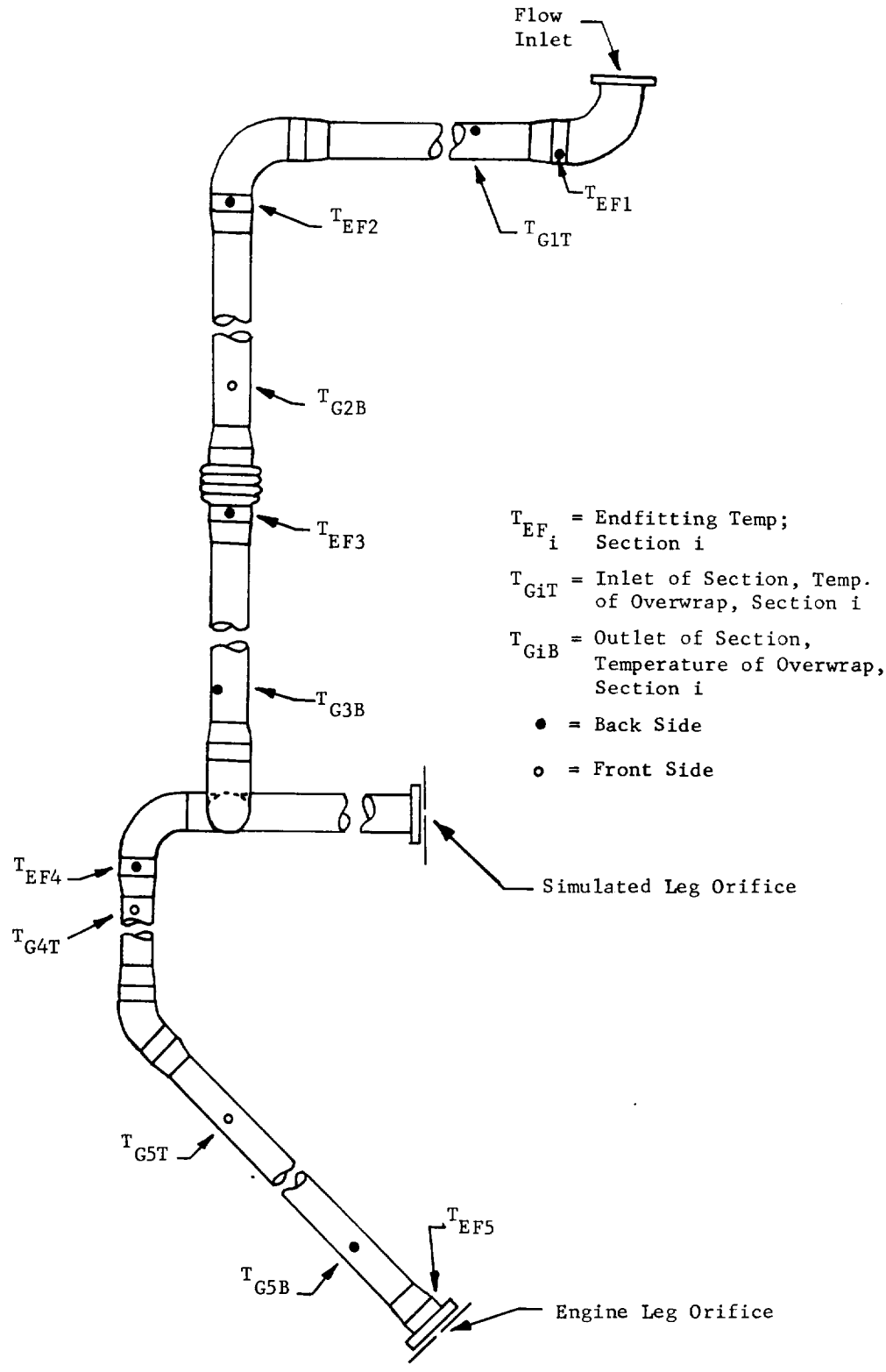

Figure 47. - Thermocouple Location for LH_2 OMS Flow Test

TABLE 16. - OUTFLOW TEST EVENT COMPARISON

Event	LN_2 Run 1	LN_2 Run 2	LH_2 Run 1
Dewar Storage			
Pressure (Pre-load Cond.)	8.3 N/sq cm (12 psi)	8.3 N/sq cm (12 psi)	17.2 - 20.7 N/sq cm (37-42 psi)
Temperature (Saturation)	75.7 K (-323.8°F)	75.7 K (-323.8°F)	23.9 - 24.4 K (-417 to -416°F)
Propellant Loading			
Duration (Approximately)	12 min.	33 min.	16 min.
Tank Pressure	8.3 - 11.4 N/sq cm (12 - 16.5 psi) (tanks vented)	Maintained between 15.2 and 22.1 N/sq cm (22 and 32 psi)	Maintained between 18.6 and 20.0 N/sq cm (27 and 29 psi)
Pressurization			
Duration	165 sec.	92 sec.	117 sec.
Tank Pressure (initial to final)	11.4 - 36.9 N/sq cm (16.5 - 53.5 psi)	8.7 - 31.4 N/sq cm (12.6 - 45.5 psi)	19.8 - 38.1 N/sq cm (28.7 - 55 psi)
Hold Period			
Duration	3.5 hours	36 sec	None
Tank Pressure	36.9 to 36.2 N/sq cm (53.5 to 52.5 psi)	31.4 to 35.4 N/sq cm (45.5 to 51.3 psi)	
Temperature Change (Orifice inlet)	+ 2K (+3°F)	None	
Outflow			
Valve Opening Method	Manual	Pneumatic	Pneumatic
Valve Opening Time	15 sec.	1 sec.	1 sec.

NOTE: Pressures are Absolute Pressure.

15 seconds. This slow opening was employed because it was believed that excessive pressure surges might occur during initiation of flow in the feedline. However, since no significant pressure surges occured, rapid pneumatic valve opening was employed in subsequent runs.

The loading procedure in LN_2 Run 2 was changed to load the tank under 15.2 to 22.1 N/sq cm absolute (22 to 32 psi) pressure. The purpose of this procedure was to obtain a saturation temperature higher than that normally maintained in the LN_2 storage dewar. No hold period was employed after pressurization in this run.

For the liquid hydrogen run, loading was accomplished with tank pressure maintained at 18.6 to 20.0 N/sq cm absolute (27 to 29 psi) to minimize boiloff. Storage pressure in the LH_2 dewar was maintained at 17.2 to 20.7 N/sq cm absolute (37 to 42 psi) so that some cooling of the propellant would be accomplished during loading.

Test results: To evaluate the chilldown process, pressure histories for the tank, the engine leg orifice inlet, and the simulated leg orifice inlet were prepared for the three outflow tests. These histories are presented in Figures 48, 49, and 50. In addition to these measured pressures, a plot of propellant saturation pressure corresponding to the temperature measured by the flow metering orifice inlet thermocouple is also included in the figures. Chilldown at the engine and simulated leg orifices was assumed to have occurred when the inlet pressures at these orifices reached the estimated saturation pressure curve. This condition is indicated in the figures as the maximum chilldown time. Beyond this time, the propellant at the orifice inlet is assumed to be subcooled.

Consideration of all three saturation pressure curves indicates a tendency to approach a constant value after a certain length of time. It is believed this pressure represents the true bulk propellant saturation in the tank. An extrapolation of this pressure back to the start of the outflow was made for each run and is indicated by the dashed line on the figures. The intersection of the extrapolation and the orifice inlet pressure curves has been identified as minimum chilldown time on each of the figures. The minimum chilldown point represents the minimum time allowable to reach essentially zero quality condition at the orifice inlets if no propellant temperature increase occurred between the tank and the orifice inlets. Table 17 summarizes the maximum and minimum chilldown times taken from the figures.

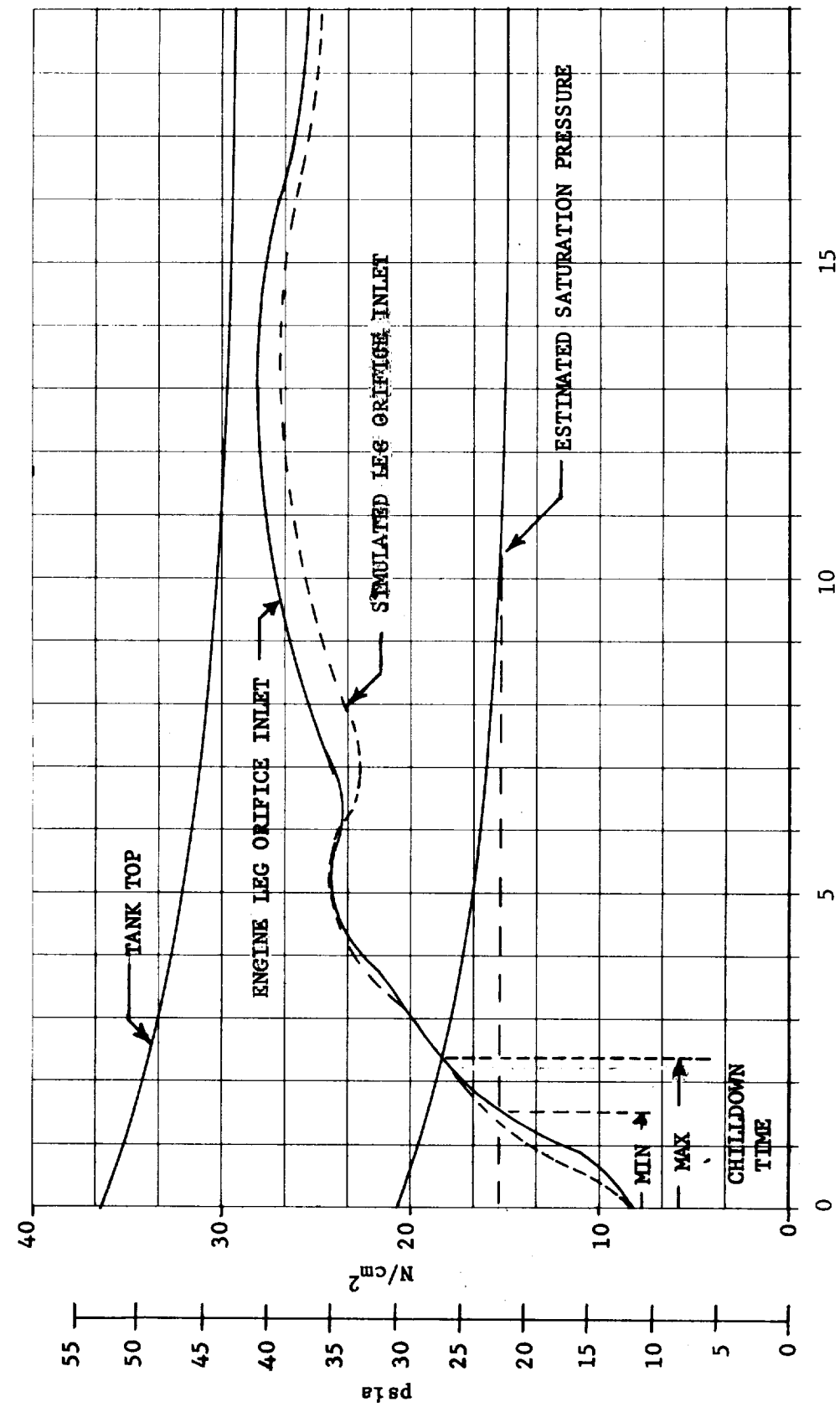

Figure 48. - Pressure Histories for LN_2 Chilldown - Run No. 1

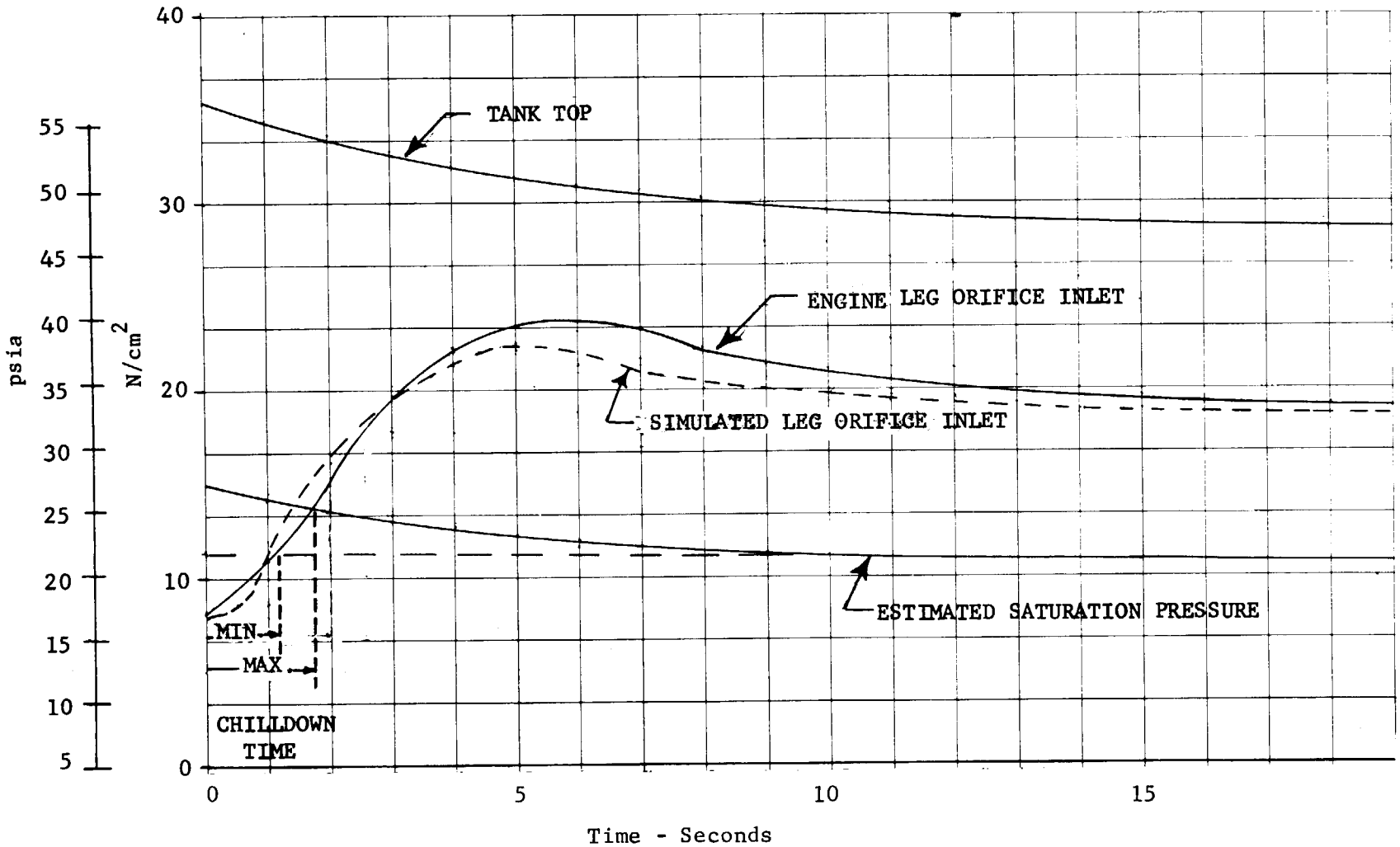

Figure 49. - Pressure Histories for LN_2 Chilldown - Run No. 2

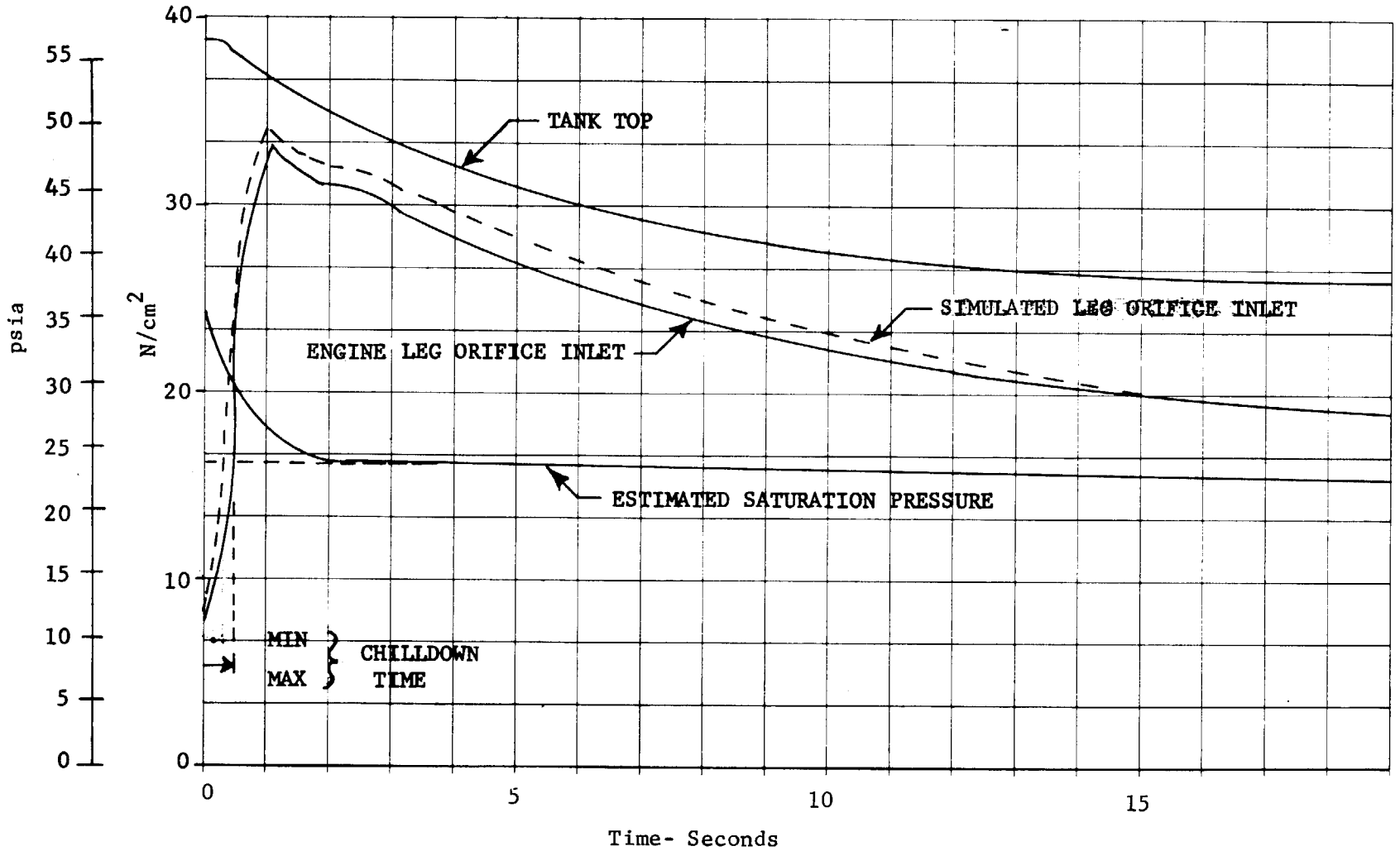

Figure 50. - Pressure Histories for LH_2 Chilldown Test

TABLE 17. - MAXIMUM AND MINIMUM CHILLDOWN TIMES

	LN_2 RUN 1	LN_2 RUN 2	LH_2 TEST
Maximum time, sec	2.3	1.8	0.4
Minimum time, sec	1.5	1.2	0.3

Propellant mass flowrates from the tank were computed from the flow metering orifice pressure drop and inlet temperature measurements. These flowrates are presented in Figure 51. Differences in valve opening procedures can be readily seen in the figure.

Temperature measurements were also made at various points on the composite feedline. Typical temperatures in the overwrap and end fitting during LN_2 Run 2 and LH_2 Run 1 are presented in Figures 52 and 53. Comparison of the data indicates that the overwrapped area tends to cool much faster than the end fittings. This is attributed to the smaller mass and lower heat capacity of this section of the tube.

Analytical Correlation. - The analysis program predicted the chilldown time for the OMS LH_2 test item to be on the order of 2 seconds. The results of the test program show a chilldown time of 0.3 to 0.4 seconds. Since the chilldown of the line is very rapid and the computer analysis gives a conservative time, no modification of the math model is planned.

The simplified analysis performed to predict the chilldown time for the OMS LOX line gave a chilldown time on the order of 0.3 seconds. No losses or heat transfer film coefficient were considered, so this represents the ideal absolute minimum chilldown time. Since chilldown testing of the OMS LOX test item was cancelled, this time was not verified by test. However, chilldown tests on the OMS LH_2 test item using liquid nitrogen show a chilldown time of 2.0 - 2.5 seconds. The simplified analysis performed on this line using LN_2 gave a predicted chilldown time of 0.8 seconds which indicates the actual chilldown time for the LOX line would be about 1.0 second.

The composite line does show a significant advantage over the all-metal line in chilldown boiloff. After an initial surge, in which the heat content of the metal liner is consumed, the boiloff drops off and is then supported only through the heat contained in the overwrap and in the heavier metal of the elbows, end fittings, etc. With an all-metal line,

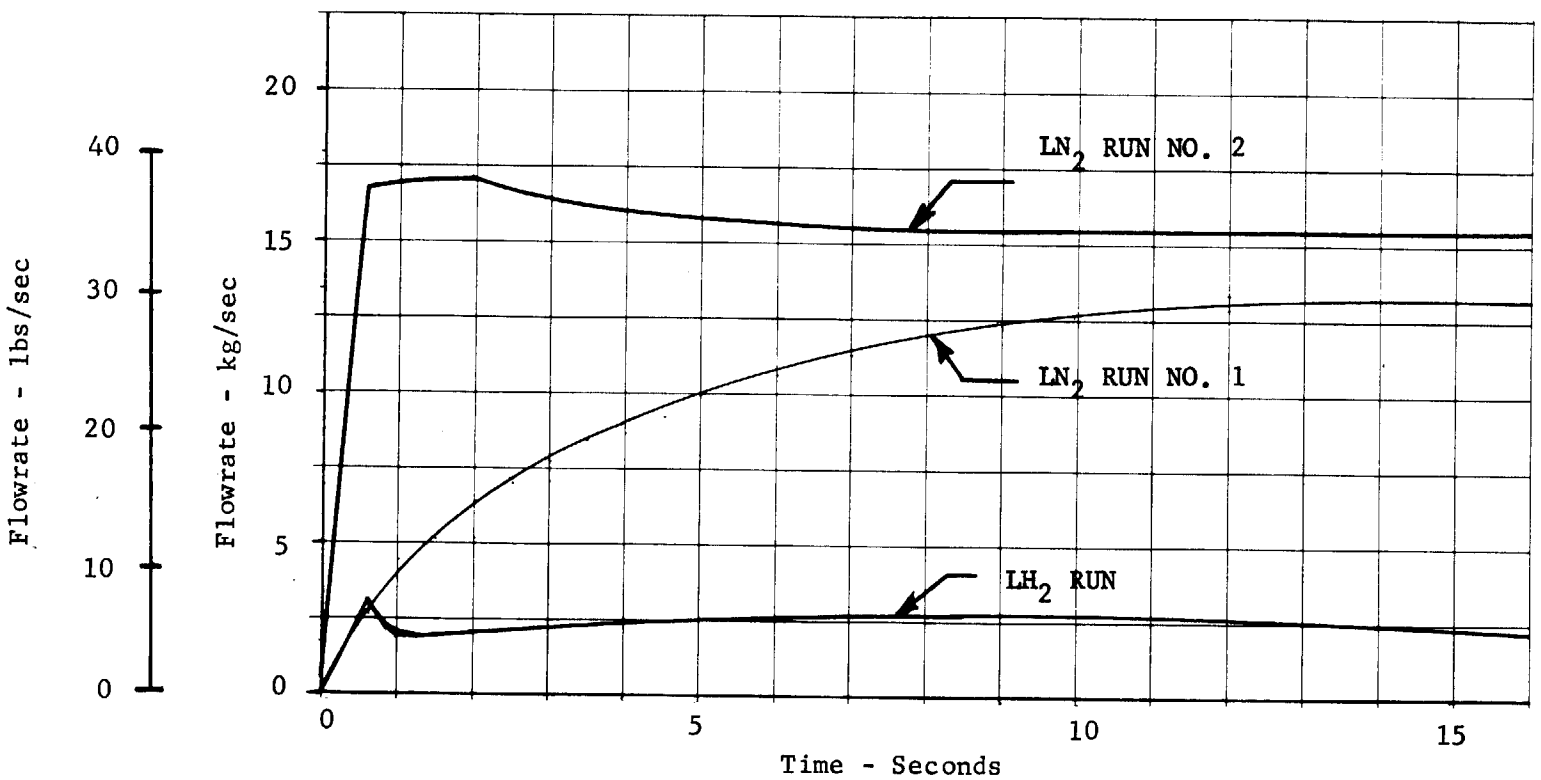

Figure 51. - Tank Mass Outflow Rate History

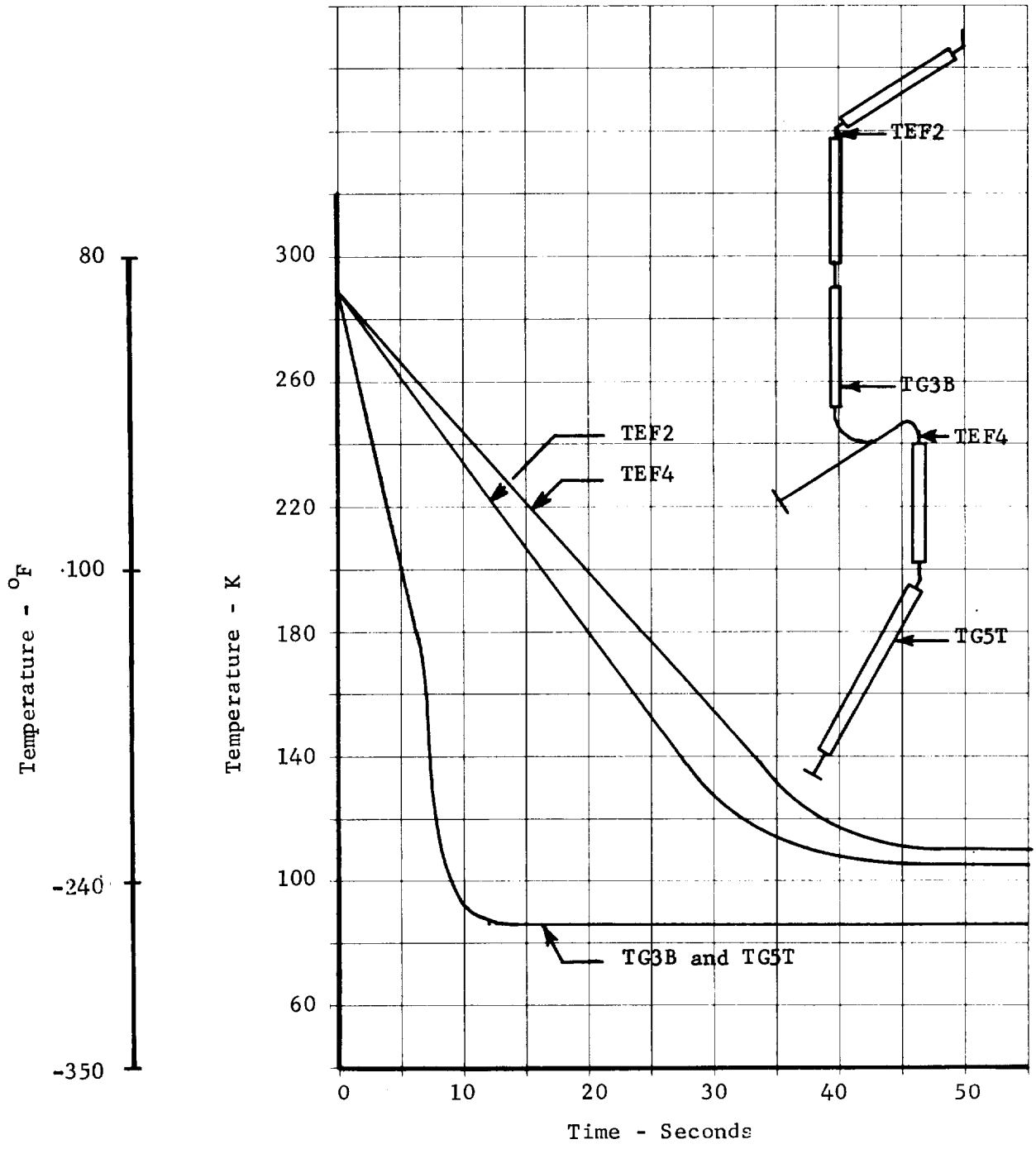

Figure 52. - Temperature History of Overwrap and End Fittings, LN_2 Run No. 2

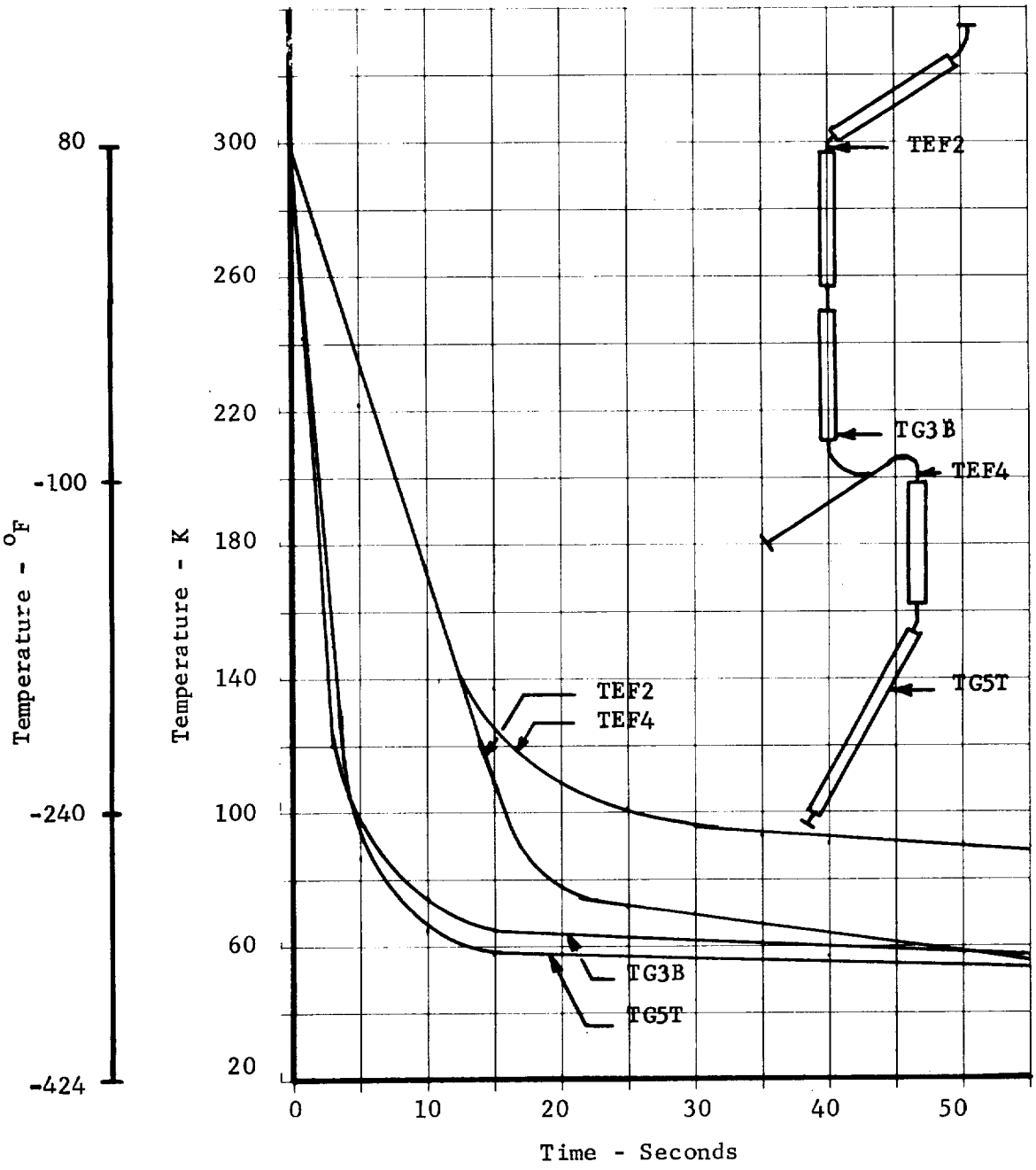

Figure 53. - Temperature History of Overwrap and End Fittings - LH_2 Run No. 1

the higher boiloff would continue for a much longer period. The heavier metal elbow structure continues to contribute to the boiloff for a much longer period as shown in Figure 54. Had the composite areas been of all-metal construction, the cooldown in those areas would have been similar to this curve and the initial high boiloff level would have continued beyond 25 seconds.

OMS LOX Steady-State Heat Input. - The thermal analysis performed on the OMS propellant feedlines considered the LOX line to be wet, that is, with the flow initiating valve located at the engine interface. The purpose of this test was to determine the steady-state heat input to the LOX test item under static (no flow) conditions while filled with simulated propellant.

For this testing, the test item shown in Figure 55 was installed in the test fixture shown schematically in Figure 56. An anti-geysering device consisting of a concentric line inside of the test item was employed to keep the test item filled with liquid nitrogen for the duration of the test runs. Three test runs were made using liquid nitrogen as the test medium. For the first test, the test item was uninsulated; for the second test, one layer of double aluminized mylar was wrapped around the test item; and for the third test, 20 layers of double aluminized mylar with each layer separated by nylon netting, were wrapped around the test item. Analysis of the test data shows the actual heat input to be less than the heat input predicted by the analytical program.

The tests were performed by filling the supply tank with LN_2 and allowing the system to stabilize. The heat input to the feedline was determined by measuring the propellant boiloff rate, using a gas flowmeter installed in the vent system. The tare heat input from the supply tank in its insulated configuration was determined by this method prior to installing the test item. The tare boiloff rate was 0.0014 m^3/hr (0.0368 gal/hr). The tare boiloff rate and the heat input were determined with the chamber evacuated to simulate a space environment.

The results of the steady-state heat input testing performed on the OMS LOX line are compared to boiloff predicted by the analysis program in Table 18. The addition of a single layer of aluminized mylar to alter the surface emissivity of the overwrap had a substantial impact on the boiloff rates as can be seen in the table.

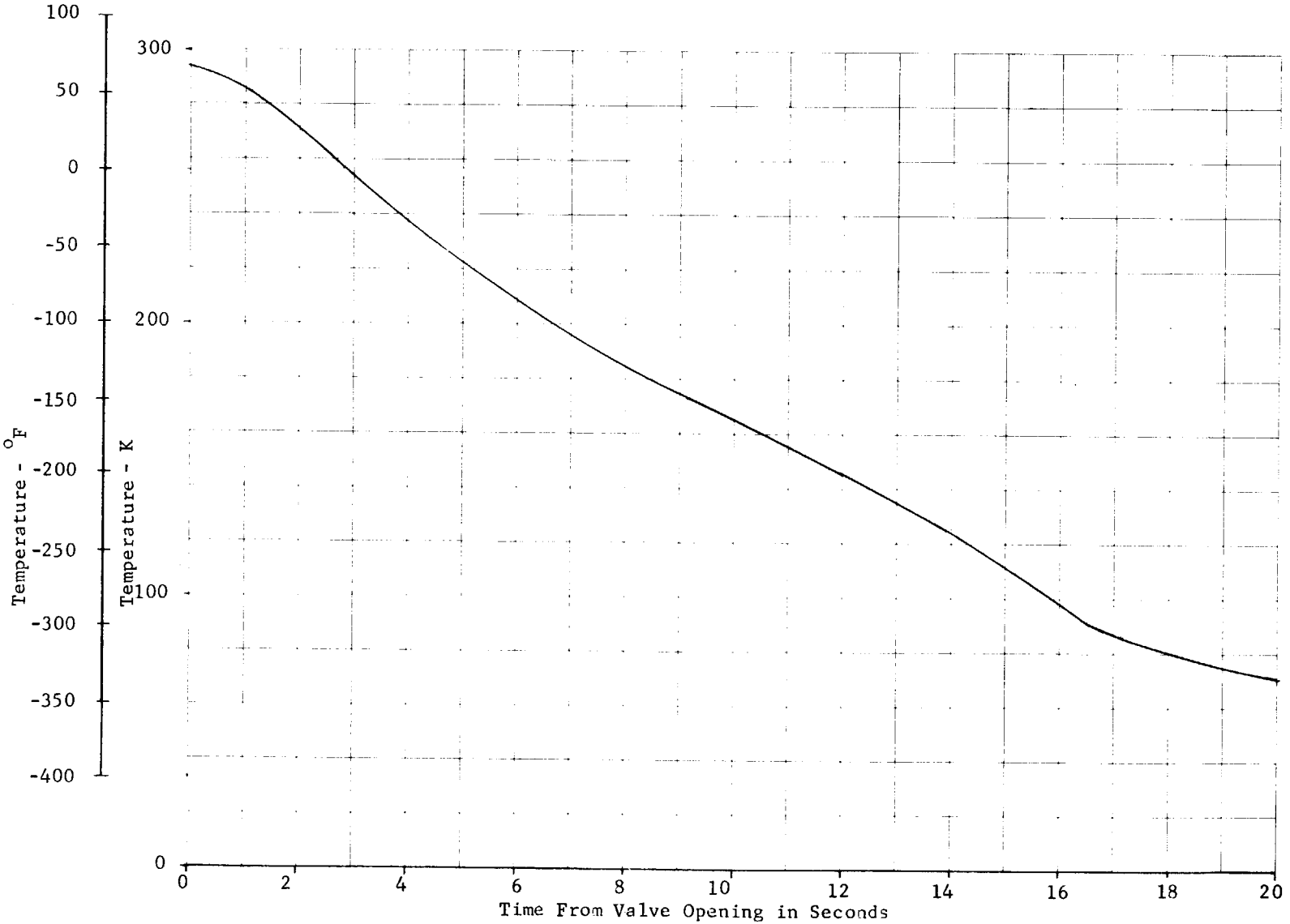

Figure 54. - Typical Metal End Fitting Temperature Response During LH_2 Chilldown

Figure 55. - OMS LOX Test Item Assembly

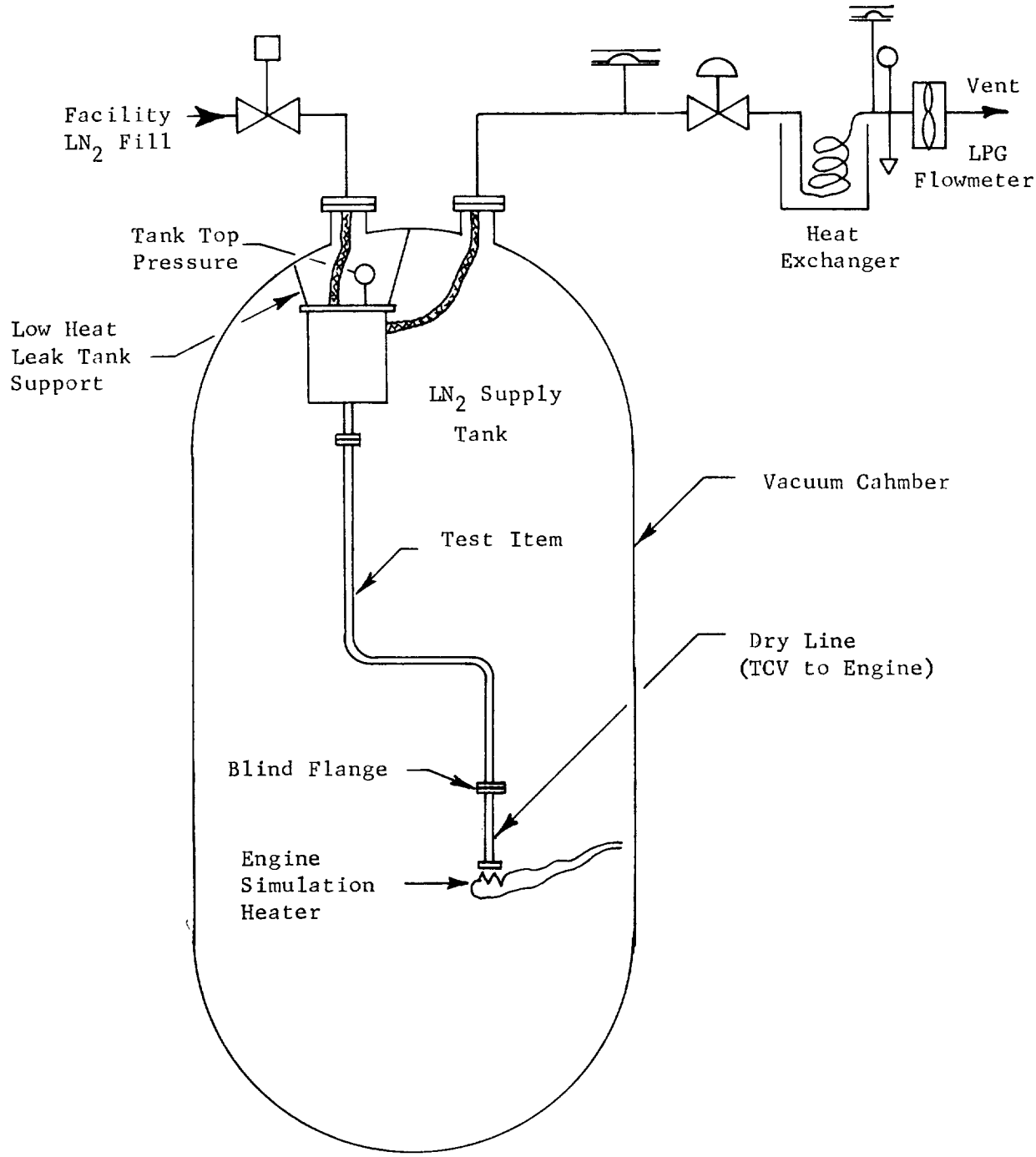

Figure 56. - OMS LOX Steady-State Heat Input
Test Installation Schematic

TABLE 18. - OMS LOX STEADY-STATE HEAT INPUT TEST RESULTS COMPARISON WITH ANALYTICAL PREDICTIONS

Line Condition	Predicted Propellant Boiloff		Actual Propellant Boiloff	
	m^3/hr	gal/hr	m^3/hr	gal/hr
Uninsulated (Bare Line)				
*Complete Contact	0.007	1.89	0.006	1.56
**Partial Contact	0.006	1.63		
Insulated *(1 Layer MLI)	0.0024	0.63	0.002	0.47
Insulated+ **(20 Layers MLI)	0.0014	0.37	0.0007	0.18

* Liner in complete contact with the overwrap.

** Liner in partial contact (50%) with the overwrap.

\+ At a density of 20-24 layers per cm (50-60 layers per inch).

The good agreement between the predicted boiloff and the test results validates the assumptions and the math models used in the analysis and, therefore, no modification of the analysis technique is required.

Radial Thermal Conductivity. - The objective of the radial thermal conductivity test was to determine the radial thermal conductivity of an OMS LH_2 composite feedline section. The test section consisted of an Inconel liner 0.008 cm (0.003 in.) thick with appropriate end fittings, overwrapped with approximately 0.05 cm (0.020 in.) of glass-fiber overwrap. The nominal tube diameter was 9.4 cm (3.7 in.).

Electric heaters were attached to the 10 cm (4 in.) long test section and guard heaters were attached on both ends of the test section to minimize end effect errors. The feedline and heaters were installed in a vacuum chamber and the feedline was filled with liquid nitrogen. The test section heaters were adjusted to maintain a desired temperature gradient radially through the test section wall. The guard heaters were controlled such that there was no axial temperature difference between the test section and the adjacent portions of the feedline.

This procedure was repeated at different radial temperature gradients and with the test section pressure at 8.27 N/sq cm absolute (12 psia) and 19.3 N/sq cm absolute (28 psia). The test setup is shown schematically in Figure 57 and the thermocouple locations and heater cross sections are shown in Figure 58.

The results of this testing showed the radial thermal conductivity of the composite feedline is much lower than that of other candidate feedline materials. The results of the radial thermal conductivity test including comparisons with other feedline materials are plotted on Figure 59. This represents a major deviation from earlier analytical predictions which can be explained by the low conductivities of the overwrap material and the lack of good contact between the liner and overwrap. The lack of contact may be more widespread than expected. Inspection of the tubes after the liner has been plastically strained, such as during burst testing, exemplifies this theory. Almost continuous hoop depressions, a significantly larger diameter than the original tube, indicate there existed a gap between the liner and overwrap in a large percent of the total surface area during routine operations.

Heat Capacity. - An experimental program was performed to determine the specific heat of a glass-fiber resin overwrap material and Inconel 718 metal for temperatures ranging from room temperature to liquid hydrogen temperature.

Test method: The average specific heat of various materials was determined for several temperature ranges by the methods indicated:

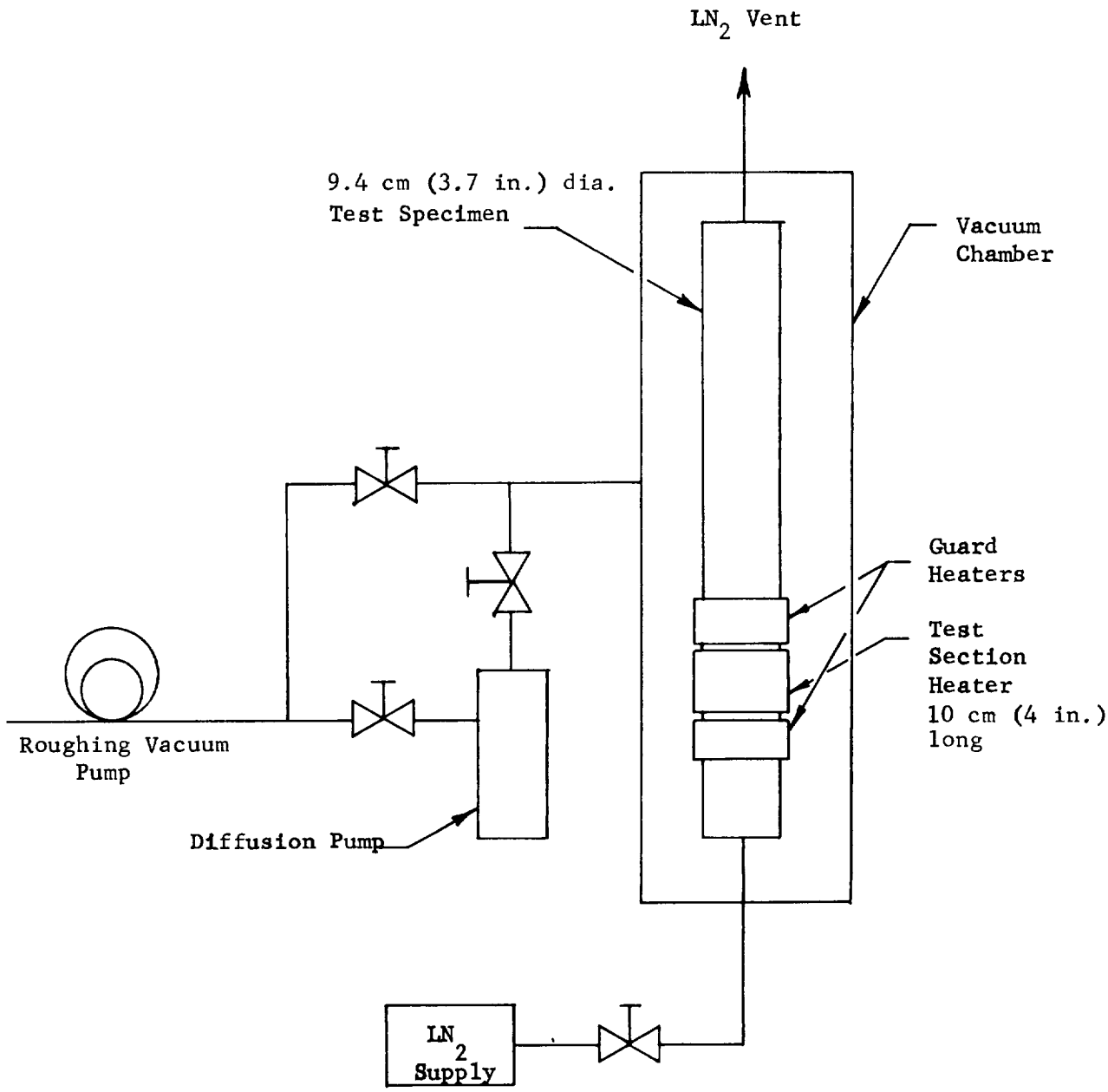

Figure 57. - Test Setup Schematic, Radial Thermal Conductivity

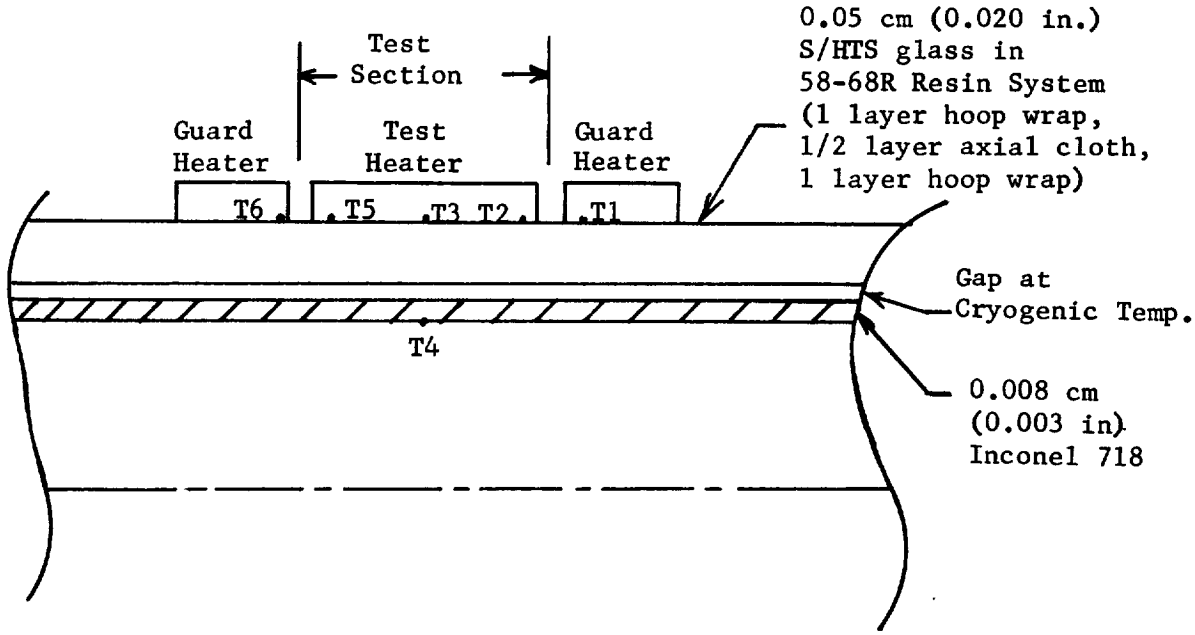

Note: Thermocouples T3 and T4 indicate the radial temperature gradient and thermocouple pairs T1 - T2 and T5 - T6 indicate the axial heat loss.

Figure 58. - Test Item Cross Section
Radial Thermal Conductivity

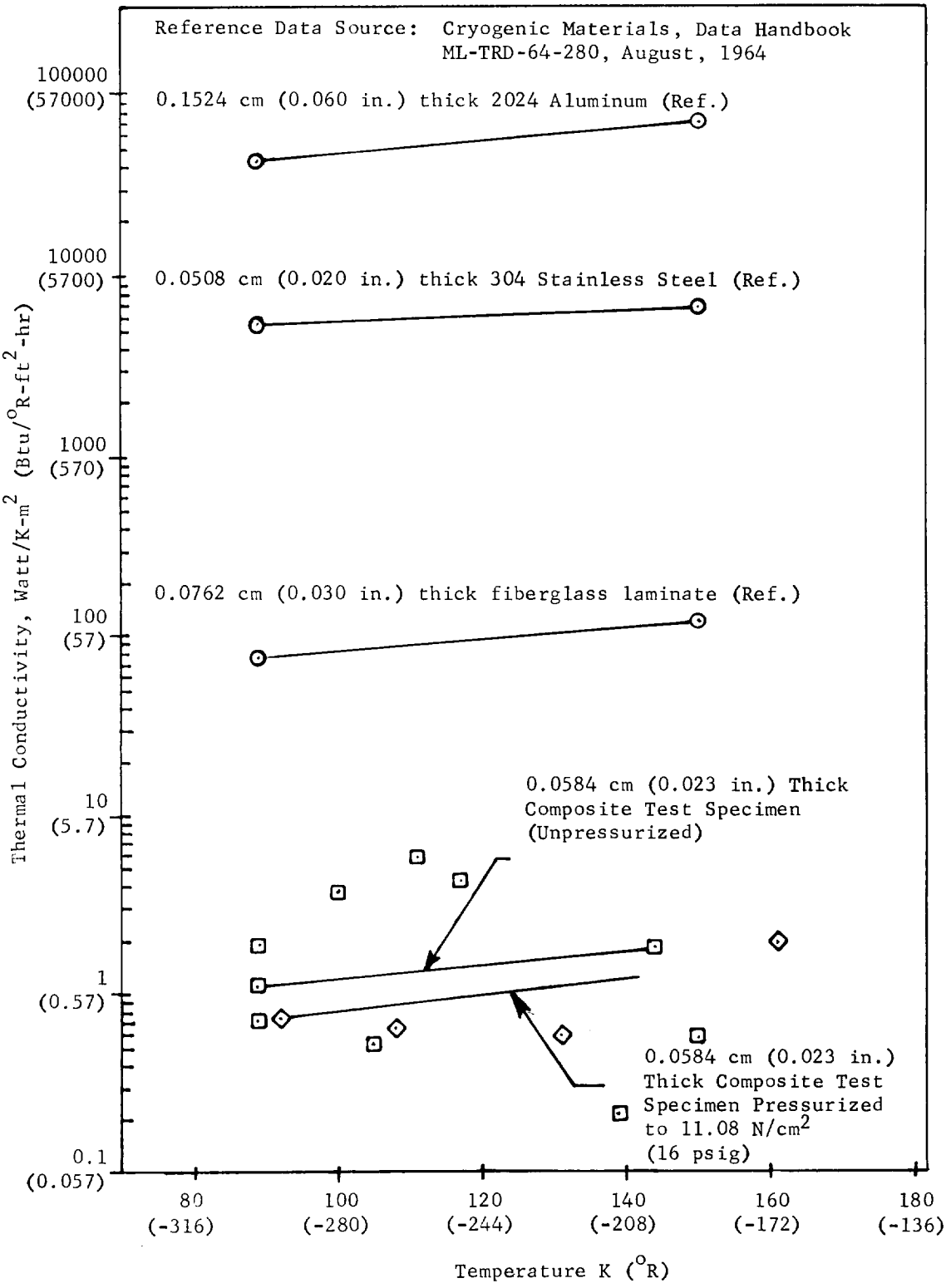

Figure 59. - Test Results, Radial Thermal Conductivity

TEMPERATURE RANGE	METHOD
294 to 350 K (70 to 170°F)	Water Bath Calorimeter
294 to 195 K (70 to -109°F)	Water Bath Calorimeter
294 to 78 K (70 to -320°F)	Water Bath Calorimeter
195 to 78 K (-109 to -320°F)	LN_2 Boiloff

The water bath calorimeter method used an insulated 1500 cc vessel, a motor-driven stirrer and a thermometer graduated in 0.01 K increments.

To facilitate calculations, the weight of water in the calorimeter was kept at 1000 g (2.2 lb) for all tests. Insulated containers of water heated to 350 K (170°F), dry ice in acetone at 195 K (-109°F) and liquid nitrogen at 78 K (-320°F) were used to condition the test specimens to the initial temperature prior to inserting them into the water bath calorimeter. The enthalpy change experienced by the water in bringing the specimen to equilibrium temperature was used to calculate the average specific heat of the specimen for the particular temperature interval.

The LN_2 boiloff method involved the use of a small LN_2 filled cryostat mounted on a balance scale graduated in 0.1 g (0.002 lb) increments. Specimens were conditioned to 195 K (-109°F) in a dry ice/acetone bath, during which time weight measurements were made to determine the cryostat weight change (LN_2 boiloff) rate. The specimen was then placed in the cryostat, and the weight versus time history again obtained. Plots of the weight versus time history were then used to determine the weight of LN_2 boiled off by the test specimen. This information, together with the known latent heat of vaporization of LN_2 was used to calculate the heat content and average specific heat of the specimen for the 195 K (-109°F) to 78 K (-320°F) interval.

Test materials: The two materials under investigation were Inconel 718 and a glass-fiber/resin overwrap material consisting of approximately 75% by weight S/HTS glass-fiber and 25% by weight 58-68R resin. In addition, reference specimens of copper, lead, 6061 aluminum and 316 stainless steel (for which published specific heat data exist) were tested to assess the validity and accuracy of the test method and apparatus. The weights of the samples were as follows:

MATERIAL	SPECIMEN WEIGHT	
	g	lb
6061 Aluminum	82.20	0.18
Copper	169.90	0.35
Lead	240.05	0.53
316 Stainless Steel	97.31	0.21
Inconel 718	28.85	0.06
Glass-Fiber/Resin Overwrap	39.80	0.09

Calibration results: The average values of published specific heat (C_p) were obtained by graphically integrating under the published curves between the temperature bounds and then dividing the area so obtained by the abscissa dimension. A comparison of these values with the test data shows a maximum deviation of 5% for the aluminum, stainless steel and lead samples and 10% for the copper sample. The calibration results indicated that the accuracy of the results subsequently obtained for the Inconel and overwrap materials should be on the order of $\pm$ 5%.

Test results: The average values of specific heat for the Inconel and overwrap test materials are shown as the shaded rectangular blocks in Figures 60 and 61. An examination of the figures shows that any data acquired by the water calorimeter method for samples conditioned at liquid hydrogen temperature would only have defined a point on the C_p curve which had already been covered by the 195 to 78 K (-109 to -320°F) tests. The usefulness of testing at LH_2 temperature was, therefore, seen to be contingent on restricting the upper bound of the temperature range to 78 K (-320°F) which is LN_2 temperature. Although it is technically feasible to determine C_p in the 21 K (-423°F) regime by either the LH_2 latent heat of vaporization method or the LN_2 calorimeter method, these techniques are relatively difficult to control to the desired accuracy levels. Furthermore, an inspection of the C_p curves shows that, since the curve must intercept the origin, any reasonable variation assumed for the curve characteristic between the origin and the intercept established for the 78 to 195 K (-320 to 109°F) regime would have only a minor effect (5% maximum) on the area under the curve (enthalpy) between the 21 and 294 K (-423 to +70°F) bounds (LH_2 system cooldown) and even less effect on the enthalpy value between 91 to 294 K (-297 to 70°F) (LOX system cooldown).

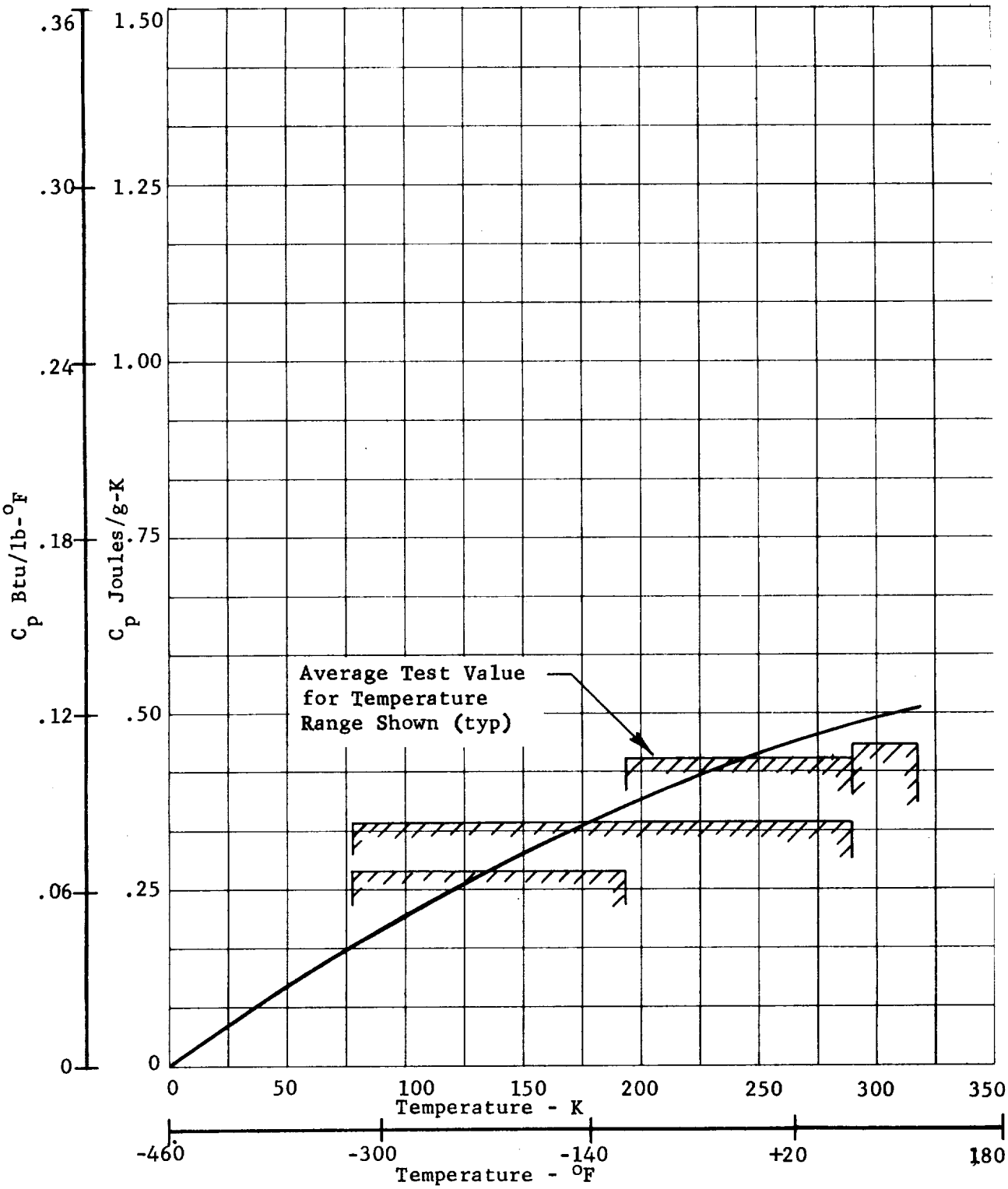

Figure 60. - Specific Heat of Inconel 718

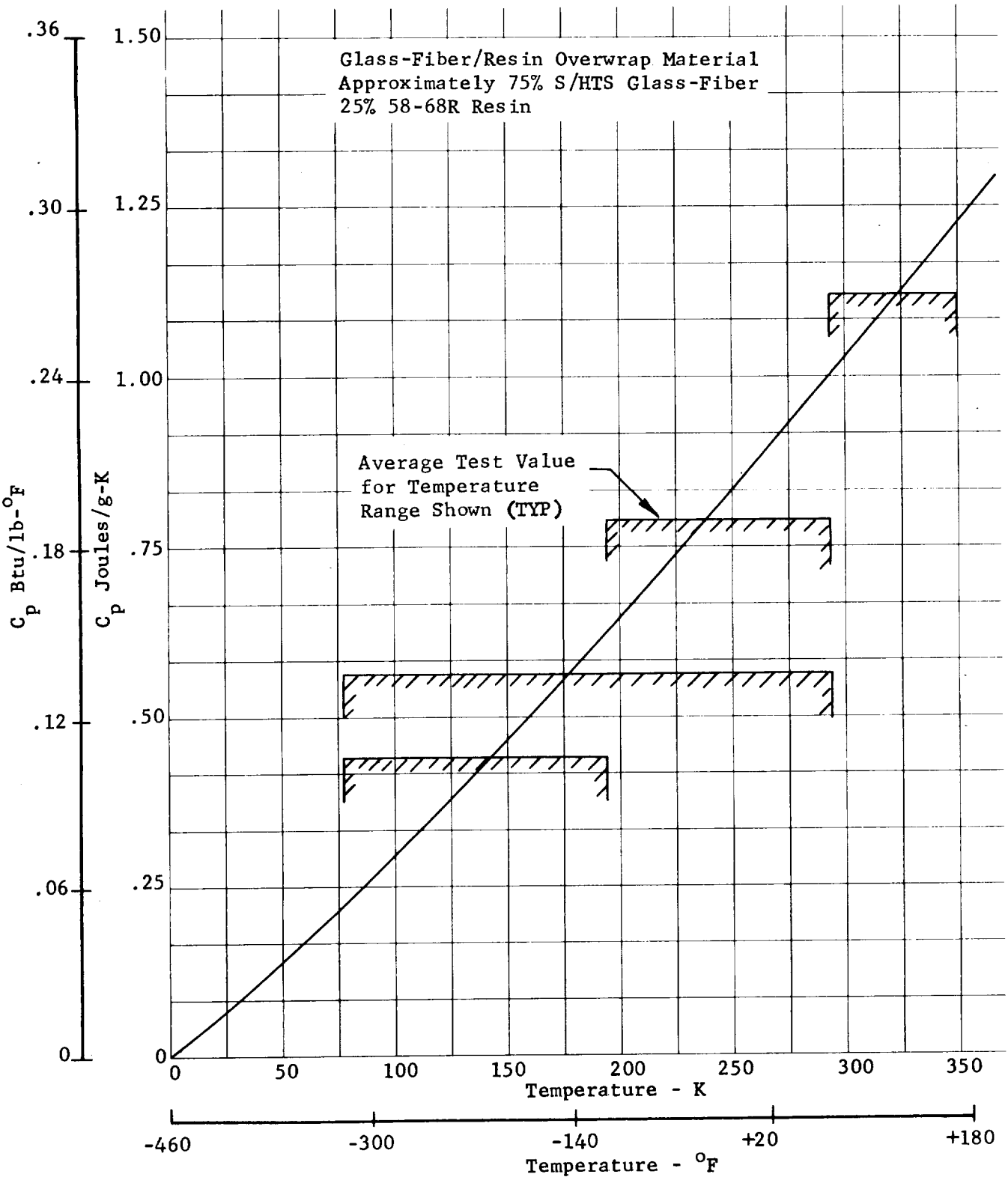

Figure 61. - Specific Heat of Glass-Fiber/Resin Overwrap Material

The curves shown in Figures 60 and 61 were fitted to provide, in each of the temperature intervals, an area under the curve equal to that of the shaded area. The curve fit for the overwrap material is considered to be very satisfactory. The curve fit for the Inconel 718 is somewhat less satisfactory, however, the area mismatch is a maximum of 4%. The enthalpy of the two materials, as given by the area under the curves, is as follows for the temperatures of interest in cryogenic propellant systems:

Change in Enthalpy

294 to 90 K (70 to -297°F)				
Material	joules/g	Btu/lbm	joules/cm^3	Btu/in.^{3}
Inconel 718	72.8	31.3	599	9.3
Glass-Fiber Resin Overwrap Material	126.5	54.4	296	4.6
294 to 21 K (70 to -423°F)				
Material	joules/g	Btu/lbm	joules/cm^3	Btu/in.^{3}
Inconel 718	82.6	35.5	676	10.5
Glass-Fiber Resin Overwrap Material	137.7	59.2	322	5.0

Analytical correlation: The specific heat of candidate feedline materials is shown in Figure 62. By integrating these data, one can conclude the total enthalpy per pound for the glass-fiber overwrap is considerably higher than for stainless steel, and considerably lower than for aluminum. However, to determine the total residual heat in a feedline, the densities must be included and the tradeoff per unit volume favors the overwrap material over both aluminum and stainless steel.

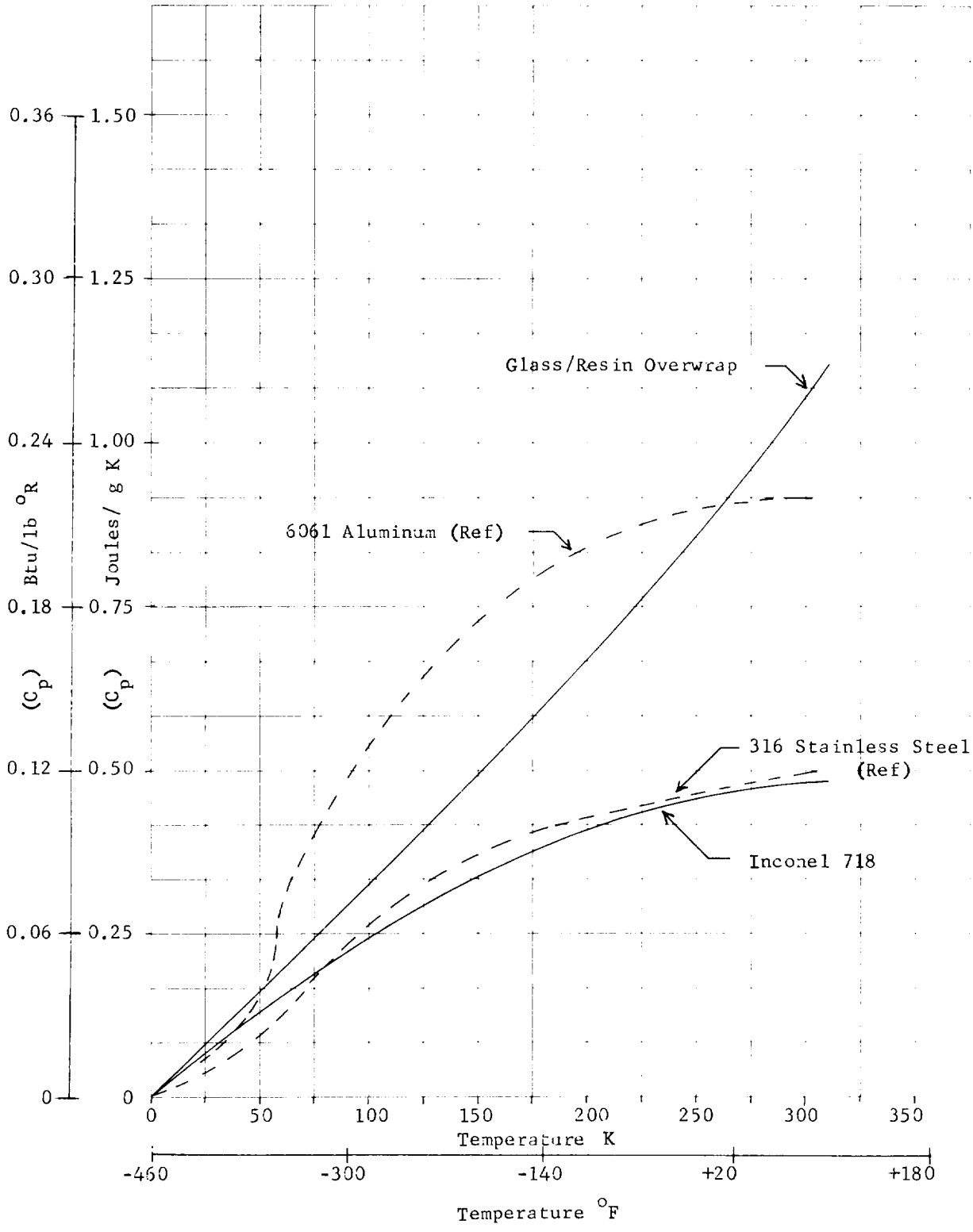

Figure 62. - Specific Heat of Candidate Feedline Materials

Vibration. - One section of the LOX OMS test item was subjected to vibration testing at sine vibration levels of: 1) 5-13 Hz at 0.6 cm (1/4 in.) single amplitude for 10 minutes; 2) 13-600 Hz at 3 g rms for 10 minutes; and 3) 600-2000 Hz at 4 1/2 g rms for 10 minutes. The vibration test was performed with the test section at ambient temperature and repeated with the test item cooled to below 89 K (-300°F) with liquid nitrogen. Leak tests performed at operating pressure 45 N/sq cm (65 psi) after each vibration test showed no degradation in the integrity of the test section. A photograph of the test item installed in the vibration test fixture is included as Figure 63.

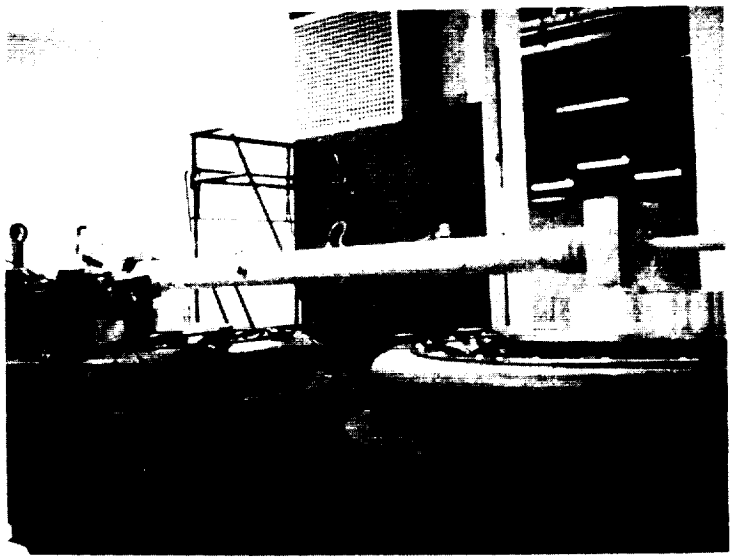

Figure 63. - Cryogenic Temperature Vibration Test

The following sketch shows the accelerometer locations on the test item:

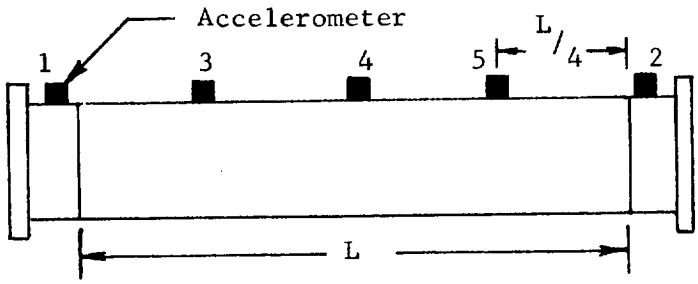

Figure 64 shows a typical plot of accelerometer output versus frequency during the cold temperature test run. The resonant frequencies and mid- and quarter-span responses determined during the test are compared with the predictions from the analytical model in Table 19.

TABLE 19. - FEEDLINE TEST DATA VERSUS ANALYTICAL RESULTS

	Frequency (Hz)	
	Test	Analysis
Mode 1	196	176
Mode 2	580	372
Mode 3	660	573
Mode 4	780	766
Mode 5	1000	956
Mode 6	1200	1143
Mode 7	1300	1331
Mid-Span Response (g)	57.3	46.9
Qtr-Span Response (g)	33.9	25.4

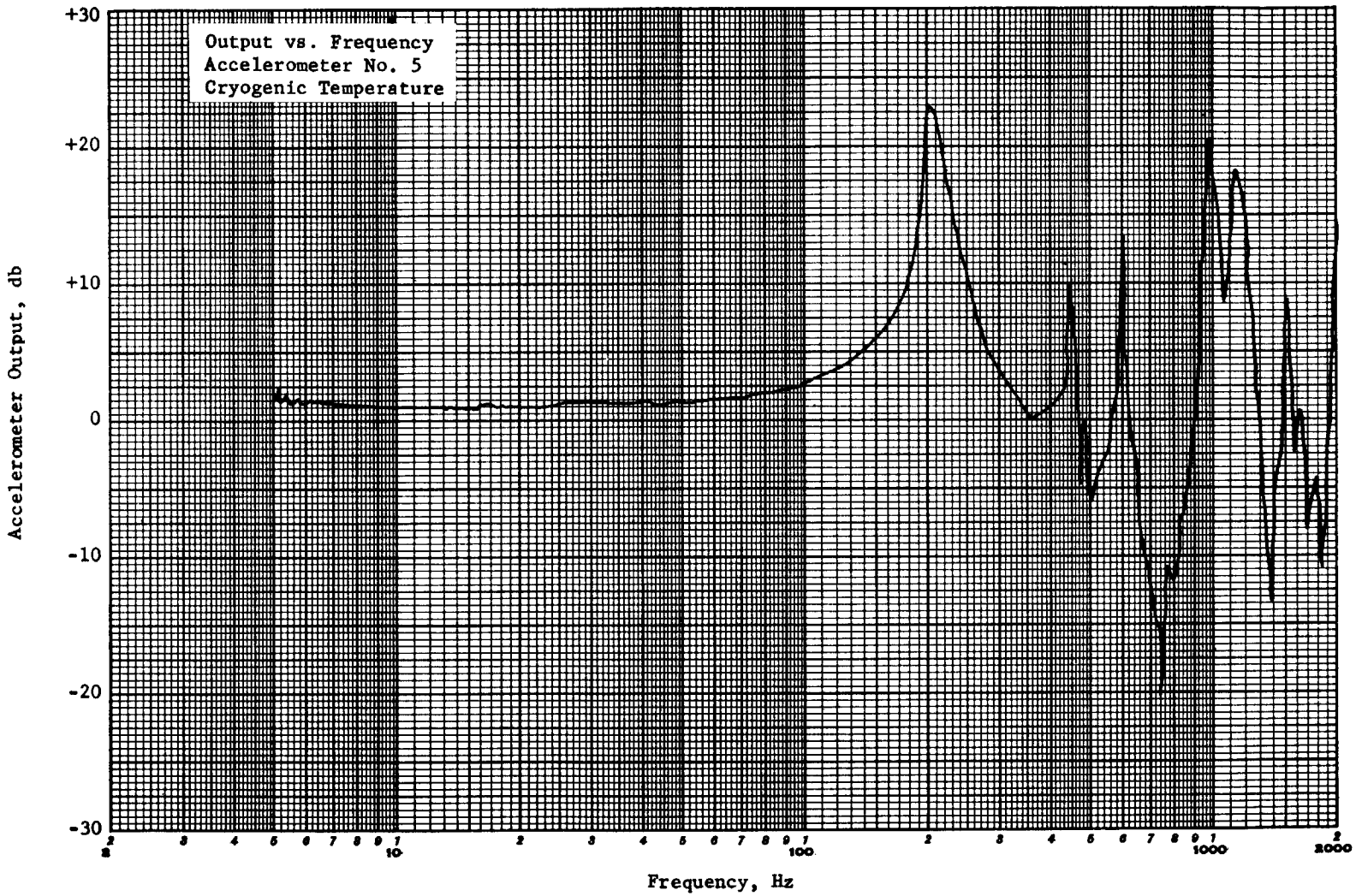

Figure 64. - Accelerometer Output vs. Frequency, OMS LOX Test Section at Cryogenic Temperature

Examination of the data shows that in general the agreement between analytical and test frequencies is good, indicating that the elastic model being used for the dynamic analysis is acceptable for future analysis.

The comparison also indicates that the agreement in response data is good, but that the analytical value used for damping was too high. The analytical value used was 5% nodal damping, whereas, the test data indicates a value of 4% should have been used.

Thermal Cycle Tests. - The LOX and LH_2 test items, both OMS and main engine, were subjected to thermal cycling from ambient temperature to operating temperature and back to ambient temperature. Two composite sections of each of the simulated OMS feedlines and the main engine LH_2 test item were subjected to 200 cycles. The failed main engine LOX test item was subjected to 50 cycles.

The thermal cycles on the OMS test items were performed with the test items installed in the test fixture shown in Figure 65. The test specimens were cooled down by flowing liquid nitrogen (LOX test items) or liquid hydrogen (LH_2 test items) from the supply through the inlet manifold and the test specimens into the outlet manifold and an outlet vent. This flow was continued until the temperatures in the overwrap became essentially stable. The test specimens were then warmed up to ambient temperature by flowing hot gaseous nitrogen from the nitrogen heater through the test specimens. The test sections were subjected to a pressure of 24 to 31 N/sq cm (35 to 45 psi) during each cooldown cycle. Leak checks performed before and after the thermal cycles showed no degradation in the structural integrity of the test sections.

The thermal cycles on the LH_2 main engine test item were performed with the tube mounted in the fixture as shown in Figure 66. A photograph of the test item installed in the fixture is included as Figure 67. Prior to performing the thermal cycles, the test item was encased in a plastic bag and leak checked at operating pressure. The test item was then coated with 13 cm (6 in.) of urethane foam insulation.

The thermal cycles on the main engine LH_2 test item were performed by precooling the test item with liquid nitrogen and then completing the cooldown with liquid hydrogen. The liquid nitrogen was sprayed inside of the test item until the overwrap temperatures dropped below 105 K ($-270^{\circ}F$). The liquid nitrogen spray was then stopped and the cooling was continued with liquid hydrogen until the temperatures in the overwrap became essentially stable. The test item was then warmed to ambient temperature with heated gaseous nitrogen. This sequence was repeated

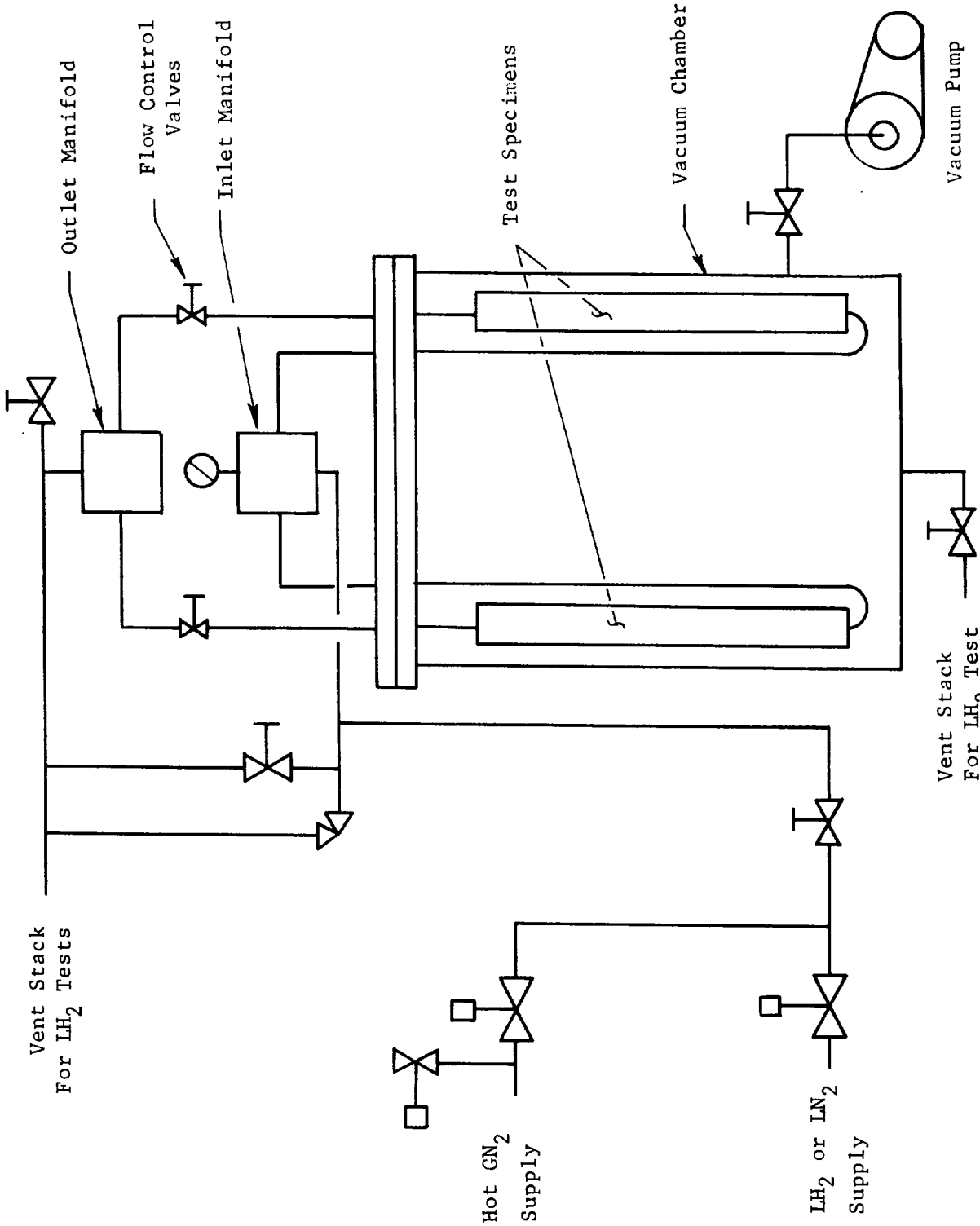

Figure 65. - OMS Thermal Cycle Test Setup Schematic

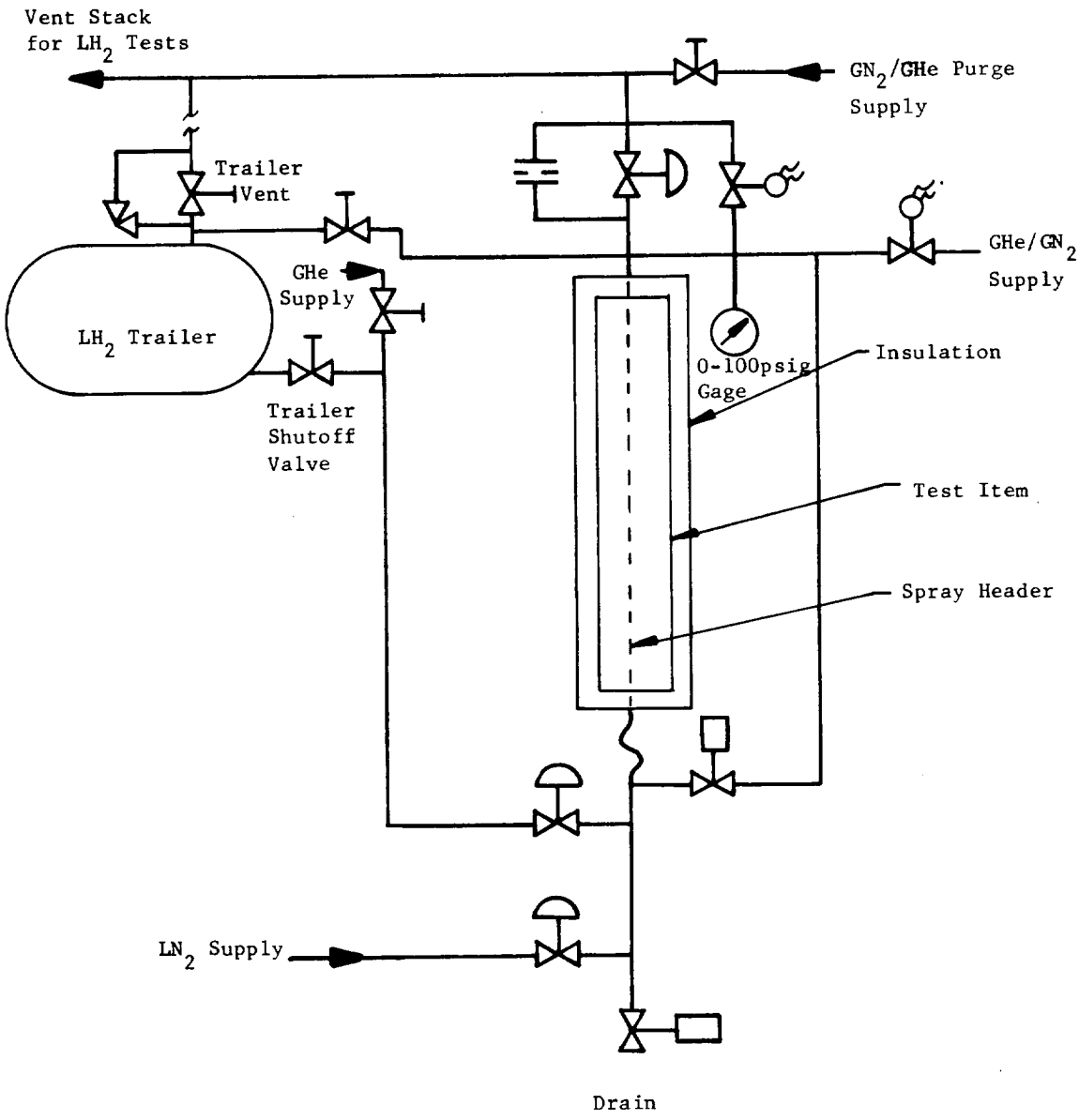

Figure 66. - Main Engine Thermal Cycle Test Fixture Schematic

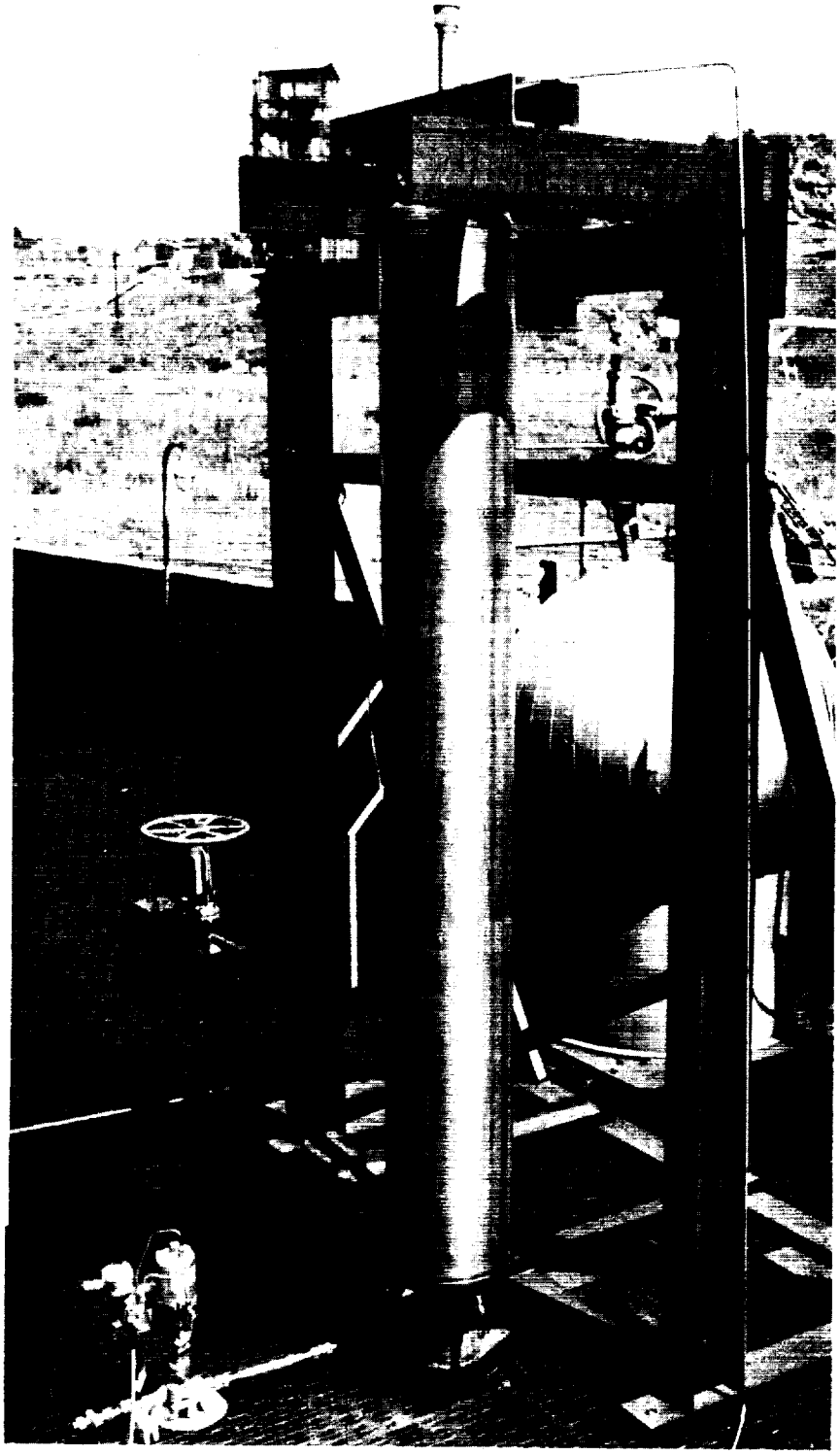

Figure 67. - Main Engine LH_2 Test Item Installed in Test Fixture Prior to Applying Insulation

until a total of 200 thermal cycles were completed, at which time the test item was subjected to a leak check at operating pressure and ambient temperature. The results of this leak test, as plotted on Figure 44, show no degradation in the integrity of the test item. A plot of temperature vs time for a typical cycle is included as Figure 68.

For the thermal cycle test on the failed LOX main engine tube, the test item was installed in the test fixture with the failed end up. The thermal cycles were performed by filling the lower one-third of the tube with liquid nitrogen and allowing the temperature to stabilize. The liquid nitrogen was then drained and the test item was warmed to ambient temperature with heated gaseous nitrogen. This sequence was repeated until a total of 50 thermal cycles were completed. The results of low pressure helium leak tests performed before starting the cycles, after completing 10 cycles, and after completing 50 cycles showed no degradation in the integrity of the explosively bonded joint. A plot of temperature vs time for a typical cycle is included on Figure 68.

Pressure Cycle Tests. - The LH_2 main engine test item was subjected to 200 pressure cycles from 10 N/sq cm (15 psi) to 69 N/sq cm (100 psi) and back. This test was performed with the test item installed in the same fixture used for thermal cycle testing. For this test the tube was filled with liquid hydrogen and allowed to stabilize. The tube was then pressurized with gaseous helium to 69 N/sq cm (100 psi) at a rate not exceeding 7 N/sq cm/sec (10 psi/sec). The test item pressure was then reduced at approximately the same rate. This sequence was repeated until a total of 200 pressure cycles were completed. A helium leak test performed after completing the cycles showed no degradation in the structural integrity of the test item.

Bending Cycle Tests. - The LH_2 main engine test item was subjected to 200 bending cycles while filled with liquid hydrogen and pressurized to 41 N/sq cm (60 psi). This test was performed with the test item installed in the same fixture used for the thermal and pressure cycle tests. The test item was filled with liquid hydrogen, allowed to stabilize, and then pressurized with gaseous helium to a pressure of 41 N/sq cm (60 psi). A lateral force of 34 kg (75 lbs) was then applied to the free end of the test item at a rate not exceeding 4.5 kg/sec (10 lbs/sec). This load was applied and relaxed until a total of 200 bending cycles were completed. The load caused a deflection of 0.95 cm (0.375 in.) at the free end of the test item.

Torsion Cycle Tests. - The LH_2 main engine test item was subjected to 200 torsion cycles while still filled with liquid hydrogen. For this test a set of rollers was installed at the free end of the test item to prevent

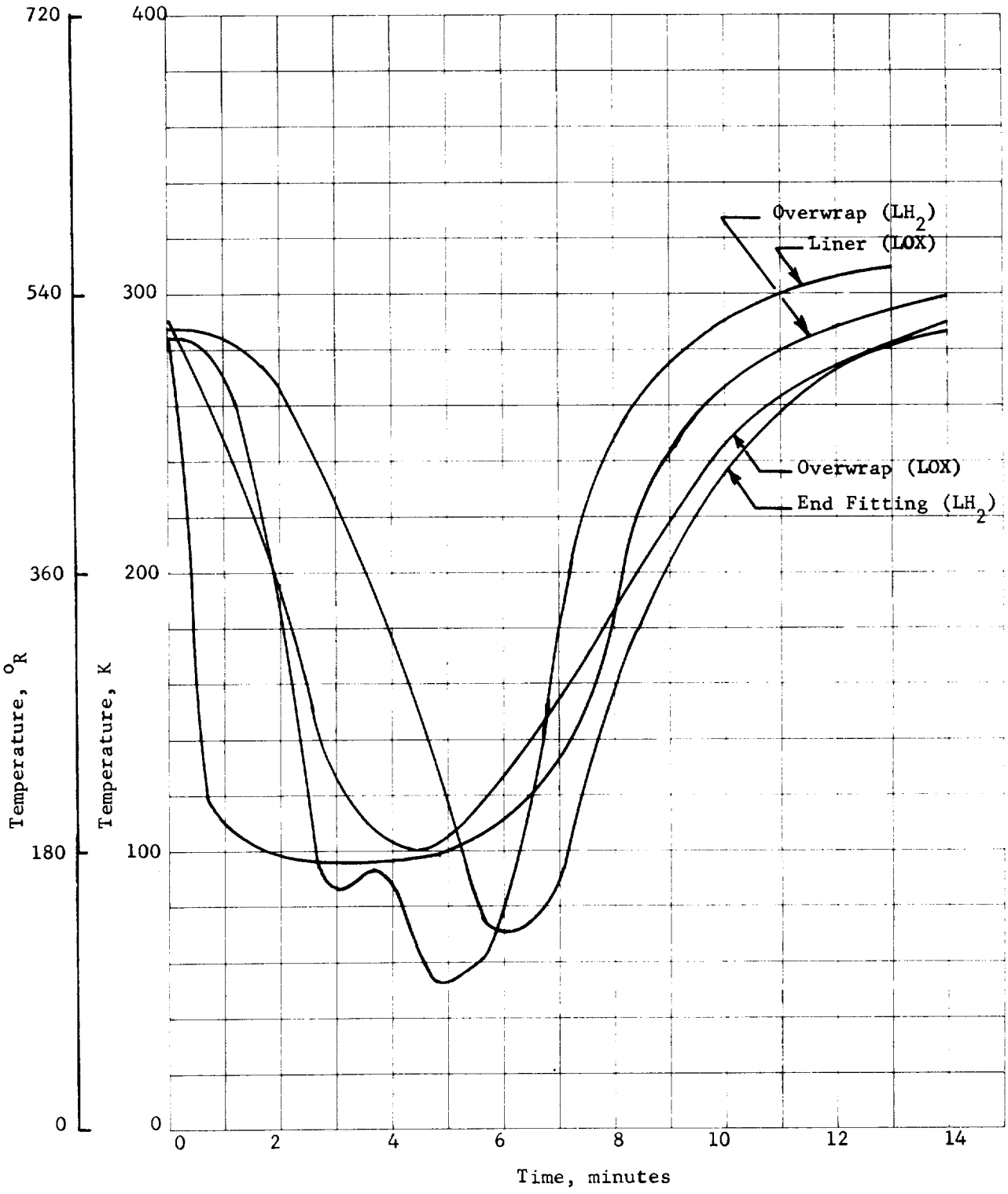

Figure 68. - Typical Thermal Cycle Main Engine Feedlines

bending and the torsion load was applied about the axial centerline of the test item. The test item was pressurized to 69 N/sq cm (100 psi) while the torsion cycles were performed. For the torsion test a load of 0.55 m-kg (4 ft-lbs) was applied for the first 37 cycles, 1.10 m-kg (8 ft-lbs) for the next 23 cycles and 2.20 m-kg (16 ft-lbs) for the remaining 140 cycles.

A helium leak test performed after completing the bending and torsion cycles showed no evidence of degradation in the structural integrity of the test item. The results of this test are plotted on Figure 44.

Burst Tests. - After completing all other testing, the test sections were subjected to ambient or cryogenic (liquid nitrogen) burst tests using a standard fixture. Table 20 compares the actual burst pressure to the predicted burst pressure for each tube section.

TABLE 20.- BURST TEST DATA VERSES ANALYTICAL PREDICTIONS

Section No.	Diameter		Temp.	Burst Pressure			
				Actual		Predicted	
	cm	in.		N/sq cm	psig	N/sq cm	psig
OMS LOX 1	6.4	2.5	AMB.	500	725	441	640
2	6.4	2.5	AMB.	562	815	441	640
4	5.1	2.0	78K(-320°F)	1138	1650	827	1200
OMS LH_2 1	9.4	3.7	AMB.	228	330	228	330
2	9.4	3.7	AMB.	221	320	228	330
3	9.4	3.7	78K(-320°F)	317	460	296	430
4	7.9	3.1	AMB.	286	415	269	390
5	7.9	3.1	AMB.	315	457	269	390
Main Engine LH_2	38	15	AMB.	124	180	105	152

The higher than predicted burst pressures indicate some transfer of axial loads to the glass-fiber overwrap. This load transfer is attributed to the friction between the liner and the overwrap when the tube is pressurized. This transfer of axial load was not considered in the tube design but was known to exist from the previous program results.

A photograph of a typical OMS test item failure at ambient or liquid nitrogen temperature is included as Figure 69 and a photograph of the failed main engine LH_2 test item is included as Figure 70. A plot of pressure versus strain during the burst test of the main engine LH_2 test item is included as Figure 71.

Weight. - Table 21 compares the actual weight of the composite feedline sections to the predicted weight of an all-metal feedline. The table also compares the predicted weight of a composite section using optimized end fittings to the all-metal feedline. If end fittings are not considered the composite lines are much lighter per unit length. For example, section 3 of the OMS LH_2 line weighs 5.58 g/cm (0.030 lbs/in.) compared to 69.36 g/cm (0.1529 lbs/in.) for the all-metal line.

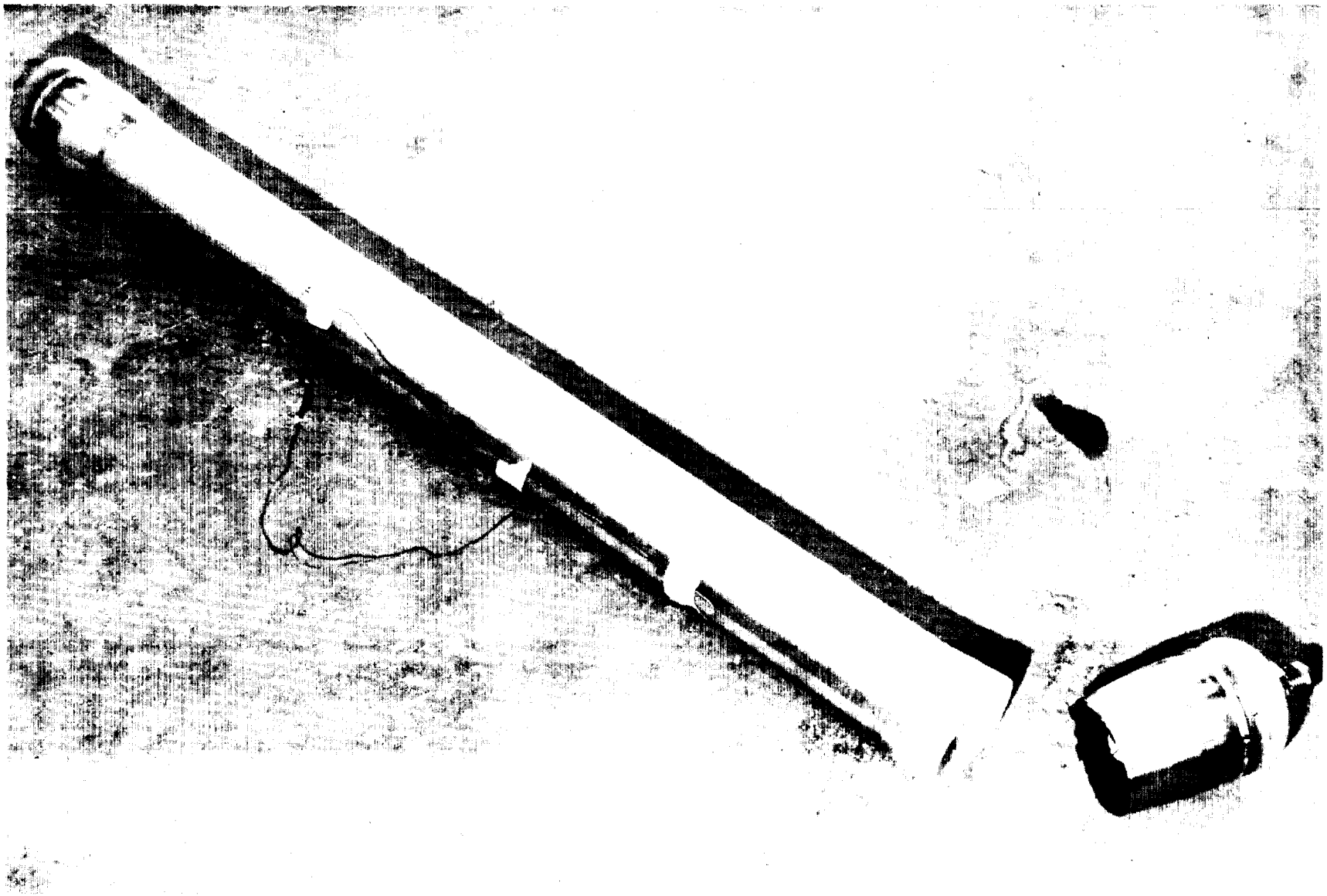

Figure 69. - Typical Burst Test Failure Mode

Figure 70. - LH_2 Main Engine Test Item
Post Burst Test

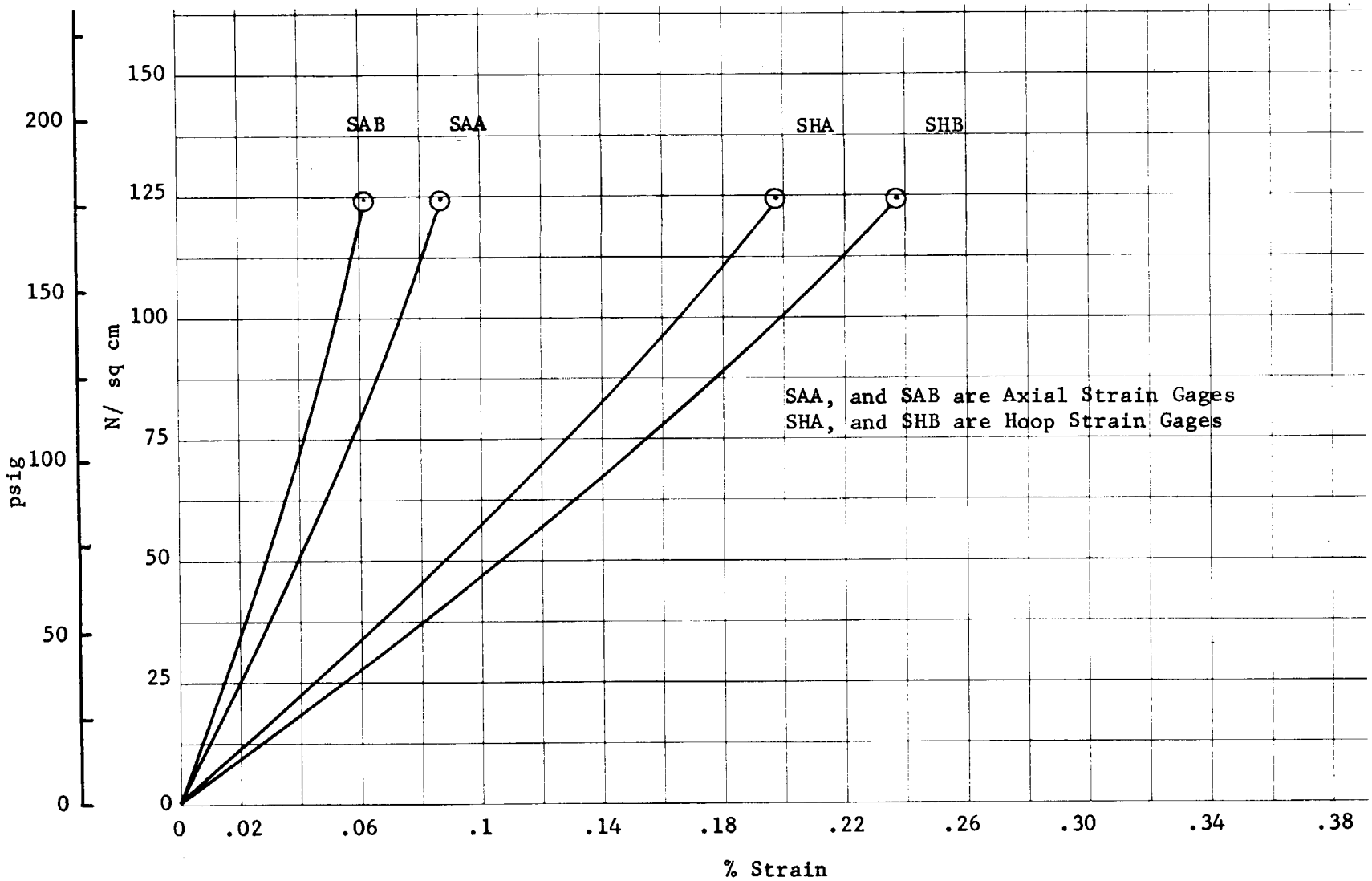

Figure 71. - LH_2 Main Engine Test Item - Burst Test Strains

TABLE 21. - OMS FEEDLINE WEIGHT COMPARISON

Line Section	*Composite				**All-metal	
	*Actual Weight		Predicted Weight Optimized End Fittings		Predicted Weight	
	g	lbs	g	lbs	g	lbs
OMS						
LOX 1 & 2	1674	3.69	1234	2.72	3846	848
3	794	1.75	617	1.36	1923	4.24
4	594	1.31	513	1.13	1538	3.39
OMS						
LH_2 1	1669	3.68	540	1.19	1873	4.13
2	2014	4.44	989	2.18	4164	9.18
3	2100	4.63	989	2.18	4164	9.18
4	1814	4.00	558	1.23	1352	2.98
5	1955	4.31	830	1.83	2250	4.96
Main Engine LH_2	8144	17.9	7775	17.1	29510	65
Main Engine LOX	12383	27.3	14122	29.4	48990	108

NOTES:

* The actual weights of the OMS composite sections include end fittings which were not weight optimized. The weights given for the main engine lines do not include end fittings.

** The weights given for the all-metal lines are for the same length of line, but do not include end fittings of any type except for the main engine LOX line. Since this line is aluminum it includes two 6800 g (15 lb) aluminum Conoseal flanges so that it can be attached to steel bellows, sliding joints or distribution manifolds.

Summary of OMS Test Results. - The results obtained from the test program on the OMS LOX and LH_2 test items are summarized in the following paragraphs:

- The actual chilldown time for the LH_2 test configuration was less than the 2 seconds predicted;
- The Inconel liners must be heat treated when very rapid chilldown of the composite tubes is anticipated. This new requirement is discussed in the next section of this report (page 149);
- The steady-state heat input to the feedline can be accurately predicted;
- The test items performance is not degraded by thermal cycling or exposure to typical space vehicle vibration environments;
- When the composite tubes are pressurized, some axial load is transferred to the overwrap, as evidenced by the higher than expected burst pressures;
- The radial thermal conductance of the tube is very low when vented and when pressurized adequately to close the gap between the overwrap and the liner;
- A single layer of MLI provides a very satisfactory correction to the high emissivity of the overwrap surface;
- The tubes are adequately low in thermal mass to consider flying the feedline dry for a variety of missions.

Summary of Main Engine Test Results. - The results obtained from the test program on the main engine test items are summarized in the following paragraphs:

- Some wrinkling and buckling of the liner during the fabrication process does not degrade the performance of the composite tube;
- Large diameter composite tubes can withstand moderate bending and torsional loads without loss of performance capabilities;
- Further development of the explosive bonding process is required to obtain a reliable bond between Inconel liners and aluminum end fittings although at least two successful bonds were obtained;
- Fabrication of large diameter tubes is very feasible, especially in liner thicknesses exceeding approximately 0.12 cm (0.005 in.).

Summary of Test Problems. - The significant problems encountered during the test program are summarized as:

- The low pressure leak checks performed during fabrication cannot be used to accurately predict leakage of the composite tubes at operating pressure;

- The temperature of the explosive bonded joint, as currently developed, must be maintained below 422 K ($300^{o}F$) to prevent unbonding of the joint during fabrication or operation. During fabrication, the temperature of the bonded joint can be controlled by using a chill ring for welding operations.

REQUIRED OR PROPOSED MODIFICATIONS

The problems encountered during the fabrication and test program suggest several modifications to future designs. The modifications or changes include:

- o Liner Heat Treatment
- o Knurling of the End Fittings
- o More Stringent Leakage Criteria

Liner Heat Treatment. - During the rapid chilldown test of the LH_2 OMS feedline assembly, a rather severe wrinkling of the annealed liner occurred. Stress analysis did not indicate the need to heat treat the liner after welding for the design pressures baselined in this program and no heat treatment was performed on the tubing liners. After the chilldown test, a stress analysis was performed assuming the overwrap remained at ambient temperature, as indicated by thermocouples during test, while the liner was chilled to 20 K ($-423^{o}F$). The analysis shows the possibility of exceeding the yield stress of annealed Inconel 718 during this rapid chilldown operation. Although some additional cost is involved, it is suggested the liners be heat treated prior to welding to the end fittings to preclude this damage unless, for a specific use, no rapid chilldown is contemplated. As a result of this test and the analysis, the chilldown test for the LOX OMS lines was deleted to prevent the same damage. Of interest, although both ends of each section of the LH_2 line were wrinkled badly, only one of the ten joints demonstrated any leakage, and the burst pressures were still higher than predicted.

Knurling of the End Fittings. - Knurls were added to the end fittings on selected designs for contract NAS3-12047[1] to provide torsional resistance and torsional load transfer from the metal liner to the overwrap. A photograph of a typical knurl is shown in Figure 72. This knurl also proved capable of providing more effective axial load transfer to the overwrap and could be used to further reduce the liner thickness. This capability to transfer load was again demonstrated during this program by burst testing the tube shown in Figure 73. The ultimate tensile stress in the liner of 62,000 N/sq cm (90,000 psi) would be attained at an internal pressure of 379 N/sq cm (550 psi). However, the tube failed at 638 N/sq cm (925 psi) when the 1/2 layer of axially oriented overwrap failed in tension and permitted an axial strain in the liner of adequate magnitude to create a gap between the end of the hoop supporting overwrap and the end fitting as shown in the figure. The liner failed in the hoop direction at this gap.

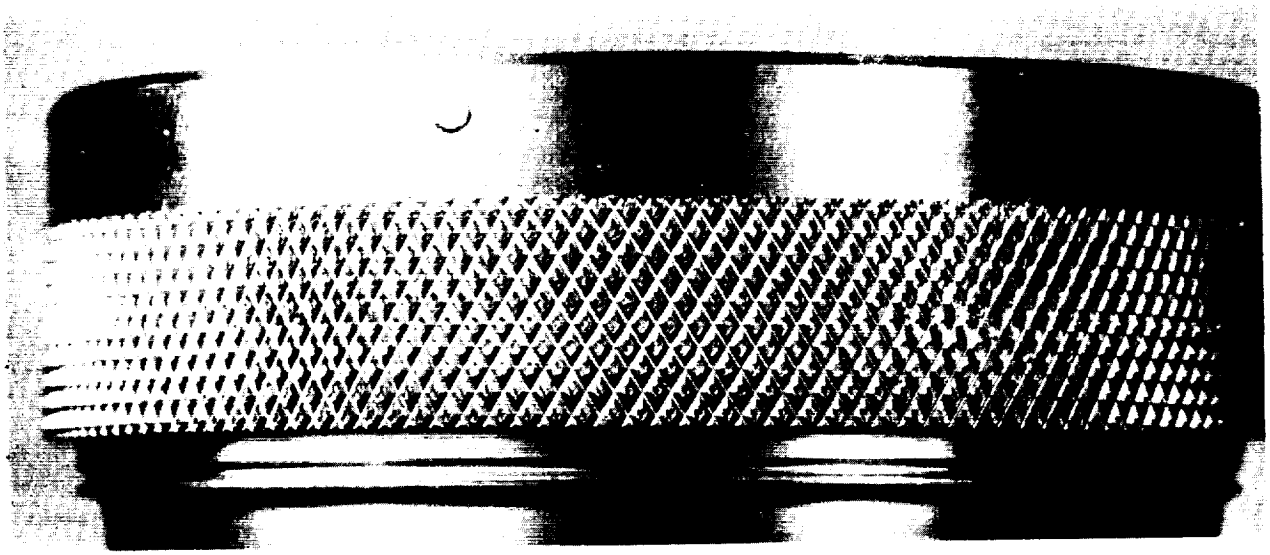

Figure 72. - Knurl on a 13 cm (5 in.) Diameter Tube

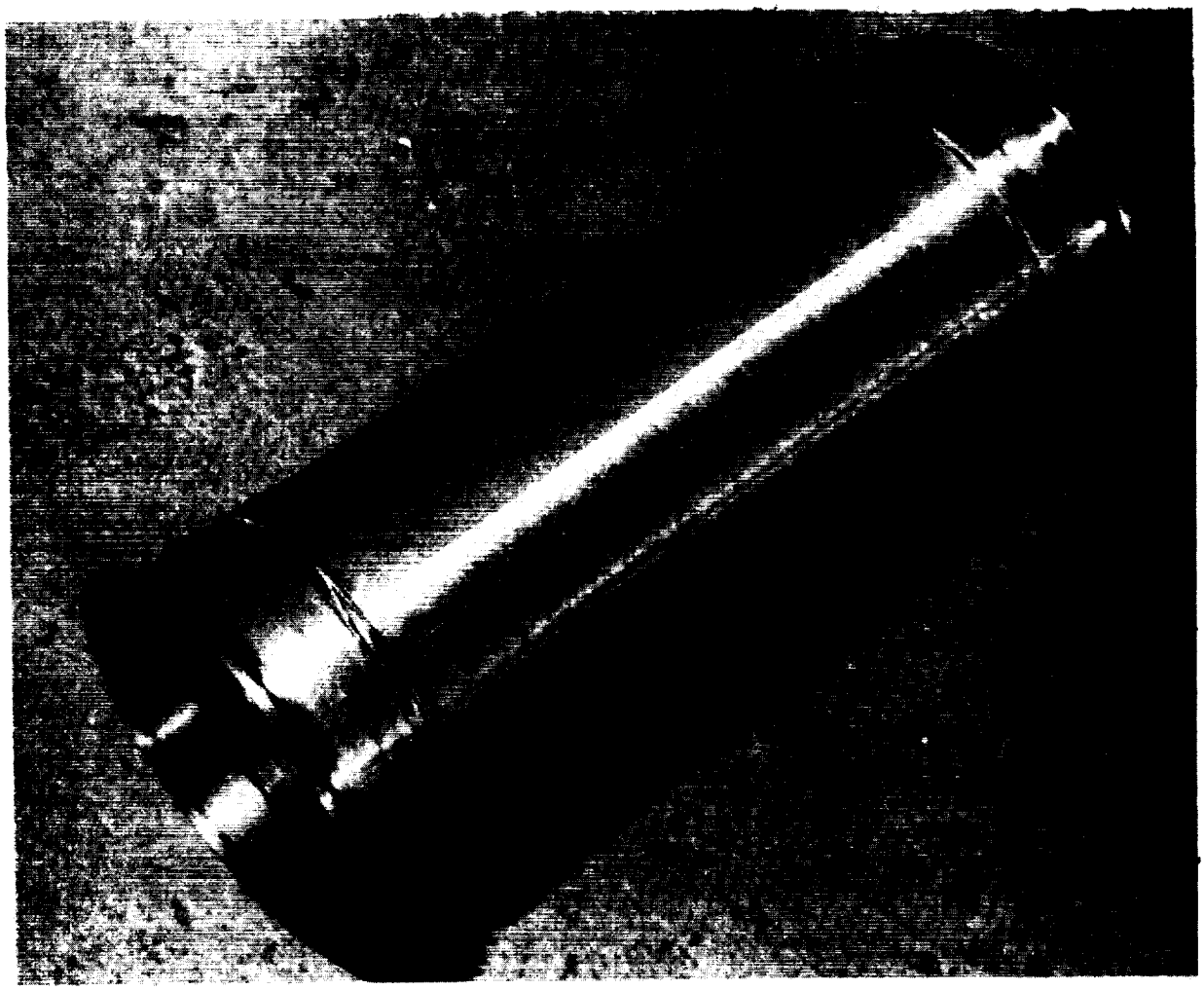

Figure 73. - Burst Test Specimen With Knurled Ends

This knurl can help solve another problem encountered on this program--that of damage during handling. During removal of the LOX OMS assembly from the vacuum chamber, one end of the horizontal tube section was allowed to catch on the edge of the chamber opening. This occurred while the tube was being lifted by an overhead crane and the resulting moment caused major damage to the tube section as shown in Figure 74. The addition of a knurled section on the end fitting would assist transfer of these excessive loads to the overwrap. However, this damage has only happened one time while handing almost 200 different specimens through a variety of fabrication and test activities on this and previous programs. Proper handling should be adequate to eliminate the concerns but the knurl could provide additional margin. The knurl can be described as a "Male Diamond Knurl - Pitch 0.048" with 21 teeth per inch, and is approximately 1.2 cm (0.5 in.) wide.

The knurl has two apparent undesirable side-effects. First there is a slight additional cost for end fitting fabrication and second, the knurl causes axial compression in the liner during cure which may result in wrinkles forming in the thinner liners. During overwrap, no release agent is applied in the knurled area and a thin coat of the resin is brushed into the knurl to assist in shear strength. The knurl may require an additional 1.2 cm (0.5 in.) length on the end fitting when using the resistance welded style joint since the weld cannot be performed in the area of the knurl.

More Stringent Leakage Criteria. - Relatively minor, but out-of-tolerance leakage in the liner-to-end fitting weld was a problem on this program, as it was on the prior program. Since the tubes can be provided in the leak-free condition at operating pressure (but with some risk of spoilage and additional cost), the prevention of leakage was not specifically addressed during the program--that is, leaky joints, are expensive to replace when making only one or a few tubes but can be relatively easily replaced during a production program.

One problem arises since leak checking the metallic liner to end fitting joint cannot usually be performed at operating pressure because of the lack of metal liner strength in the hoop direction or safety (without the overwrap). This creates problems in locating a leak and suggests a review of the applicabilities of lower pressure to determine leakage rates at higher pressure. Frequently tubes thought to be leak-free at this low pressure have significant leaks at higher pressure. Assuming viscous flow of the gas through a leak, Poiseville's law can be used to quantify the leak which occurs when the mean free path of the gas is smaller than the cross section dimension of the hole[10]. Viscous flow normally occurs with positive pressure methods such as mass spectrometer probing.

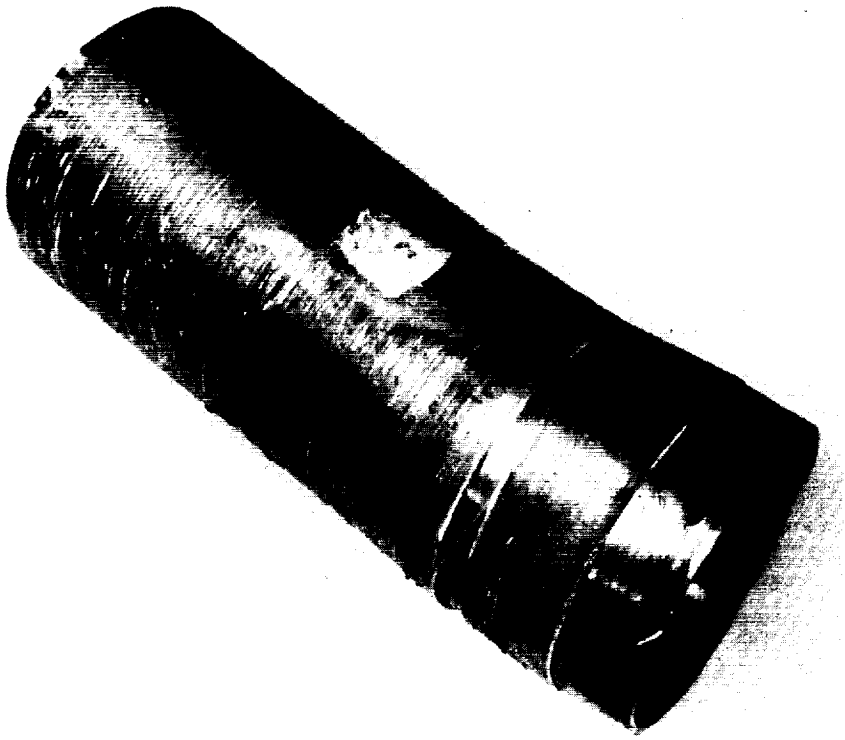

Side View

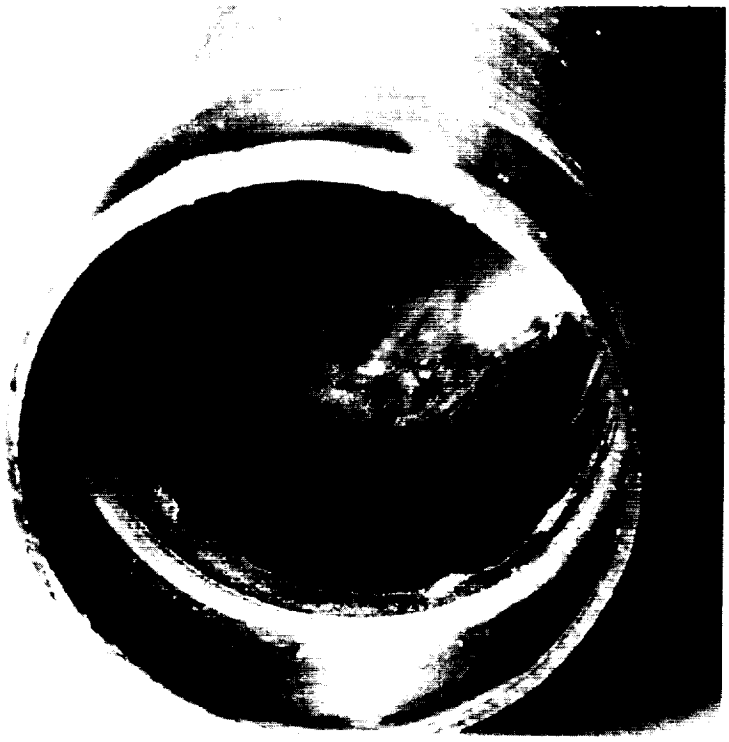

End View

Figure 74. - Damaged LOX OMS Tube

From Reference 10:

$$Q = \frac{\pi r^4}{16 \mu l} \quad (10^{-3}) \quad (P_1^2 - P_2^2)$$

Where Q = Flow Rate, micron liters/sec
r = Radius of the leak path, cm
μ = Viscosity of the gas, poise
l = Length of the leak path, cm
P_1 = Upstream Pressure, microns
P_2 = Downstream Pressure, microns

The only variable for a fixed hole or leak path is pressure, and in viscous flow, the leakage is proportional to the difference of the squares of the pressures. A leak of helium gas at 1 atmosphere delta pressure which is the typical level of leak checks at this stage of fabrication can be compared to a working pressure of 45 N/sq cm (65 psi) using this equation with the pressure as the only variable.

At the leak test level

$$P_1^2 - P_2^2 = 1.7 \times 10^{12} \text{ microns}^2$$

and at the operating pressure level

$$P_1^2 - P_2^2 = 1.6 \times 10^{13} \text{ microns}^2$$

which is a difference of one order of magnitude. This indicates a leak check at the lower pressure level should be satisfactory.

An additional loss of sensitivity takes place because of the inability to evacuate the inside of the liner and remove the air which is trapped inside (1 atmosphere). The addition of 1 atmosphere of helium to the trapped air will result in a 50% solution of helium. Under viscous flow, the two gases, air and helium, both will flow through a leak at the same rate regardless of the concentrations in the mixture. Thus the sensitivity will be 1/2 that with pure helium.

In practice, the leaks at operating pressures do not correlate at the theoretical levels with the low pressure leak checks, indicating some other variable exists which results in several orders of magnitude difference in the respective leak rates. This difference can be explained by a review of the configuration of the leak path. As the pressure increases, metal strains increase and, quite likely, the radius of the leak path will increase, again assuming a circular leak for simplicity. This radius is a fourth power function in the equation and a small increase can account for substantial additional leakage.

The suggested criteria for the low pressure leak checks, in production hardware, is no detectable leaks with a helium mass spectrometer at the maximum safe pressure. While this will not assure no leakage at operating pressure, it should assure levels sufficiently low to provide good service even if the line is a part of a vacuum jacketed assembly.

RECOMMENDATIONS AND ADDITIONAL WORK REQUIRED

As a result of the knowledge and experience gained from this program, Martin Marietta Corporation makes the following recommendations for additional work:

1) Further development of explosive bonding techniques as a method of attaching end fittings, especially using the lightweight aluminum end fittings and the efficient Inconel or stainless steel tube liners.

2) Quantification of the effects on the liner of a variety of overwrap tensions and cure temperatures. Development of a useful equation to determine the required internal pressure to offset the stresses caused by these tensions and temperatures.

3) Extension of the upper temperature limits for the composite lines to include the Space Shuttle LOX pressurization line, currently required to be operated up to 667 K (+740^{o}F).

4) Evaluation of the low density overwrap candidates including PRD49-III, graphite, and boron. The evaluation should include analytical modeling, fabrication of tubes, and empirical verifications.

5) Comparison between the thermal performance of all-metal tubes and candidate overwrapped composite feedlines by empirical evaluation of the two using identical test settings.

6) Application and evaluation of thermal coatings for use in modifying the surface emissivity of the composite. The coatings may be useful when a layer of aluminized mylar would be exposed to damage.

7) An evaluation of the feasibility of using a braiding technique to apply the overwrap.

SUMMARY OF RESULTS

The purpose of this program was to investigate the feasibility of using metal lined glass-fiber tubing as propellant outflow lines on cryogenic space vehicles such as the Space Shuttle booster and orbiter.

The concept of the composite tubes includes thin walled metal liners, to provide leak-free service and reduce conductive heat transfer, with an overwrap of glass-fibers to provide structural integrity and handling ability. The tubes are very lightweight when compared to conventional tubing.

Results obtained during the course of the program include the following:

1) The most efficient use of the lines would be to locate the composite section as near the tank as possible and make it as long as is practical;

2) The composite tubes are lightweight and could provide a significant weight saving in the vehicle;

3) The composite tubes are sufficiently strong and rigid so that no special handling techniques, other than ordinary care, are required;

4) Some wrinkling or slight buckling of the liner during fabrication or assembly does not degrade the performance of the completed composite line;

5) The test program confirms the analytical predictions for the tube performance in weight, thermal characteristics, vibration, and burst pressures;

6) The chilldown characteristics of the tubes could prove valuable by permitting a long term use system to use a "dry" feedline, thus eliminating the need for elaborate recirculation systems to keep the system chilled during coast periods;

7) The tubes are cost competitive for the Space Shuttle external tank, which allows an expenditure of $66/kg ($30/lb) of weight saved per launch vehicle. A weight savings of approximately 540 kg (1200 lb) per external tank can be realized by using the composite lines. This weight saving represents a $36,000 saving for each launch vehicle;

8) Manufacturing methods required to fabricate the thin metal liners and apply the glass-fiber overwrap are available in the present state-of-the-art; however, further development of the explosive bonding technique may be warranted. While successful aluminum to

Inconel bonds were made on the 38 cm (15 in.) diameter LOX main engine line, subsequent damage to one of the joints created the need for a rebonding which was not successful. This process if refined, can reduce feedline weight substantially;

9) While the 0.008 cm (0.003 in.) thick liner for the LH_2 main engine feedline was successfully fabricated and the tube passed all tests, a minimum gage of 0.013 cm (0.005 in.) is suggested for tubes over 25 cm (10 in.) in diameter;

10) One of the LOX OMS tube sections was fabricated to include thicker ends [0.012 cm (0.005 in.)] and an optimized thickness in other areas. This process, accomplished by selectively redrawing the tube, provides for easier, more reliable welding to the end fittings without sacrificing weight.

REFERENCES

1) C. A. Hall, T. J. Pharo, J. M. Phillips, and J. P. Gille: Low Thermal Flux Glass-Fiber Tubing for Cryogenic Service. Martin Marietta Corporation, Denver, Colorado, NASA CR-72797, March, 1971.

2) Part 11-2 (A), Technical Summary, Orbiter. McDonnell Douglas Aircraft Corporation, Martin Marietta Corporation - Denver Division, TRW Systems Incorporated, Pan American World Airways. Space Shuttle System, Phase B, Final Report. MDC E0308, June 1971.

3) Part 11 (A), Detail Mass Properties Report, Orbiter Details. McDonnell Douglas Aircraft Corporation, Martin Marietta Corporation - Denver Division, TRW Systems Incorporated, Pan American World Airways. Space Shuttle System, Phase B Study, Final Report. MDC E0377, June 1971.

4) Part 11-3, Technical Summary, Booster. McDonnell Douglas Aircraft Corporation, Martin Marietta Corporation - Denver Division, TRW Systems Incorporated, Pan American World Airways. Space Shuttle System, Phase B Study, Final Report MDC E0308, June 1971.

5) Part 111 (B), Detail Mass Properties Report, Booster Details. McDonnell Douglas Aircraft Corporation, Martin Marietta Corporation - Denver Division, TRW Systems Incorporated, Pan American World Airways. Space Shuttle System, Phase B Study, Final Report. MDC E0377, June 1971.

6) Baseline Tug Definition Document. Rev. A, National Aeronautics and Space Administration, George C. Marshall Space Flight Center, Huntsville, Alabama, June 26, 1972.

7) J. W. H. Chi: Cooldown Temperatures and Cooldown Time During Mist Flow. Advances in Cryogenic Engineering, Vol. 10, Sec. A-L, pg. 330, Plenum Press, 1964.

8) F. E. Ruccia and R. B. Hinckley: The Surface Emittance of Vacuum-Metallized Polyester Film. Advances in Cryogenic Engineering, Vol. 12, Plenum Press, New York, 1967.

9) Capillary Insulation Feedline. Report No. D-71-48774-004, Martin Marietta Corporation, Denver, Colorado, September, 1972.

10) Leak Detection Manual. Bell and Howell, CEC/Analytical Instruments Division, Monrovia, California, January, 1969.

11) Alexander Mendelion: Plasticity: Theory and Application. MacMillan Co., N. Y., 1968.

12) Saturn Feedline Specifications, Space Division of North American Rockwell Corporation.

ME271-0010 Line Assembly, Engine Feed, LOX
ME271-0011 Line Assembly, Engine Feed, LH_2
ME271-0012 Line Assembly, Fill and Drain, LOX

13) R. J. Roark: Formulas for Stress and Strain. 4th Edition, McGraw-Hill, 1954.

14) G. W. Howell, T. M. Weathers: Aerospace Fluid Component Designers Handbook. TRW Systems Group, Redondo Beach, California, RPL-TDR-64-25, March, 1967.

DISTRIBUTION LIST

Report Copies	Recipient
	National Aeronautics & Space Administration Lewis Research Center 21000 Brookpark Road Cleveland, Ohio 44135
1	Attn: Contracting Officer, MS 500-313
5	E. A. Bourke, MS 500-205
1	Technical Report Control Office, MS 5-5
1	Technology Utilization Office, MS 3-16
2	AFSC Liaison Office, 501-3
2	Library
1	Office of Reliability & Quality Assurance, MS 500-211
1	J. W. Gregory, Chief, MS 500-203
5	J. J. Notardonato, Project Manager, MS 500-203
1	N. T. Musial, MS 500-113
1	E. M. Krawczonek, MS 500-209
1	J. R. Barber, MS 500-203
1	Director, Physics & Astronomy Programs, SG Office of Space Science NASA Headquarters Washington, D. C. 20546
1	Director, Planetary Programs, SL Office of Space Science NASA Headquarters Washington, D. C. 20546
1	Director, Manned Space Technology Office, RS Office of Aeronautics & Space Technology NASA Headquarters Washington, D. C. 20546
2	Director Space Prop. and Power, RP Office of Aeronautics & Space Technology NASA Headquarters Washington, D. C. 20546

Report Copies	Recipient
1	Director, Launch Vehicles & Propulsion, SV Office of Space Science NASA Headquarters Washington, D. C. 20546
1	Director, Materials & Structures Div, RW Office of Aeronautics & Space Technology NASA Headquarters Washington, D. C. 20546
1	Director, Advanced Manned Missions, MT Office of Manned Space Flight NASA Headquarters Washington, D. C. 20546
1	National Aeronautics & Space Administration Ames Research Center Moffett Field, California 94035 Attn: Library
1	National Aeronautics & Space Administration Flight Research Center P. O. Box 273 Edwards, California 93523 Attn: Library
1	Director, Technology Utilization Division Office of Technology Utilization NASA Headquarters Washington, D. C. 20546
1	Office of the Director of Defense Research & Engineering Washington, D. C. 20301 Attn: Office of Asst. Dir. (Chem. Technology)
1	Office of Aeronautics & Space Technology, R NASA Headquarters Washington, D. C. 20546
10	NASA Scientific and Technical Information Facility P. O. Box 33 College Park, Maryland 20740 Attn: NASA Representative

Report Copies	Recipient
1	National Aeronautics & Space Administration Goddard Space Flight Center Greenbelt, Maryland 20771 Attn: Library
1	National Aeronautics & Space Administration John F. Kennedy Space Center Cocoa Beach, Florida 32931 Attn: Library
1	National Aeronautics & Space Administration Langley Research Center Langley Station Hampton, Virginia 23365 Attn: Library
1	National Aeronautics & Space Administration Manned Spacecraft Center Houston, Texas 77001 Attn: Library
1	W. Chandler
1	W. Dusenberry
1	C. Yodzis
1	National Aeronautics & Space Administration George C. Marshall Space Flight Center Huntsville, Alabama 35912 Attn: Library
1	J. M. Stuckey
1	I. G. Yates
1	E. H. Hyde
1	Jet Propulsion Laboratory 4800 Oak Grove Drive Pasadena, California 91103 Attn: Library
1	L. Stimson
1	J. Kelly
1	R. Breshears
1	Defense Documentation Center Cameron Station Building 5 5010 Duke Street Alexandria, Virginia 22314 Attn: TISIA

Report Copies	Recipient
1	RTD (RTNP) Bolling Air Force Base Washington, D. C. 20332
1	Arnold Engineering Development Center Air Force Systems Command Tullahoma, Tennessee 37389 Attn: Library
1	Advanced Research Projects Agency Washington, D. C. 20525 Attn: Library
1	Aeronautical Systems Division Air Force Systems Command Wright-Patterson Air Force Base Dayton, Ohio Attn: Library
1	AFML (MAAE)
1	AFML (MAAM)
1	Air Force Rocket Propulsion Laboratory (RPM) Edwards, California 93523 Attn: Library
1	Air Force FTC (FTAT-2) Edwards Air Force Base, California 93523 Attn: Library
1	Air Force Office of Scientific Research Washington, D. C. 20333 Attn: Library
1	Space & Missile Systems Organization Air Force Unit Post Office Los Angeles, California 90045 Attn: Technical Data Center
1	Office of Research Analyses (OAR) Holloman Air Force Base, New Mexico 88330 Attn: Library RRRD

Report Copies	Recipient
1	U. S. Air Force Washington, D. C. Attn: Library
1	Commanding Officer U. S. Army Research Office (Durham) Box CM, Duke Station Durham, North Carolina 27706 Attn: Library
1	Bureau of Naval Weapons Department of the Navy Washington, D. C. Attn: Library
1	Director (Code 6180) U. S. Naval Research Laboratory Washington, D. C. 20390
1	Picatinny Arsenal Dover, New Jersey 07801 Attn: Library
1	Air Force Aero Propulsion Laboratory Research & Technology Division Air Force Systems Command United States Air Force Wright-Patterson AFB, Ohio 45433 Attn: APRP (Library)
1	Electronics Division Aerojet-General Corporation P. O. Box 296 Azusa, California 91703 Attn: Library
1	Space Division Aerojet-General Corporation 9200 East Flair Drive El Monte, California 91734 Attn: Library

Report Copies	Recipient
1	Aerojet Ordnance and Manufacturing Aerojet-General Corporation 11711 South Woodruff Avenue Fullerton, California 90241 Attn: Library
1	Aerojet Liquid Rocket Company P. O. Box 15847 Sacramento, California 95813 Attn: Technical Library 2484-2015A
1	Aeronutronic Division of Philco-Ford Corp. Ford Road Newport Beach, California 92663 Attn: Technical Information Department
1	Aerospace Corporation 2400 E. El Segundo Blvd. Los Angeles, California 90045 Attn: Library-Documents
1	Arthur D. Little, Inc. 20 Acorn Park Cambridge, Massachusetts 02140 Attn: Library
1	R. B. Hinckley
1	Astropower Laboratory McDonnell-Douglas Aircraft Company 2121 Paularino Newport Beach, California 92163 Attn: Library
1	Susquehanna Corporation Atlantic Research Division Shirley Highway & Edsall Road Alexandria, Virginia 22314 Attn: Library
1	Beech Aircraft Corporation Boulder Facility Box 631 Boulder, Colorado Attn: Library

Report Copies	Recipient
1	Bell Aerosystems, Inc. Box 1 Buffalo, New York 14240 Attn: Library
1	Instruments & Life Support Division Bendix Corporation P. O. Box 4508 Davenport, Iowa 52808 Attn: Library
1	Boeing Company Space Division P. O. Box 868 Seattle, Washington 98124 Attn: Library
1	D. H. Zimmerman
1	Boeing Company 1625 K Street, N.W. Washington, D. C. 20006
1	Chemical Propulsion Information Agency Applied Physics Laboratory 8621 Georgia Avenue Silver Spring, Maryland 20910
1	Chrysler Corporation Missile Division P. O. Box 2628 Detroit, Michigan Attn: Library
1	Chrysler Corporation Space Division P. O. Box 29200 New Orleans, Louisiana 70129 Attn: Library
1	Curtiss-Wright Corporation Wright Aeronautical Division Woodridge, New Jersey Attn: Library

Report Copies	Recipient
1	University of Denver Denver Research Institute P. O. Box 10127 Denver, Colorado 80210 Attn: Security Office
1	Fairchild Stratos Corporation Aircraft Missiles Division Hagerstown, Maryland Attn: Library
1	Research Center Fairchild Hiller Corporation Germantown, Maryland Attn: Library
1	Republic Aviation Fairchild Hiller Corporation Farmington, Long Island New York
1	General Dynamics/Convair P. O. Box 1128 San Diego, California 92112 Attn: Library
1	R. Tatro
1	Missiles and Space Systems Center General Electric Company Valley Forge Space Technology Center P. O. Box 8555 Philadelphia, Pa. 19101 Attn: Library
1	General Electric Company Flight Propulsion Lab. Department Cincinnati, Ohio Attn: Library
1	Grumman Aircraft Engineering Corporation Bethpage, Long Island, New York Attn: Library

Report Copies	Recipient
1	Honeywell Inc. Aerospace Division 2600 Ridgeway Road Minneapolis, Minnesota Attn: Library
1	IIT Research Institute Technology Center Chicago, Illinois 60616 Attn: Library
1	Ling-Temco-Vought Corporation P. O. Box 5907 Dallas, Texas 75222 Attn: Library
1	Lockheed Missiles and Space Company P. O. Box 504 Sunnyvale, California 94087 Attn: Library
1	Linde--Division of Union Carbide P. O. Box 44 Tonawanda, New York 11450 Attn: G. Nies
1	Marquardt Corporation 16555 Saticoy Street Box 2013 - South Annex Van Nuys, California 91409
1	Denver Division Martin Marietta Corporation P. O. Box 179 Denver, Colorado 80201 Attn: Library
1	C. G. Skartvedt
1	Western Division McDonnell Douglas Astronautics 5301 Bolsa Avenue Huntington Beach, California 92647 Attn: Library
1	P. Klevatt

Report Copies	Recipient
1	McDonnell Douglas Aircraft Corporation P. O. Box 516 Lambert Field, Missouri 63166 Attn: Library
1	L. F. Kohrs
1	Rocketdyne Division North American Rockwell Inc. 6633 Canoga Avenue Canoga Park, California 91304 Attn: Library, Department 596-306
1	Space & Information Systems Division North American Rockwell 12214 Lakewood Blvd. Downey, California Attn: Library
1	E. Hawkinson
1	Northrop Space Laboratories 3401 West Broadway Hawthorne, California Attn: Library
1	Purdue University Lafayette, Indiana 47907 Attn: Library (Technical)
1	Goodyear Aerospace Corporation 1210 Massilon Road Akron, Ohio 44306 Attn: C. Shriver
1	Hamilton Standard Corporation Windsor Locks, Connecticut 06096 Attn: Library
1	Stanford Research Institute 333 Ravenswood Avenue Menlo Park, California 94025 Attn: Library

Report Copies	Recipient
1	TRW Systems, Inc. 1 Space Park Redondo Beach, California 90278 Attn: Tech. Lib. Doc. Acquisitions
1	United Aircraft Corporation Pratt & Whitney Division Florida Research & Development Center P. O. Box 2691 West Palm Beach, Florida 33402 Attn: Library
1	United Aircraft Corporation United Technology Center P. O. Box 358 Sunnyvale California 94038 Attn: Library
1	Vickers Incorporated Box 302 Troy, Michigan
1	Airesearch Mfg. Div. Garrett Corporation 9851 Sepulveda Blvd Los Angeles, California 90009
1	Airesearch Mfg. Div. Garrett Corporation 402 South 36th Street Phoenix, Arizona 85034 Attn: Library
1	Commanding Officer U. S. Naval Underwater Ordnance Station Newport, Rhode Island 02844 Attn: Library
1	National Science Foundation, Engineering Division 1800 G. Street, N.W. Washington, D. C. 20540 Attn: Library

Report Copies	Recipient
1	G. T. Schjeldahl Company Northfield, Minn. 55057 Attn: Library
1	General Dynamics P. O. Box 748 Fort Worth, Texas 76101
1	Cryonetics Corporation Northwest Industrial Park Burlington, Massachusetts
1	Institute of Aerospace Studies University of Toronto Toronto 5, Ontario Attn: Library
1	FMC Corporation Chemical Research & Development Center P. O. Box 8 Princeton, New Jersey 08540
1	Westinghouse Research Laboratories Beulah Road, Churchill Boro Pittsburgh, Pennsylvania 15235
1	Cornell University Department of Materials Science & Engr. Ithaca, New York 14850 Attn: Library
1	Marco Research & Development Co. Whittaker Corporation 131 E. Ludlow Street Dayton, Ohio 45402
1	General Electric Company Apollo Support Dept. P. O. Box 2500 Daytona Beach, Florida 32015 Attn: C. Bay

Report Copies	Recipient
1	E. I. DuPont, DeNemours and Company Eastern Laboratory Gibbstown, New Jersey 08027 Attn: Library
1	Esso Research and Engineering Company Special Projects Units P. O. Box 8 Linden, New Jersey 07036 Attn: Library
1	Minnesota Mining and Manufacturing Company 900 Bush Avenue St. Paul, Minnesota 55106 Attn: Library
1	Alloy Spotwelders 2035 Granville Avenue Los Angeles, California 90025
1	Metal Bellows Corporation 20977 Knapp Street Chatsworth, California 91311 Attn: H. Johnson
1	Gardner Bellows Corp. 15934 Strathern Street Van Nuys, California 91406
1	BV Machine Co., Inc. 2090 West Bates Avenue Englewood, Colorado 80110
1	Explosive Forming Industries 1301 Courtesy Louisville, Colorado 80027